A 67-year-old woman presented to the emergency department with a 6-week history of progressive exertional dyspnea. Her medical history was notable for lung transplantation that had been performed 8 years earlier. Laboratory studies showed normocytic anemia, with a hemoglobin level of 6.9 g per deciliter (reference range, 11.9 to 17.2). White-cell and platelet counts were normal. The reticulocyte index was 0%. Bone marrow aspiration was performed and showed giant proerythroblasts with basophilic and vacuolated cytoplasm, uncondensed chromatin, and large, intranuclear, purple-colored inclusions. What is the diagnosis?

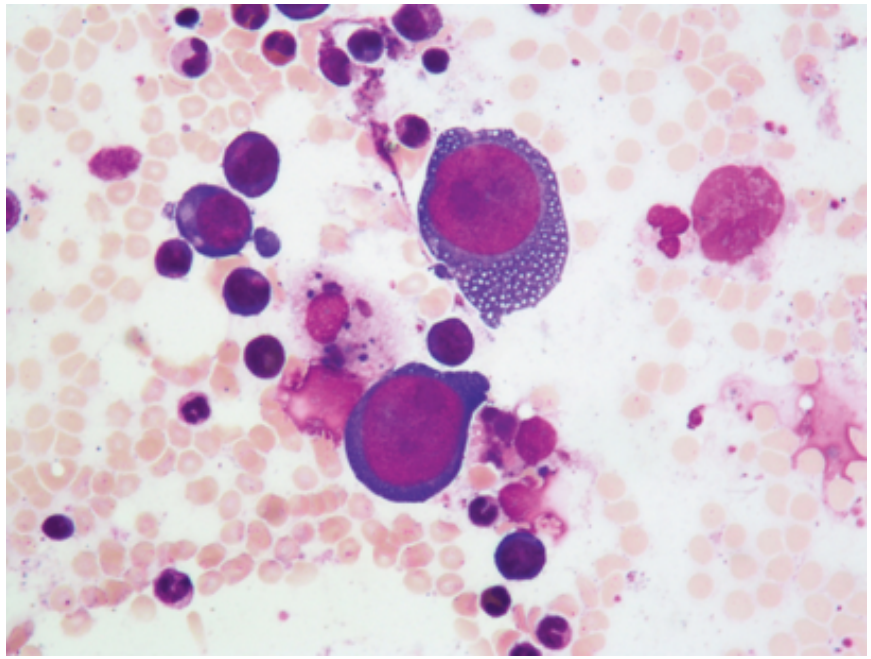

Chronic lung allograft dysfunction

Acute promyelocytic leukemia

Adverse reaction to an immunosuppressant

Parvovirus B19 infection

Acute hepatitis B infection

Correct!
These findings supported a diagnosis of parvovirus B19 infection, which was confirmed by polymerase-chain-reaction testing. The patient was treated with red-cell transfusions and intravenous immune globulin.

Parvovirus B19 (von lat. parvus = klein) ist ein kleines Einzelstrang-DNA-Virus aus der Familie der Parvoviren und Erreger der Ringelröteln (Erythema infectiosum). Es war bis zur Entdeckung des ersten Humanen Bocavirus 2005 das einzige bekannte humanpathogene Virus aus der Gattung Erythrovirus. 1974 wurde es durch Zufall durch die australische Virologin Yvonne Cossart entdeckt. Seinen Namen trägt es nach der Laborprobe mit der Nummer B19, in der es gefunden wurde. Es hat einen Durchmesser von nur 20 bis 24 nm und gehört damit zu den kleinsten bekannten Viren. Das Parvovirus B19 ist der Erreger der Ringelröteln (Erythema infectiosum). Aufgrund einer nach der Infektion lebenslang bestehenden Immunität kommt die Erkrankung häufig bei Kindern vor. Parvovirus B19 vermehrt sich ausschließlich in den Erythroblasten, den Vorläuferzellen der roten Blutkörperchen (Erythrozyten) im Knochenmark. Die Infektion löst daher eine vorübergehende Anämie aus, die bei immun-geschwächten oder bereits anämischen Patienten zu Komplikationen bis hin zum Tod führen kann, die jedoch durch rechtzeitige Bluttransfusionen behandelt werden können. Patienten, die bereits vor der Infektion mit Parvovirus B19 an einer Änamie – beispielsweise Sichelzellenanämie – leiden, haben ein erhöhtes Risiko für eine Aplastische Krise. Auch in der Schwangerschaft kann es zu Spontanaborten und weiteren Komplikationen wie Hydrops fetalis kommen, der den Fetus schwer schädigen kann, wenn er nicht erkannt wird.

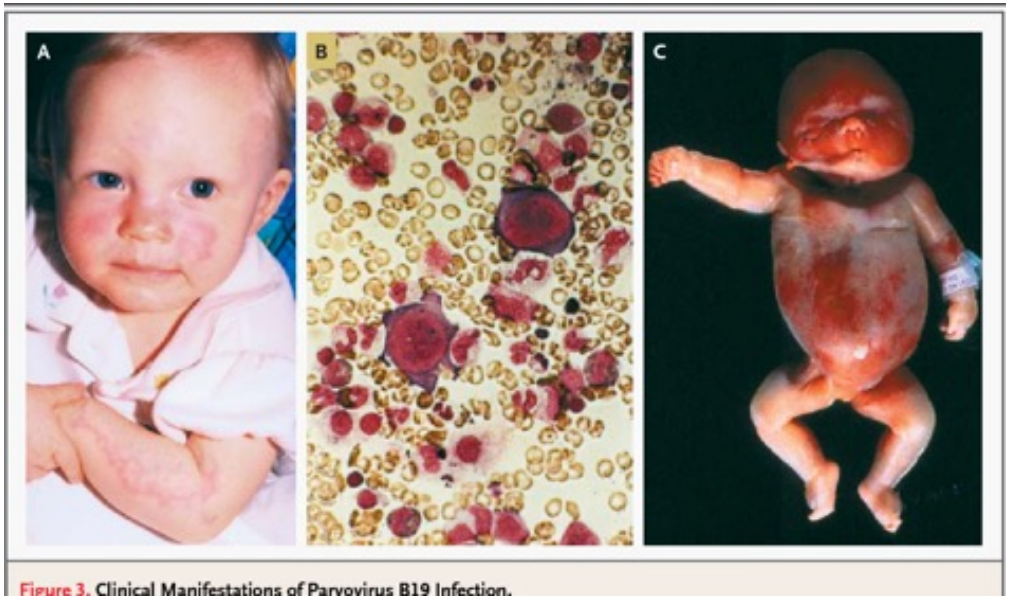

Figure 3. Clinical Manifestations of Parvovirus B19 Infection.

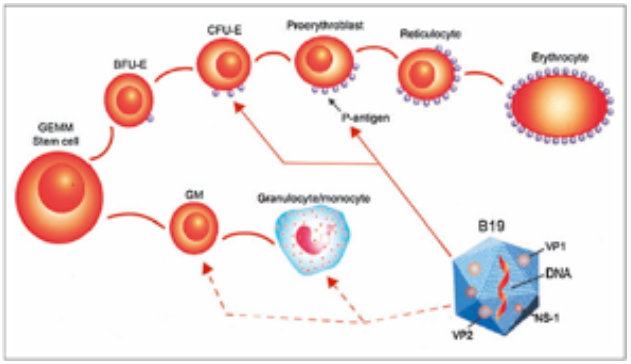

Alter	% seropositiv
4 – 6 Jahre	35 %
10 – 15 Jahre	58 %
25 – 29 Jahre	70 %
65 – 69 Jahre	79 %

Pantoprazol ist ein Arzneistoff aus der Gruppe der Protonenpumpenhemmer, der zur Behandlung von Magen- und Zwölffingerdarmgeschwüren sowie bei Refluxösophagitis eingesetzt wird. Pantoprazol entfaltet seine Wirkung in den Parietalzellen der Magenschleimhaut, wo es als irreversibler Hemmstoff der H+/K+-ATPase dient. Dadurch kommt es zu einer Verminderung der Salzsäureproduktion im Magen, und der pH-Wert des Magensafts steigt an. Dies führt zu weniger aggressivem Magensaft, was wiederum die beschleunigte Heilung von Magenwandverletzungen (bspw. Schleimhauterosionen oder Magengeschwüren) begünstigt. 2013 wurde in einer Studie festgestellt, dass bei einer Langzeitmedikation das Risiko eines Vitamin-B12-Mangels deutlich ansteigt. Nach einer Bonner Studie von 2016 haben ältere Menschen, die Pantoprazol oder Omeprazol über längere Zeit einnehmen, ein erhöhtes Demenzrisiko. Pantoprazol kann bei Urin-Schnelltests ein falsch-positives Ergebnis zu THC verursachen.

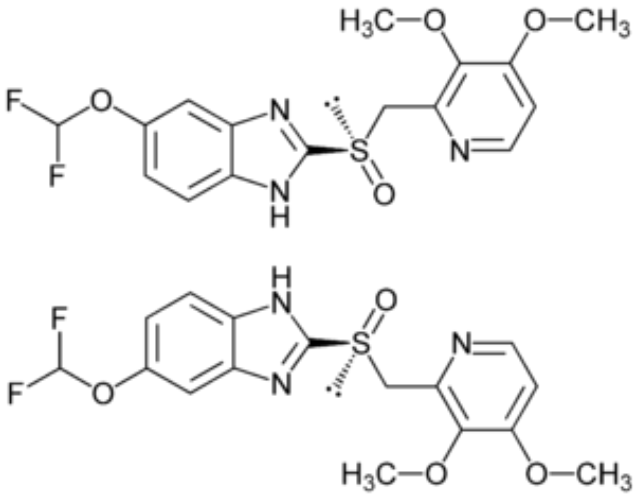

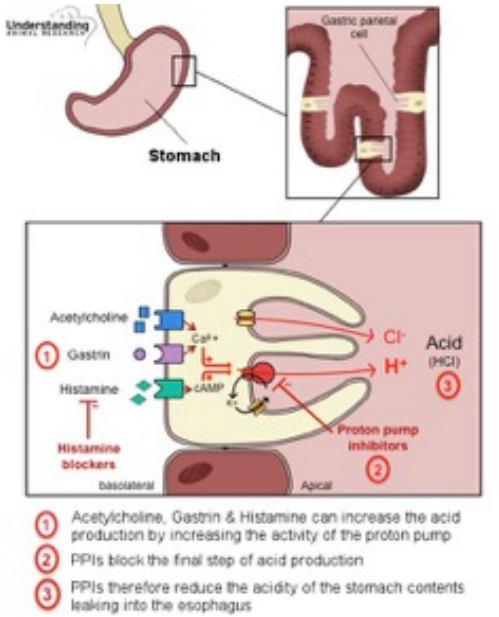

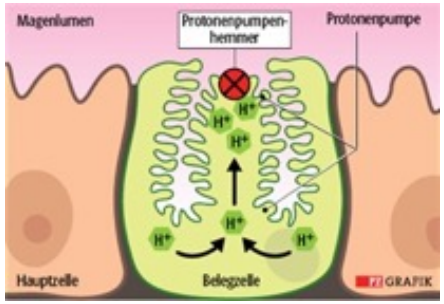

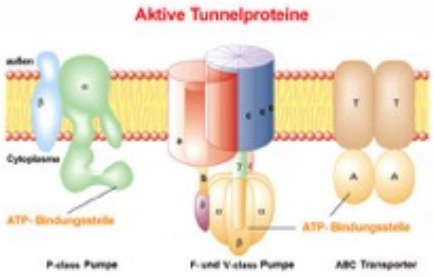

Pantoprazole in Patients at Risk for Gastrointestinal Bleeding in the ICU

Prophylaxis for gastrointestinal stress ulceration is frequently given to patients in the intensive care unit (ICU), but its risks and benefits are unclear. In this European, multicenter, parallel-group, blinded trial, we randomly assigned adults who had been admitted to the ICU for an acute condition (i.e., an unplanned admission) and who were at risk for gastrointestinal bleeding to receive 40 mg of intravenous pantoprazole (a proton-pump inhibitor) or placebo daily during the ICU stay. The primary outcome was death by 90 days after randomization.

Characteristic	Pantoprazole (N=1644)	Placebo (N=1647)
Median age (IQR) — yr	67 (56–75)	67 (55–75)
Male sex — no. (%)	1039 (63)	1067 (65)
Coexisting conditions — no. (%)		
Chronic lung disease†	351 (21)	306 (19)
Previous myocardial infarction	156 (9)	142 (9)
Chronic heart failure‡	100 (6)	99 (6)
Use of glucocorticoids§	35 (2)	27 (2)
Hematologic cancer¶	64 (4)	55 (3)
Metastatic cancer ‖	56 (3)	55 (3)
AIDS**	6 (<1)	1 (<1)
Coagulopathy††	352 (21)	299 (18)
Admission to university hospital — no. (%)	1183 (72)	1189 (72)
Median time from ICU admission to randomization (IQR) — hr	15 (5–28)	14 (6–25)
Median time from hospital admission to randomization (IQR) — days	1 (1–3)	1 (1–3)
ICU admission type — no. (%)		
Medical	998 (61)	941 (57)
Emergency surgery	490 (30)	558 (34)
Elective surgery	156 (9)	148 (9)
Use of invasive mechanical ventilation — no. (%)	1273 (77)	1316 (80)
Use of vasopressors or inotropes — no. (%)	1103 (67)	1093 (66)
Use of any renal-replacement therapy — no. (%)	123 (7)	99 (6)
Median SAPS II (IQR)‡‡	49 (39–59)	48 (37–59)
Median SOFA score (IQR)§§	9 (7–11)	9 (7–11)

Outcomes	Pantoprazole	Placebo	Relative Risk (95% CI)*	P Value†
Primary outcome: death by day 90 — no./total no. (%)	510/1642 (31.1)	499/1640 (30.4)	1.02 (0.91–1.13)	0.76
Secondary outcomes				
One or more clinically important events — no./total no. (%)‡	360/1644 (21.9)	372/1647 (22.6)	0.96 (0.83–1.11)	—
One or more episodes of clinically important gastrointestinal bleeding — no./total no. (%)	41/1644 (2.5)	69/1647 (4.2)	0.58 (0.40–0.86)	—
One or more infectious adverse events — no./total no. (%)§	276/1644 (16.8)	279/1647 (16.9)	0.99 (0.84–1.16)	—
Severe adverse reaction — no./total no. (%)¶	0/1644 (0)	0/1647 (0)	—	—
Median percentage of days alive without the use of life support (IQR)‖	92 (60–97)	92 (65–97)	—	—

Figure legend. Time to Death and Relative Risk of Death at Day 90. Panel A shows the survival curves with data censored at day 90 for the two groups in the intention-to-treat population. The nine patients who were lost to 90-day follow-up — two patients in the pantoprazole group and seven patients in the placebo group — were included in the survival curves until the last day they were known to be alive; at that time point, data from these patients were censored. One patient in the pantoprazole group was known to be dead at day 90, but the date of death was unknown. This patient was excluded from the survival curves. Panel B shows relative risks with 95% confidence intervals for the primary outcome measure of death at day 90 in the pantoprazole group as compared with the placebo group, among all the patients and in the six predefined subgroups, assessed by logistic-regression analysis with adjustment for the stratification variables. Shock was defined as at least one of the following: systolic blood pressure of less than 90 mm Hg, mean arterial pressure of less than 70 mm Hg, use of vasopressors or inotropes (norepinephrine, epinephrine, phenylephrine, vasopressin or dopamine, dobutamine, milrinone, or levosimendan), or a lactate level of more than 4 mmol per liter. Coagulopathy included both acute coagulopathy, defined as a platelet count of less than 50×10^9 per liter, an international normalized ratio of more than 1.5, or a prothrombin time of more than 20 seconds at ICU admission, and a history of coagulopathy, defined as coagulopathy within 6 months before hospital admission. A history of liver disease was defined as portal hypertension; cirrhosis proved by biopsy, computed tomography, or ultrasonography; history of variceal bleeding; or hepatic encephalopathy in the medical history. A medical admission was defined as a hospital admission during which no surgery was performed or an ICU admission in which surgery had been performed more than 1 week before admission. The Simplified Acute Physiology Score (SAPS) II was calculated from 17 baseline variables and ranges from 0 to 163, with higher scores indicating greater severity of disease. One or more variables were missing for 134 patients in the pantoprazole group and 115 patients in the placebo group for the calculation of the SAPS II; these patients were not included in the SAPS II subgroup analysis.

A Time to Death

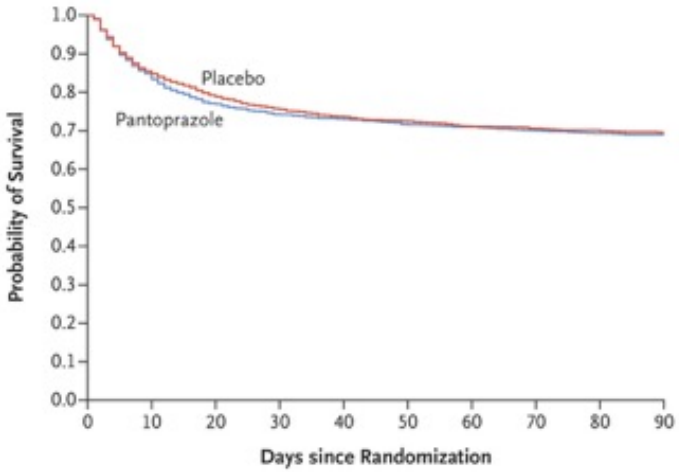

No. at Risk				
Placebo	1647	1243	1167	1141
Pantoprazole	1643	1219	1163	1133

B Relative Risk of the Primary Outcome

Subgroup	Pantoprazole	Placebo	Relative Risk (95% CI)	P Value for Heterogeneity
	no. of events/no. of patients in subgroup			
Shock at randomization				0.92
Yes	413/1251	395/1210	1.01 (0.90–1.13)	
No	97/391	104/430	1.02 (0.80–1.31)	
Mechanical ventilation at randomization				0.74
Yes	399/1272	400/1310	1.03 (0.91–1.16)	
No	111/370	99/330	0.98 (0.77–1.25)	
Coagulopathy at randomization				0.54
Yes	135/352	118/299	0.95 (0.77–1.17)	
No	375/1290	381/1341	1.03 (0.91–1.16)	
History of liver disease				0.69
Yes	20/44	25/48	0.93 (0.60–1.44)	
No	490/1598	474/1592	1.02 (0.92–1.14)	
Type of ICU admission				0.38
Medical	361/1045	328/994	1.04 (0.92–1.18)	
Surgical	149/597	171/646	0.94 (0.78–1.14)	
SAPS II score >53				0.05
Yes	272/579	229/558	1.13 (0.99–1.30)	
No	205/929	231/967	0.92 (0.78–1.09)	
All patients	510/1642	499/1640	1.02 (0.91–1.13)	

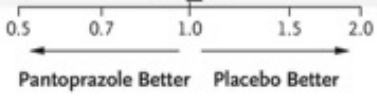

In this international, blinded, placebo-controlled, randomized trial involving adult patients in the ICU who were at risk for gastrointestinal bleeding, we found that 90-day mortality, percentages of days alive without the use of life support, and numbers of patients with clinically important events, infectious adverse events, or serious adverse reactions were similar between those treated with pantoprazole and those who received placebo. Fewer patients in the pantoprazole group than in the placebo group had clinically important gastrointestinal bleeding in the ICU, and the 95% confidence intervals (which were not adjusted for multiple comparisons) for the relative risk did not cross 1; however, the absence of correction for multiple comparisons of secondary outcomes limits inferences from this observation. The results of this trial apply only to patients who meet the entry criteria used in the trial, including a high risk of gastrointestinal bleeding.

Critical illness can disrupt local and systemic mechanisms that protect against upper gastrointestinal bleeding, a condition that may be associated with increased mortality, particularly among patients receiving extracorporeal life support. On the basis of randomized trials performed over a period of 40 years, most guidelines recommend preventive therapy with either histamine H_2–receptor antagonists or proton-pump inhibitors (PPIs) for patients in the intensive care unit (ICU) who are at risk for the development of stress ulceration and bleeding.

In our view, the take-home message from this trial is that, given the low incidence of clinically important upper gastrointestinal bleeding in the ICU, prophylaxis with a PPI, if initiated, should be reserved for seriously ill patients who are at high risk for this complication. (An important problem, of course, is that the definition of a high risk of bleeding varies between guidelines and needs to be standardized.) Although 90-day mortality was not affected by pantoprazole administration in the current trial, the between-group difference in the rate of important upper gastrointestinal bleeding may still support the recommendation of using a prophylactic PPI, particularly given the absence of a difference in the rate of adverse events between the pantoprazole group and the placebo group. We base this view mainly on the admittedly small (1.7-percentage-point) difference in bleeding rates between the groups.

Mucine (lateinisch mucus ‚Schleim ‘) sind der strukturgebende Bestandteil des Schleims von Organismen. Diese protektiven Substanzen können von sehr vielen Mikroorganismen (namensgebend für Schleimpilze), Pflanzen und Tieren gebildet werden. Sie können äußerlich (z. B. bei Prokaryoten, Einzellern, Weichtieren) oder zum auskleidenden Schutz von inneren Organen auf den Schleimhäuten (Mucosa) dienen. Mucine sind Glykoproteine, also Makromoleküle aus einer zentralen Proteinkette und (langen) Seitenketten aus Zuckerverbindungen (Polysacchariden). Die Polysaccharide verleihen den Mucinen eine hohe Wasserbindungskapazität und schützen das zentrale Protein vor enzymatischem Abbau (Proteolyse) oder Einwirkung von Säuren (im Verdauungssystem). Mucine spielen eine Rolle für die Barrierefunktion durch die Schleimhäute und die Adhäsion.

Die Mucine werden funktional in zwei Gruppen eingeteilt: in *membrangebundene* und in *abgesonderte* Mucine. Unabhängig davon werden sie beim Menschen mit dem Kürzel „MUC“, gefolgt von einer Zahl benannt beziehungsweise durchnummeriert (MUC1, MUC2, MUC3A usw.). Im Jahr 2002 waren sechzehn Mucin-Gene im Menschen bekannt: MUC1, MUC2, MUC3A, MUC3B, MUC4, MUC5AC, MUC5B, MUC6–9, MUC11–13, MUC16 und MUC17. Diese Benennung wurde jedoch kritisiert, da sie die Existenz einer Familie von Genen suggeriert, während zwischen den Genen der verschiedenen Mucine die entsprechende Sequenzhomologie oft fehlt.

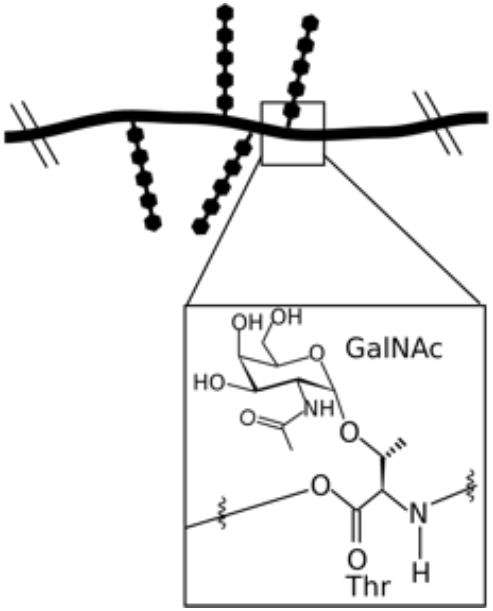

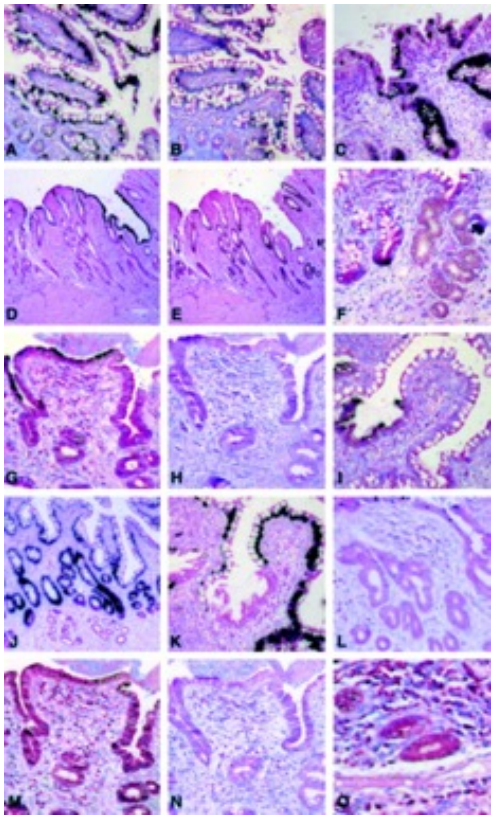

MUC5B Promoter Variant and Rheumatoid Arthritis with Interstitial Lung Disease

Interstitial lung disease (ILD) is detected in up to 60% of patients with RA on high-resolution computed tomography (CT), is clinically significant in 10% of cases, and is a leading cause of illness and death in patients with RA. RA-associated ILD (RA-ILD) shares several characteristics with idiopathic pulmonary fibrosis, including common environmental risk factors, a high prevalence of a pattern of usual interstitial pneumonia (UIP), progressive lung fibrosis, and poor survival.

Given the phenotypic similarities between rheumatoid arthritis (RA)–associated interstitial lung disease (ILD) (hereafter, RA-ILD) and idiopathic pulmonary fibrosis, we hypothesized that the strongest risk factor for the development of idiopathic pulmonary fibrosis, the gain-of-function *MUC5B* promoter variant rs35705950, would also contribute to the risk of ILD among patients with RA. Using a discovery population and multiple validation populations, we tested the association of the *MUC5B* promoter variant rs35705950 in 620 patients with RA-ILD, 614 patients with RA without ILD, and 5448 unaffected controls.

The common gain-of-function variant rs35705950 in the promoter of *MUC5B*, encoding mucin 5B, is the strongest genetic risk factor for idiopathic pulmonary fibrosis; it is observed in at least 50% of patients with idiopathic pulmonary fibrosis and accounts for 30% of the risk of developing this disease.

Characteristic	RA-ILD (N=620)	RA without ILD (N=614)	Crude P Value	Adjusted P Value†
Female sex — no./total no. (%)	345/565 (61.1)	446/540 (82.6)	8.12×10^{-15}	3.7×10^{-12}‡
Age at inclusion — yr	69.0±10.8	60.4±12.6	1.20×10^{-24}	1.3×10^{-21}
Age at onset of RA — yr	55.7±14.6	45.7±13.5	7.0×10^{-23}	5.6×10^{-14}
Duration of RA — yr	13.3±11.5	14.8±10.2	0.03	0.38
Age at onset of ILD — yr	62.7±11.8			
Duration of ILD — yr	4.3±4.0			
Ever smoked				
No./total no. (%)	282/516 (54.7)	168/465 (36.1)	7.59×10^{-9}	0.53
Pack-yr of smoking	28.0±21.8	22.4±30.7	0.07	0.37
Current smoker				
No./total no. (%)	46/415 (11.1)	67/463 (14.5)	0.14	0.06
Pack-yr of smoking	33.0±26.6	23.9±19.7	0.08	0.42
Ever used methotrexate — no./total no. (%)§	260/318 (81.8)	142/153 (92.8)	0.002	0.69
Manifestations of RA				
Positivity for ACPA or rheumatoid factor — no./total no. (%)	449/506 (88.7)	446/468 (95.3)	0.001	0.72
Erosive disease — no./total no. (%)	224/482 (46.5)	274/469 (58.4)	2.33×10^{-4}	0.30
Disease pattern on high-resolution CT of the chest				
UIP or possible UIP — no./total no. (%)	207/505 (41.0)			
Inconsistent with UIP — no./total no. (%)	298/505 (59.0)			
Pulmonary function				
Forced vital capacity — % of predicted value	78.2±25.0			
D_{LCO} — % of predicted value	57.6±23.4			
Total lung capacity — % of predicted value	81.3±20.3			

Genotyping

Genotyping of the *MUC5B* rs35705950 single-nucleotide polymorphism involved the use of TaqMan Genotyping Assays (Applied Biosystems), as reported previously. The additional common risk variants for idiopathic pulmonary fibrosis on 3q26, 4q22, 5p15, 6p21.3, 6p24, 7q22, 10q24, 11p15.5, 13q34, 15q14–15, and 19p13 were genotyped by a TaqMan quantitative polymerase-chain-reaction assay (Thermo Fisher Scientific).

Lung-Tissue Analysis

To determine whether MUC5B was expressed in the lung tissue of patients with RA-ILD, we analyzed lung tissue from nine patients with RA-ILD undergoing lung transplantation (University of California, San Francisco) as compared with six unaffected controls without ILD or RA (National Heart, Lung, and Blood Institute [NHLBI] Lung Tissue Research Consortium) and two controls with fibrotic ILD without RA (both with desquamative interstitial pneumonia) (NHLBI Lung Tissue Research Consortium).

Table 2. Genotypic Association of *MUC5B* rs35705950 Single-Nucleotide Polymorphism in Patients with RA, with and without ILD, and Unaffected Controls.*

Variable	France†	Greece	The Netherlands	United States–1	United States–2	Mexico	Japan	China	Multiethnic Replication Sample	Combined Analysis
No. of persons										
Controls	1229	1795	249	500	—	347	315	1013	4219	5448
RA without ILD	105	—	—	68	72	69	300	—	509	614
RA-ILD	118	56	40	99	48	55	182	22	502	620
Minor allele frequency of *MUC5B* rs35705950 — %										
Controls	10.9	3.8	9.0	10.7	—	5.3	0.2	0.8	—	—
RA without ILD	12.9	—	—	11.0	12.5	3.6	0.5	—	—	—
RA-ILD	32.6	26.8	30.0	28.8	13.5	16.4	1.1	2.3	—	—
Genotypic association test										
RA without ILD vs. controls										
Crude odds ratio for RA without ILD (95% CI)	1.2 (0.8–1.8)	—	—	1.0 (0.6–1.8)	—	0.7 (0.2–1.6)	3.2 (0.4–64.3)	—	1.0 (0.6–1.5)	1.1 (0.8–1.5)
Crude P value	0.40	—	—	0.91	—	0.42	0.32	—	0.90	0.60
Adjusted odds ratio for RA without ILD (95% CI)‡	1.3 (0.8–1.9)	—	—	1.0 (0.5–1.7)	—	0.7 (0.2–1.7)	3.7 (0.5–75.1)	—	1.0 (0.6–1.5)	1.1 (0.8–1.5)
Adjusted P value‡	0.28	—	—	0.99	—	0.42	0.26	—	0.83	0.54
RA-ILD vs. controls										
Crude odds ratio for RA-ILD (95% CI)	3.8 (2.8–5.2)	13.2 (7.6–22.9)	5.6 (2.9–11.2)	4.1 (2.7–6.3)	—	3.4 (1.8–6.2)	7.1 (1.0–138.6)	3.0 (0.2–15.6)	5.5 (4.2–7.2)	4.7 (3.8–5.8)
Crude P value	3.8×10^{-17}	2.2×10^{-20}	5.0×10^{-7}	5.8×10^{-11}	—	1.1×10^{-4}	0.08	0.30	3.9×10^{-35}	1.3×10^{-49}
Adjusted odds ratio for RA-ILD (95% CI)‡	3.8 (2.8–5.2)	13.2 (7.6–23.0)	4.9 (2.2–11.5)	4.1 (2.7–6.3)	—	3.6 (1.8–7.3)	5.5 (0.6–119.1)	4.9 (0.3–27.5)	5.5 (4.2–7.3)	4.7 (3.9–5.8)
Adjusted P value‡	9.7×10^{-17}	6.2×10^{-20}	1.2×10^{-4}	5.6×10^{-11}	—	2.2×10^{-4}	0.16	0.14	4.7×10^{-35}	1.3×10^{-49}
RA-ILD vs. RA without ILD										
Crude odds ratio for RA-ILD (95% CI)	3.8 (2.2–6.8)	—	—	5.4 (2.6–11.7)	1.1 (0.5–2.5)	5.7 (2.1–18.6)	2.2 (0.5–11.4)	—	3.1 (2.0–5.0)	3.4 (2.4–4.8)
Crude P value	5.9×10^{-6}	—	—	7.9×10^{-6}	0.80	0.002	0.30	—	5.3×10^{-7}	1.6×10^{-11}
Adjusted odds ratio for RA-ILD (95% CI)§	3.1 (1.6–6.3)	—	—	NA	NA	3.8 (1.2–13.3)	3.1 (0.3–28.0)	—	2.9 (1.1–8.4)	3.1 (1.8–5.4)
Adjusted P value§	9.4×10^{-4}	—	—	NA	NA	0.03	0.30	—	0.04	7.4×10^{-5}

* The two case series from the United States are designated United States–1 and United States–2. CI denotes confidence interval, and RA-ILD rheumatoid arthritis–associated interstitial lung disease.
† The case series from France represents the discovery population.
‡ P values and odds ratios were adjusted for sex and country of origin.
§ P values and odds ratios were adjusted for sex, age at inclusion, smoking status (ever smoked vs. never smoked), and country of origin. Some odds ratios and P values are not available (NA) because not all covariates were available for adjustment.

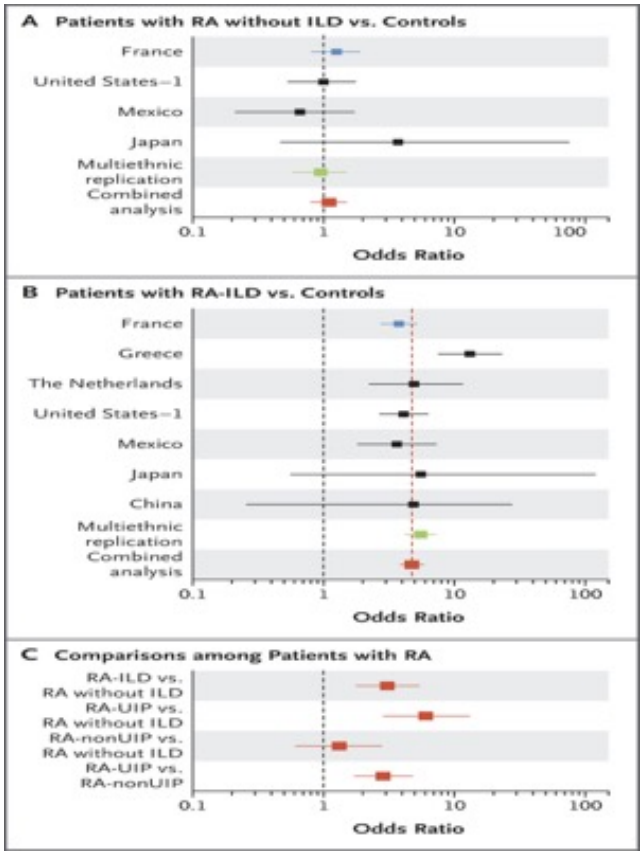

Comparison of patients with RA without ILD and controls revealed that none of the case series (discovery population and multiethnic case series) showed a significant difference in the frequency of the *MUC5B* promoter variant, findings that suggest a lack of association between the *MUC5B* promoter variant and RA. In the discovery population, the minor allele frequency of the *MUC5B* promoter variant was 10.9% in unaffected controls and 32.6% in patients with RA-ILD; this variant was in Hardy–Weinberg equilibrium in the discovery population.

An analysis of the multiethnic case series showed a significant association between the *MUC5B* promoter variant and RA-ILD (adjusted odds ratio, 5.5; 95% CI, 4.2 to 7.3; $P=4.7 \times 10^{-35}$), and an analysis of all the series (discovery population together with the other case series) combined showed a similar significant association for this comparison (adjusted odds ratio, 4.7; 95% CI, 3.9 to 5.8; $P=1.3 \times 10^{-49}$).

To investigate whether the *MUC5B* promoter variant rs35705950 contributes to the risk of ILD among patients with RA, we compared patients with RA-ILD and those with RA without ILD, adjusting for sex, age at inclusion, and smoking status. In the discovery population, the *MUC5B* promoter variant was associated with RA-ILD (adjusted odds ratio, 3.1; 95% CI, 1.6 to 6.3; $P=9.4 \times 10^{-4}$), and this finding was replicated in the aggregate multiethnic case series (adjusted odds ratio, 2.9; 95% CI, 1.1 to 8.4; P=0.04)

Table 3. Dominant Genotypic Association of *MUC5B* rs35705950 Single-Nucleotide Polymorphism in Patients with RA-ILD and a Pattern of Usual Interstitial Pneumonia (UIP) or Possible UIP and in Patients with RA-ILD and a Pattern Inconsistent with UIP.*

Variable	France†	Greece	The Netherlands	United States–1	Mexico	Japan	China	Multiethnic Replication Sample	Combined Analysis
No. of patients									
RA-ILD with UIP or possible UIP pattern	50	18	18	34	19	60	8	157	207
RA-ILD with pattern inconsistent with UIP	31	38	22	42	36	122	7	267	298
Minor allele frequency of *MUC5B* rs35705950 — %									
RA-ILD with UIP or possible UIP pattern	34.0	36.1	33.3	33.8	28.9	1.7	0	—	—
RA-ILD with pattern inconsistent with UIP	12.9	21.1	25.0	23.8	8.3	0.8	7.1	—	—
Genotypic association test									
Crude odds ratio for RA-ILD with UIP or possible UIP pattern (95% CI)	6.1 (2.3–17.5)	3.6 (1.1–13.1)	2.0 (0.6–7.6)	2.3 (0.9–6.0)	6.9 (2.0–26.0)	2.1 (0.2–17.6)	NA‡	2.9 (1.7–5.0)	3.5 (2.2–5.6)
Crude P value	3.9×10^{-4}	0.04	0.29	0.08	0.003	0.47	1.0	1.5×10^{-4}	3.6×10^{-7}
Adjusted odds ratio for RA-ILD with UIP or possible UIP pattern (95% CI)§	4.9 (1.8–14.6)	2.9 (0.8–12.1)	1.6 (0.4–6.7)	2.1 (0.7–6.3)	3.8 (0.9–16.8)	NA‡	NA‡	2.3 (1.3–4.1)	2.9 (1.7–4.8)
Adjusted P value§	0.003	0.12	0.51	0.18	0.07	0.99	1.0	0.006	5.1×10^{-5}

* Patients with RA-ILD and a pattern inconsistent with UIP had the following patterns on high-resolution computed tomography: nonspecific interstitial pneumonia, organizing pneumonia, or unclassifiable ILD.
† The case series from France represents the discovery population.
‡ Odds ratios are not available (NA) because of the small proportion of carriers with risk genotypes.
§ P values and odds ratios were adjusted for sex, age at inclusion, smoking status (ever smoked vs. never smoked), and country of origin.

The *MUC5B* promoter variant was associated with an increased risk of a usual interstitial pneumonia (UIP) pattern among patients with RA-ILD through a dominant model in the discovery population, aggregate multiethnic case series, and combined analysis; the odds of having a UIP or possible UIP pattern among patients with RA-ILD who carried at least one *MUC5B* risk allele were 2.9 times as high as those among persons who had the GG genotype (adjusted odds ratio, 2.9; 95% CI, 1.7 to 4.8; $P=5.1\times10^{-5}$). After adjusting for covariates, we observed no effect of tobacco smoking on the association of the *MUC5B* promoter variant and UIP pattern of RA-ILD.

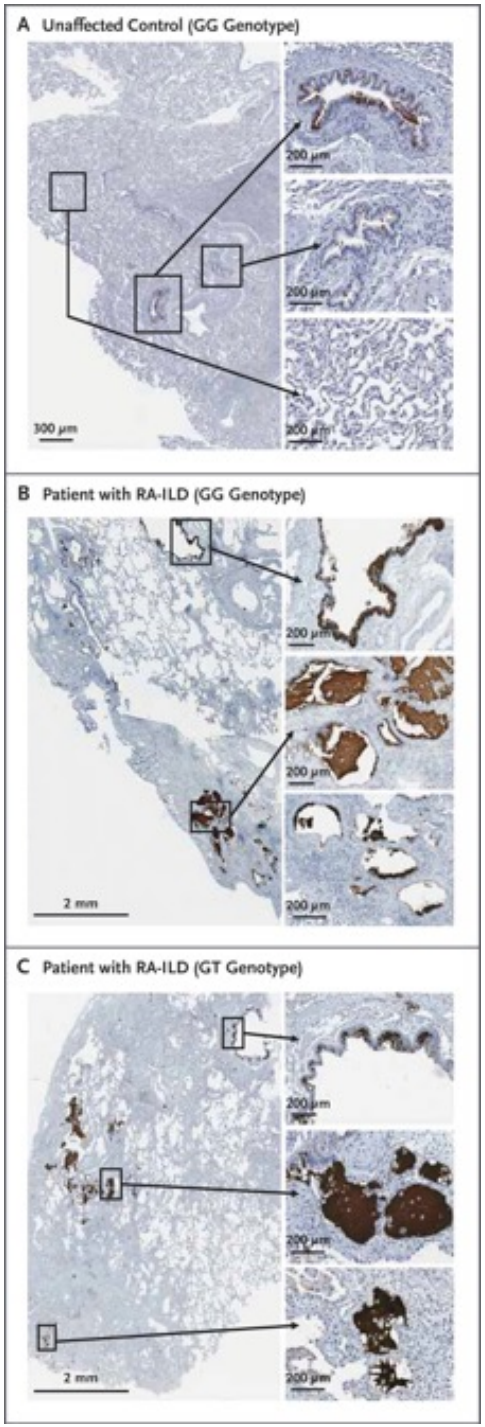

MUC5B Expression in Explanted Lung Tissue from Patients with RA-ILD and an Unaffected Control. Shown are representative lung-tissue images from an unaffected control with a GG genotype (Panel A), a patient with RA-ILD and a GG genotype (Panel B), and a patient with RA-ILD and a GT genotype (Panel C). Panel A includes a low-power view (left) of normal lung, top and middle insets with a high-power view of bronchiole with MUC5B staining, and a bottom inset with a high-power view of alveolar epithelia. Panels B and C each include a low-power view (left) of the UIP pattern in explanted lung tissue, a top inset with a high-power view of bronchiole with MUC5B staining, and middle and bottom insets with a high-power view of MUC5B staining in metaplastic epithelia lining honeycomb cysts and MUC5B staining of mucus in honeycomb cysts.

Similar to observations of MUC5B expression in the lungs of persons with idiopathic pulmonary fibrosis, staining of the lung tissue of patients with RA-ILD showed MUC5B in the cytoplasm of bronchioles and in areas of microscopic honeycombing, including in the metaplastic epithelia lining the honeycomb cysts and mucus within cysts, which presumably produce mucus containing MUC5B. MUC5B expression was limited to mucus and the epithelium in the bronchioles in unaffected controls and in patients with desquamative interstitial pneumonia.

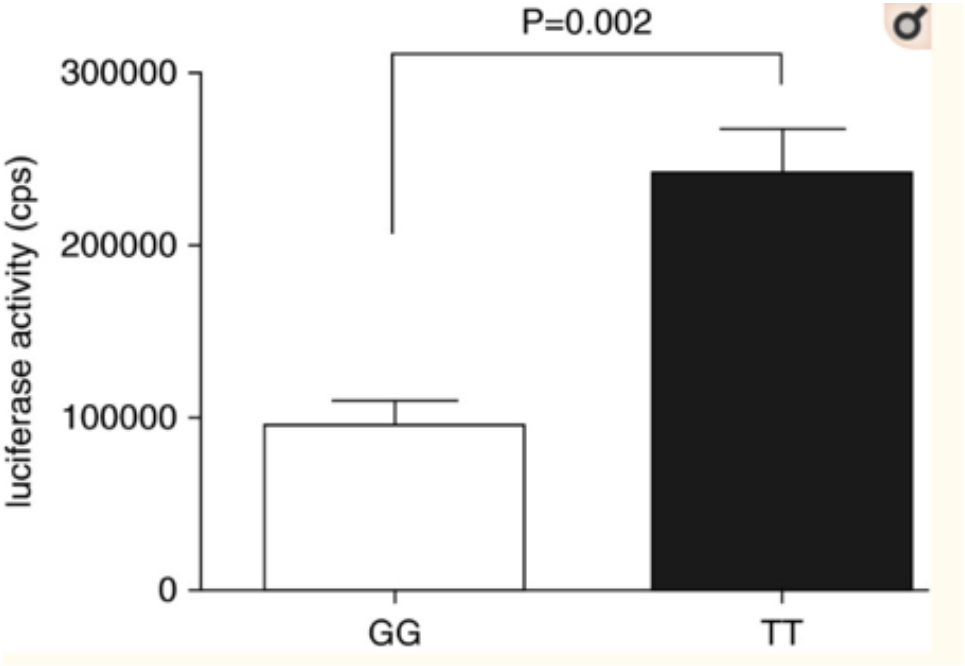

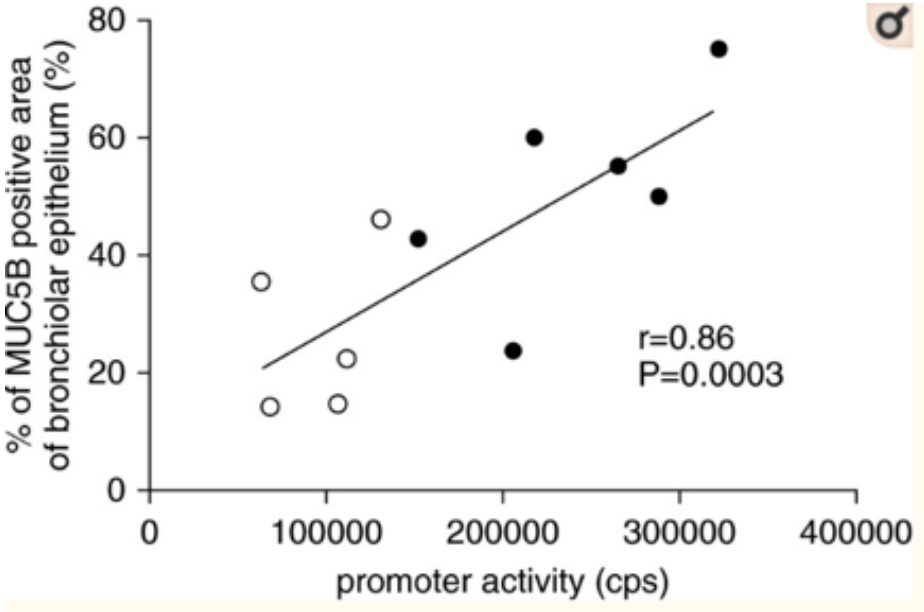

Effects of site-directed mutagenesis of the *MUC5B* promoter variant. *MUC5B* promoter activity of the TT group was significantly higher than that of the GG group in the A549 cell line. Correlation between *MUC5B* promoter activity and percentage of MUC5B-positive area of the small airway epithelium in idiopathic pulmonary fibrosis lung. *Solid circles* represent GG samples, and *open circles* represent TT samples.

Discussion

We found that the *MUC5B* promoter variant rs35705950, the strongest genetic risk factor for idiopathic pulmonary fibrosis, was also a strong risk factor for RA-ILD, especially among patients with evidence of a UIP pattern on imaging. The effect of the *MUC5B* promoter variant on the development of ILD in patients with RA was similar in magnitude and direction to that observed in patients with idiopathic pulmonary fibrosis. However, the *MUC5B* promoter variant does not appear to be a risk factor for the development of RA, a finding supported by previous genomewide association studies involving patients with RA.[31] In aggregate, our results suggest that RA consists of genetic subphenotypes and that the *MUC5B* promoter variant is associated with an increased risk of RA-ILD.

Our work on understanding the genetic architecture of RA-ILD has resulted in several observations. First, RA-ILD is a complex genetic phenotype, with the minor allele of the *MUC5B* promoter variant rs35705950 identified as a risk factor for the disease. The point estimates for the association of the *MUC5B* promoter variant with RA-ILD are equivalent to those observed with idiopathic pulmonary fibrosis and are substantively higher than those for the most common other risk factors for RA-ILD, including cigarette smoking and the human leukocyte antigen locus for RA. Second, our findings, together with those of others, suggest that the *MUC5B* promoter variant is a risk factor for the UIP pattern in general. Third, our findings suggest that the *MUC5B* promoter variant could be used to detect preclinical ILD in patients with RA. Fourth, non-*MUC5B* risk variants for idiopathic pulmonary fibrosis might also contribute to the genetic background of RA-ILD. Given the shared genetic background between idiopathic pulmonary fibrosis and RA-ILD in general and RA-ILD with a UIP or possible UIP pattern in particular, we would propose that drugs that are known to be effective in treating patients with idiopathic pulmonary fibrosis be evaluated in the treatment of RA-ILD

Ein Kleinzelliges Bronchialkarzinom (small-cell lung cancer, SCLC) ist eine Form von Lungenkrebs, die sehr schnell wächst. Es bilden sich auch schon früh Tochtergeschwülste (Metastasen) in anderen Körperregionen. Deshalb ist ein Kleinzelliges Bronchialkarzinom sehr gefährlich. Lesen Sie hier, wie häufig das SCLC ist und wie es behandelt wird! Als kleinzelliges Bronchialkarzinom, kurz SCLC, bezeichnet man ein Bronchialkarzinom, das bei mikroskopischer Betrachtung aus kleinen Zellen (APUD-Zellen) besteht. APUD steht für "Amine Precursor Uptake and Decarboxylation" und ist die veraltete Bezeichnung für endokrin wirksame Zellen, die sich außerhalb der endokrinen Organe in den Epithelien anderer Organsysteme befinden. Etwa 25% aller Bronchialkarzinome sind kleinzellige BC. Es ist meist zentral in der Lunge lokalisiert.

Durch lymphogene und hämatogene Metastasierung kommt es frühzeitig zu einer Tumoraussaat in Gehirn, Knochen, Leber und Nebennierenrinde.

Da es sich um endokrine (hormonausschüttende) Zellen handelt, kann der Tumor Hormone produzieren, die unter physiologischen Umständen nicht in der Lunge gebildet werden. Dies führt zur Entstehung eines so genannten paraneoplastischen Syndroms. So kann z.B. durch die ACTH-Produktion eines kleinzelligen Bronchialkarzinoms ein Cushing-Syndrom entstehen.

Als paraneoplastische Begleiterscheinung des kleinzelligen Bronchialkarzinoms kann ebenfalls ein Lambert-Eaton-Syndrom (PLEMS) auftreten - in einigen Fällen lange, bevor der Tumor klinisch manifest wird.

Das kleinzellige Bronchialkarzinom ist in der überwiegenden Zahl der Fälle leider zum Zeitpunkt der Diagnosestellung bereits metastasiert (besonders ins Gehirn, Knochen, Leber, Nebennieren) und daher inoperabel.

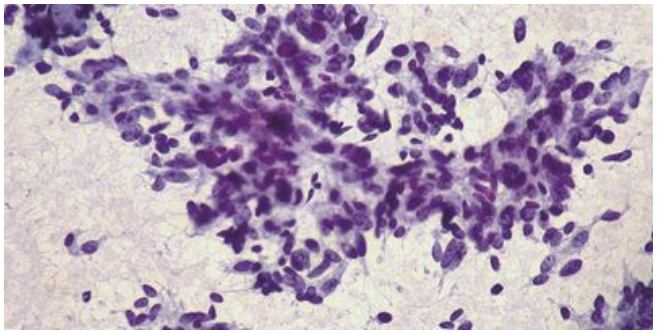

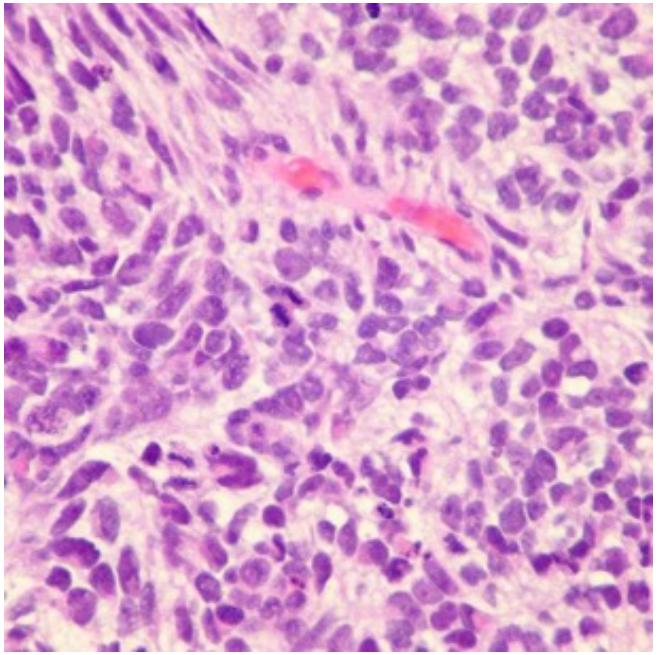

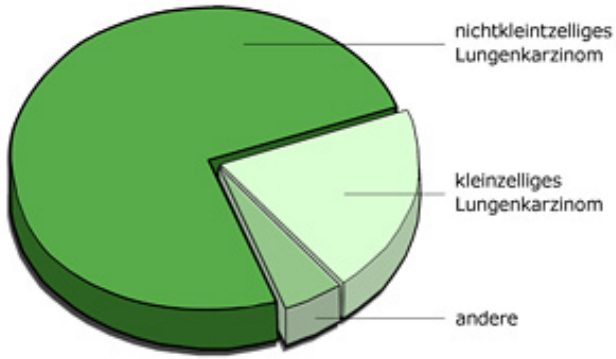

First-Line Atezolizumab plus Chemotherapy in Extensive-Stage Small-Cell Lung Cancer

Enhancing tumor-specific T-cell immunity by inhibiting programmed death ligand 1 (PD-L1)–programmed death 1 (PD-1) signaling has shown promise in the treatment of extensive-stage small-cell lung cancer. Combining checkpoint inhibition with cytotoxic chemotherapy may have a synergistic effect and improve efficacy. We conducted this double-blind, placebo-controlled, phase 3 trial to evaluate atezolizumab plus carboplatin and etoposide in patients with extensive-stage small-cell lung cancer who had not previously received treatment. Patients were randomly assigned in a 1:1 ratio to receive carboplatin and etoposide with either atezolizumab or placebo for four 21-day cycles (induction phase), followed by a maintenance phase during which they received either atezolizumab or placebo (according to the previous random assignment) until they had unacceptable toxic effects, disease progression according to Response Evaluation Criteria in Solid Tumors, version 1.1, or no additional clinical benefit. The two primary end points were investigator-assessed progression-free survival and overall survival in the intention-to-treat population.

Characteristic	Atezolizumab Group (N=201)	Placebo Group (N=202)
Median age (range) — yr	64 (28–90)	64 (26–87)
Age group — no. (%)		
<65 yr	111 (55.2)	106 (52.5)
≥65 yr	90 (44.8)	96 (47.5)
Male sex — no. (%)†	129 (64.2)	132 (65.3)
ECOG performance-status score — no. (%)†‡		
0	73 (36.3)	67 (33.2)
1	128 (63.7)	135 (66.8)
Smoking status — no. (%)		
Never smoked	9 (4.5)	3 (1.5)
Current smoker	74 (36.8)	75 (37.1)
Former smoker	118 (58.7)	124 (61.4)
Brain metastasis at enrollment — no. (%)†	17 (8.5)	18 (8.9)
Blood-based tumor mutational burden — no./total no. (%)§		
<10 mutations/Mb	71/173 (41.0)	68/178 (38.2)
≥10 mutations/Mb	102/173 (59.0)	110/178 (61.8)
<16 mutations/Mb	133/173 (76.9)	138/178 (77.5)
≥16 mutations/Mb	40/173 (23.1)	40/178 (22.5)
Median sum of longest diameter of target lesions at baseline (range)	113.0 (12.0–325.0)	105.5 (15.0–353.0)
Previous anticancer treatments — no. (%)		
Chemotherapy or nonanthracycline¶	8 (4.0)	12 (5.9)
Radiotherapy	25 (12.4)	28 (13.9)
Cancer-related surgery	33 (16.4)	25 (12.4)

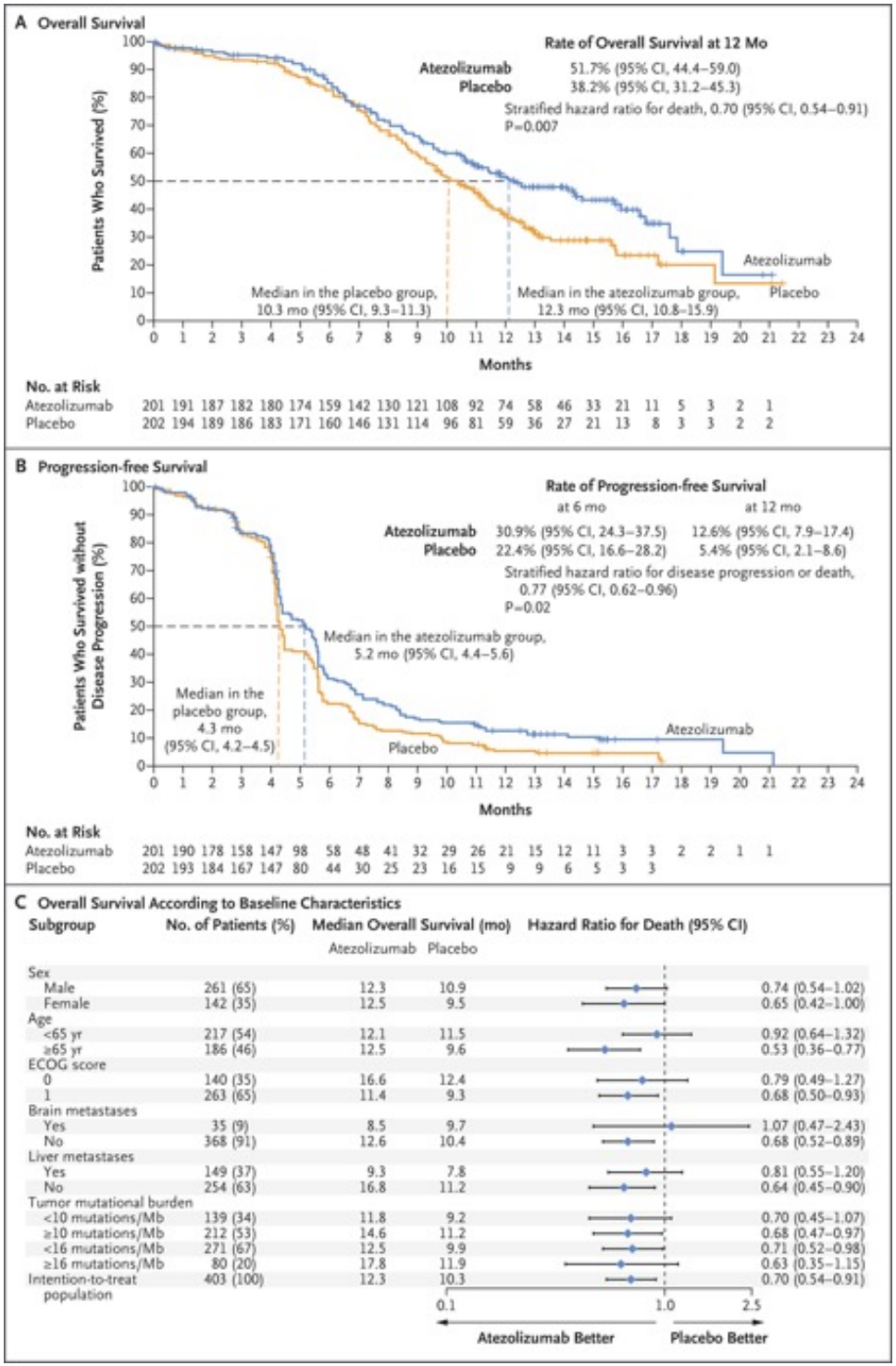

Overall Survival and Investigator-Assessed Progression-free Survival in the Intention-to-Treat Population.

Panel A shows the Kaplan–Meier estimates of overall survival, and Panel B the Kaplan–Meier estimates of investigator-assessed progression-free survival. Tick marks indicate censored data. Panel C shows a subgroup analysis of overall survival according to baseline characteristics. Eastern Cooperative Oncology Group (ECOG) performance-status scores range from 0 to 5, with higher scores reflecting greater disability. Tumor mutational burden was assessed with the use of a blood-based assay.

Variable	Atezolizumab Group (N = 201)	Placebo Group (N = 202)
Objective confirmed response†	121 (60.2 [53.1–67.0])	130 (64.4 [57.3–71.0])
Complete response — no. (% [95% CI])	5 (2.5 [0.8–5.7])	2 (1.0 [0.1–3.5])
Partial response — no. (% [95% CI])	116 (57.7 [50.6–64.6])	128 (63.4 [56.3–70.0])
Median duration of response (range) — mo‡	4.2 (1.4§–19.5)	3.9 (2.0–16.1§)
Ongoing response at data cutoff — no./total no. (%)	18/121 (14.9)	7/130 (5.4)
Stable disease — no. (% [95% CI])	42 (20.9 [15.5–27.2])	43 (21.3 [15.9–27.6])
Progressive disease — no. (% [95% CI])	22 (10.9 [7.0–16.1])	14 (6.9 [3.8–11.4])

Event	Atezolizumab Group (N = 198)			Placebo Group (N = 196)		
	Grade 1 or 2	Grade 3 or 4	Grade 5	Grade 1 or 2	Grade 3 or 4	Grade 5
	number of patients (percent)					
Any adverse event	73 (36.9)	112 (56.6)	3 (1.5)	68 (34.7)	110 (56.1)	3 (1.5)
Adverse events with an incidence of ≥10% in any grade category or events of grade 3 or 4 with an incidence of ≥2% in either group						
Neutropenia	26 (13.1)	45 (22.7)	1 (0.5)	20 (10.2)	48 (24.5)	0
Anemia	49 (24.7)	28 (14.1)	0	41 (20.9)	24 (12.2)	0
Alopecia	69 (34.8)	0	0	66 (33.7)	0	0
Nausea	62 (31.3)	1 (0.5)	0	58 (29.6)	1 (0.5)	0
Fatigue	39 (19.7)	3 (1.5)	0	37 (18.9)	1 (0.5)	0
Decreased neutrophil count	7 (3.5)	28 (14.1)	0	12 (6.1)	33 (16.8)	0
Decreased appetite	39 (19.7)	2 (1.0)	0	26 (13.3)	0	0
Thrombocytopenia	12 (6.1)	20 (10.1)	0	14 (7.1)	15 (7.7)	0

Discussion

At the time of the primary analysis of progression-free survival and the interim analysis of overall survival, this randomized, placebo-controlled, phase 3 trial showed that the addition of atezolizumab to carboplatin and etoposide resulted in significantly longer overall and progression-free survival than chemotherapy alone. The median overall survival was 2 months longer in the atezolizumab group than in the placebo group, and the 1-year overall survival rate was approximately 13 percentage points higher in the atezolizumab group than in the placebo group (51.7% vs. 38.2%). Benefits with respect to overall survival and progression-free survival were consistent across patient subgroups. Objective response rates and median duration of response were similar in the two groups; however, more patients in the atezolizumab group than in the placebo group had an ongoing response at the time of data cutoff. In addition, a single-group, phase 2 study of maintenance pembrolizumab in extensive-stage small-cell lung cancer did not show longer progression-free survival or overall survival when compared with historical data. In contrast, the current trial showed a significant improvement in progression-free survival and overall survival with the addition of atezolizumab to chemotherapy as first-line treatment. This suggests that combining checkpoint inhibition with cytotoxic therapy during induction may be beneficial and potentially necessary to improve overall survival beyond that seen with the current standard of care, and thus it may be a preferred treatment approach over maintenance checkpoint-inhibitor therapy alone. Further studies directly comparing the two treatment approaches are needed.

In summary, this multinational trial in the first-line treatment of extensive-stage small-cell lung cancer in a patient population typical for this disease showed that the addition of atezolizumab to carboplatin and etoposide was associated with significantly longer overall survival and progression-free survival, with a safety profile consistent with the defined toxic effects of the individual agents.

Laktation ist der Fachausdruck für die Milchabgabe von Säugetieren, einschließlich der Abgabe von Frauenmilch beim Menschen. Die Milchabsonderung erfolgt über die Milchdrüsen und fängt für gewöhnlich nach der Geburt an. Zwei bis acht Tage nach der Geburt beginnt die Ausschüttung der Muttermilch (Laktation), zuerst unter hormonellem Einfluss (plötzlich verminderte Östrogen- und Gestagenspiegel, vermehrte Produktion von Prolaktin aus der Hypophyse), dann reflektorisch durch den Saugreiz des Kindes, der – ebenfalls aus der Hirnanhangdrüse – die Ausschüttung des Hormons Oxytocin bewirkt. Unter Einfluss von Oxytocin kontrahieren sich auch die Myoepithelzellen um die milchbildenden Drüsenbläschen (Alveolen), sodass die Milch während des Stillens aktiv ausgetrieben wird. Prolaktin oder Prolactin (PRL), auch laktotropes Hormon (LTH), Lactotropin oder Laktotropin genannt, ist ein Hormon, das in den laktotropen Zellen (azidophil, ca. 20 % der Adenohypophyse) im Hypophysenvorderlappen gebildet wird und vor allem für das Wachstum der Brustdrüse im Verlauf der Schwangerschaft und für die Milchsekretion (Laktation) während der Stillzeit verantwortlich ist, und ferner psychische Funktionen besitzt. Bei der Hündin ist Prolaktin in der zweiten Hälfte des Zyklus (auch in der Trächtigkeit) für den Erhalt des Gelbkörpers zuständig.

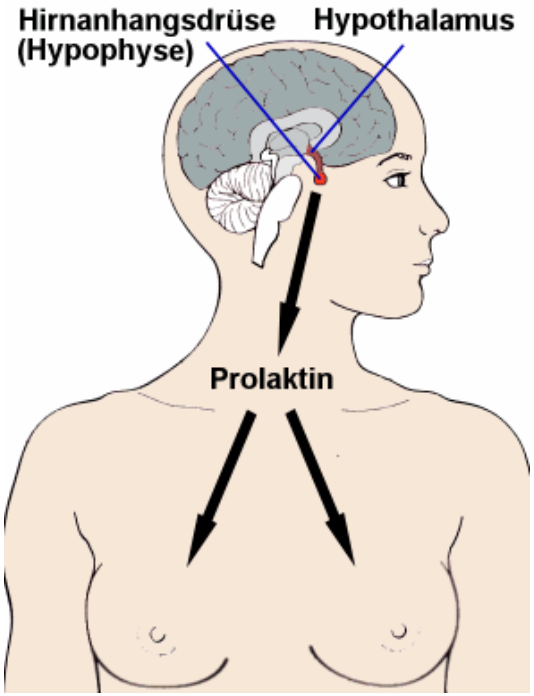

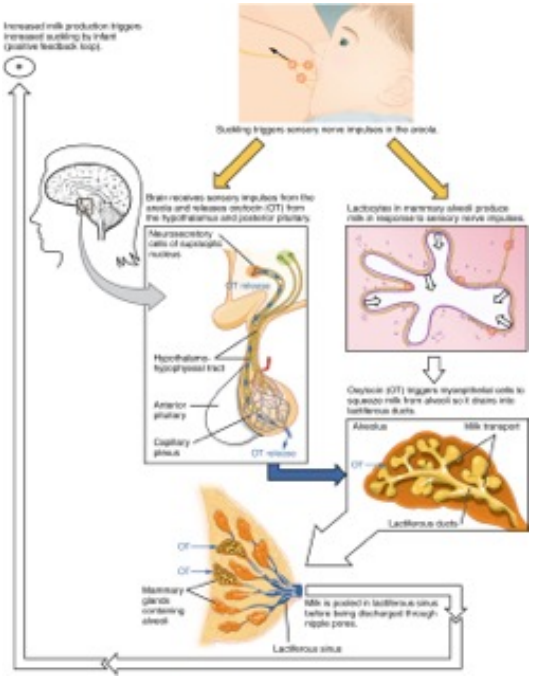

Variant Prolactin Receptor in Agalactia and Hyperprolactinemia

A loss-of-function variant in the gene encoding the prolactin receptor (*PRLR*) was reported previously in a woman with persistent postpartum galactorrhea; however, this paradoxical phenotype is not completely understood. Here we describe a 35-year-old woman who presented with idiopathic hyperprolactinemia that was associated with a complete lack of lactation after each of her two deliveries. She is a compound heterozygote for loss-of-function variants of *PRLR*. Her unaffected parents are heterozygotes. These findings are consistent with previous work showing that mice deficient in functional *Prlr* do not lactate.

Prolactin, a pituitary hormone, plays diverse roles in vertebrates; its known roles in humans are in the processes of lactation and reproduction. A loss-of-function variant in the gene encoding the prolactin receptor (*PRLR*) has been reported in a proband with persistent postpartum galactorrhea and hyperprolactinemia. The proband and her two sisters were heterozygous for a missense variant (H212R). The proband received dopamine agonist therapy to terminate the persistent galactorrhea after all (four) of her deliveries. She and a sister were oligomenorrheic; her other sister was infertile.

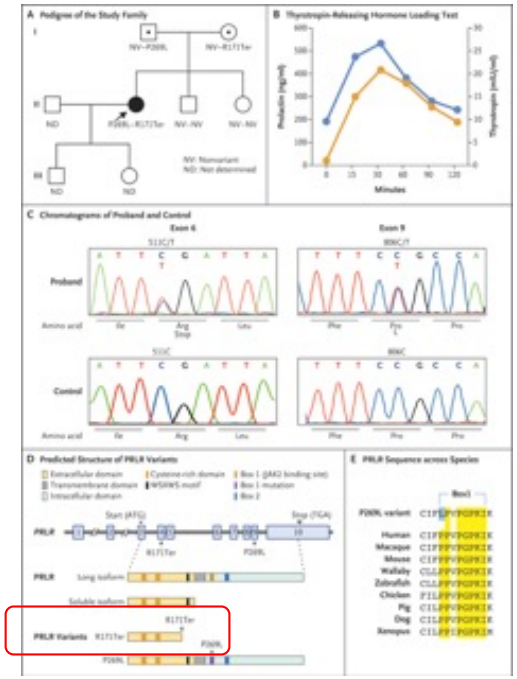

Panel A shows the pedigree of the family, with *PRLR* genotypes identified by bidirectional sequencing. Squares indicate male persons, and circles female persons. The arrow indicates the proband. The open symbols, dotted symbols, and solid symbols represent nonvariant, heterozygote, and compound heterozygote for mutations, respectively. Panel B shows serum levels of prolactin (blue) and thyrotropin (orange) after loading 500 µg of synthetic thyrotropin-releasing hormone. Panel C shows chromatograms obtained by direct sequencing of polymerase-chain-reaction products. Arg denotes arginine, Ile isoleucine, Leu leucine, Phe phenylalanine, and Pro proline. Panel D shows a schematic representation of the *PRLR*, full-length complementary DNA, and protein-domain structure. Variants and the predicted effect on protein are also shown. Panel E shows the alignment of the PRLR sequence across species. The conserved sequence is indicated by a yellow background; the P269L variant is highlighted in blue.

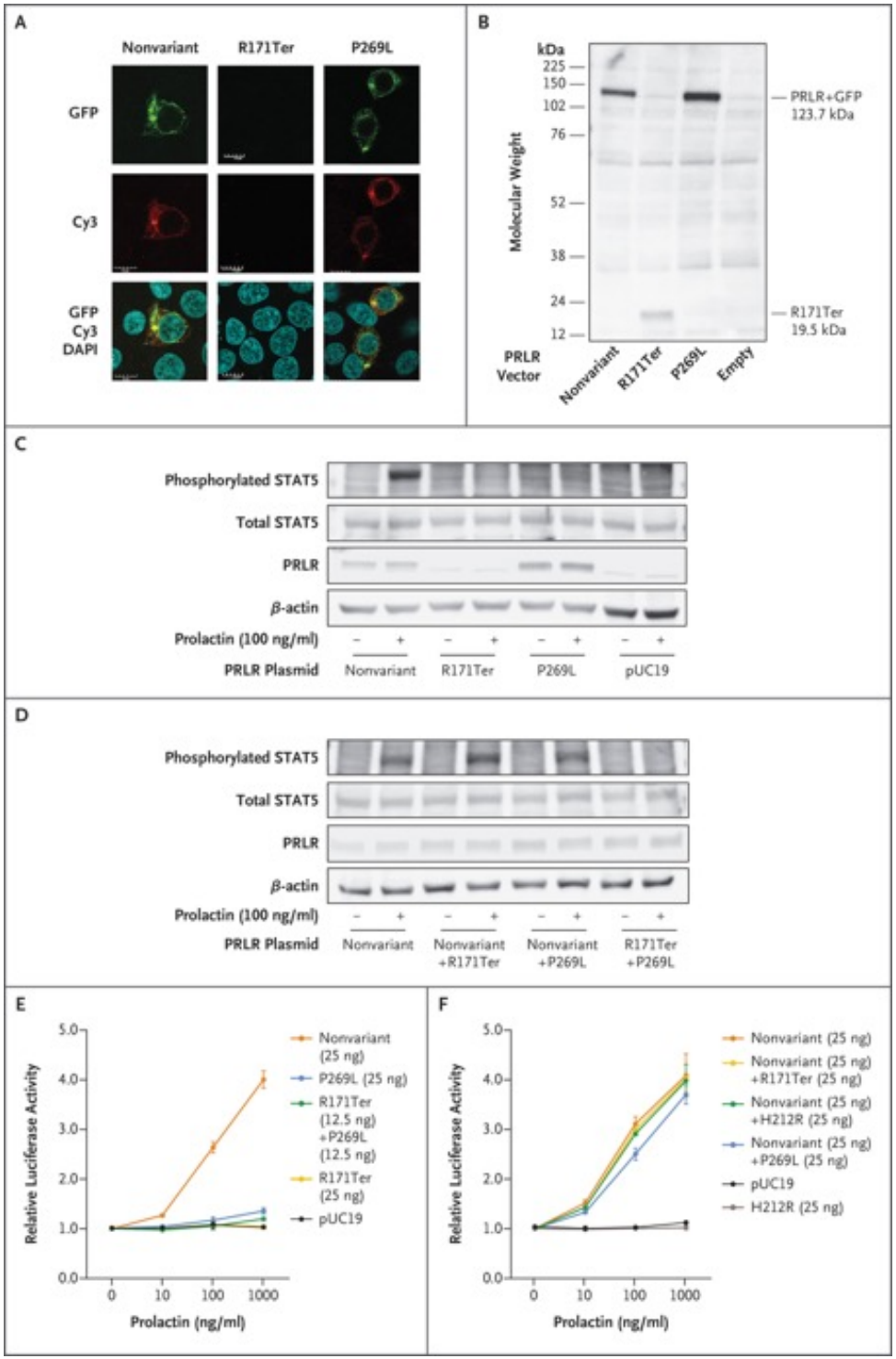

Expression and Function of the Variants in PRLR.

Panel A shows expression of the prolactin receptor (PRLR). Human embryonic kidney (HEK) 293T cells were transiently transfected with a vector carrying nonvariant or variant *PRLR* sequences with a *GFP* tag. Confocal imaging detected the signals for green fluorescent protein (GFP) (top row) and Cy3 (middle row). The bottom row shows the superimposition of GFP, Cy3, and 4′,6-diamidino-2-phenylindole (DAPI) staining. Panel B shows a Western blot analysis of nonvariant and variant receptors expressed by HEK 293T cells. At 24 hours after transfection, HEK 293T cells were lysed and blotted with the use of anti-PRLR antibody. Panel C shows a Western blot analysis to detect STAT5 phosphorylation in HEK 293T cells on exposure to prolactin. HEK 293T cells were incubated with prolactin (100 ng per milliliter) for 30 minutes, 24 hours after transfection with plasmids carrying nonvariant *PRLR*, R171Ter *PRLR*, P269L *PRLR*, or pUC19 (1.6 μg DNA per well on a six-well plate). Panel D shows a Western blot analysis to detect functional interactions on the basis of STAT5 phosphorylation status after exposure to prolactin by HEK 293T cells expressing different types of PRLR. Panel E shows the dose–response curve of the gene encoding cytokine-inducible SRC homology 2 domain protein (CISH) promoter luciferase reporter in HEK 293T cells transfected with plasmids carrying nonvariant *PRLR*, variant *PRLR*, or pUC19. Panel F shows the results of a CISH assay to query the effect of variant receptor on the function of nonvariant receptor.

Here we describe a woman with compound heterozygous germline inactivating variants of *PRLR* and hyperprolactinemia associated with postpartum agalactia. Biochemical data indicate that the variants negatively affect the prolactin receptor signaling pathway. Although we report the results of a single patient who may have other genetic variants (other than those in *PRLR*) that affect lactation, our data are consistent with the notion that signal transduction by means of the prolactin receptor is essential for lactation in humans. Our data are also consistent with possibility that reduced lactation during breast-feeding is caused by heterozygous loss-of-function variants. The proband's mother, who was heterozygous for the R171Ter variant, reportedly had "insufficient" lactation. Similarly, mice that are heterozygous for a *Prlr* null allele have shown diminished lactation. That being said, we cannot rule out the possibility that insufficient lactation by the proband's mother was a coincidental symptom and unrelated to the allelic status of *PRLR.* Our data support the idea that loss of prolactin receptor signaling does not disturb fertility in humans. The proband's parents, who are heterozygotes, were fertile. The proband, who is a compound heterozygote, had normal gonadotropin secretion, had a normal menstrual cycle, and was fertile, although the first pregnancy was achieved by means of intrauterine insemination after 1 year of trying to conceive without medical assistance.

The results of our study involving a woman who was a compound heterozygote for loss-of-function mutations in *PRLR* and had agalactia associated with hyperprolactinemia would suggest that only lactation (and not other biologic functions) is dependent on prolactin–PRLR signaling, although further study is required in order to test this hypothesis.

Mapping Symptoms to Brain Networks with the Human Connectome

The study of focal brain lesions has traditionally been used to map neurologic symptoms to specific regions; however, many neurologic and psychiatric symptoms correspond more closely to networks of connected regions. A new resource termed the human connectome, derived from functional neuroimaging of thousands of healthy persons, provides a map of these brain connections. With the use of the connectome, lesions in different locations that cause the same symptom can be linked to common networks in ways not previously possible. This approach, termed lesion network mapping, is being applied to lesions associated with a variety of neuropsychiatric symptoms, including hallucinations, delusions, abnormal movements, pain, coma, and cognitive or social dysfunction. Connectome localizations may expose new treatment targets for patients with complex neurologic and psychiatric symptoms. To appreciate this new approach to symptom localization, it is helpful to understand the evolution of classic lesion localization, functional imaging, the human brain connectome, and the analytic method of lesion network mapping.

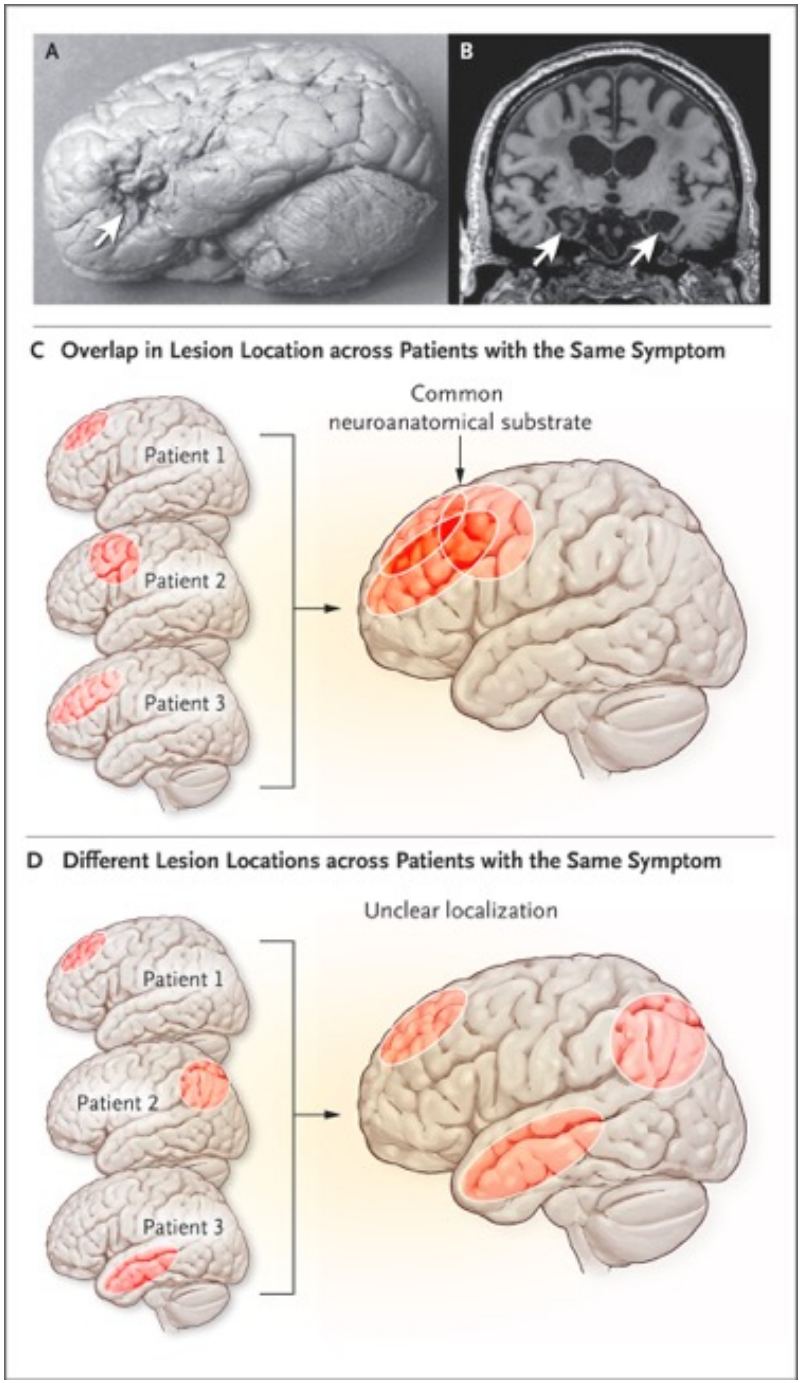

Symptom Localization from Focal Brain Lesions. Shown are index cases in which focal brain lesions (arrows) caused impairment in language (in Patient Tan)[6] (Panel A) or memory (in Patient H.M.)[7] (Panel B). Overlap in lesion location across patients with the same symptom (Patient 1 through Patient 3) can identify a common neuroanatomical substrate (arrow) (Panel C). In practice, lesions that cause the same symptom often occur in different locations, so localization remains unclear (Panel D).

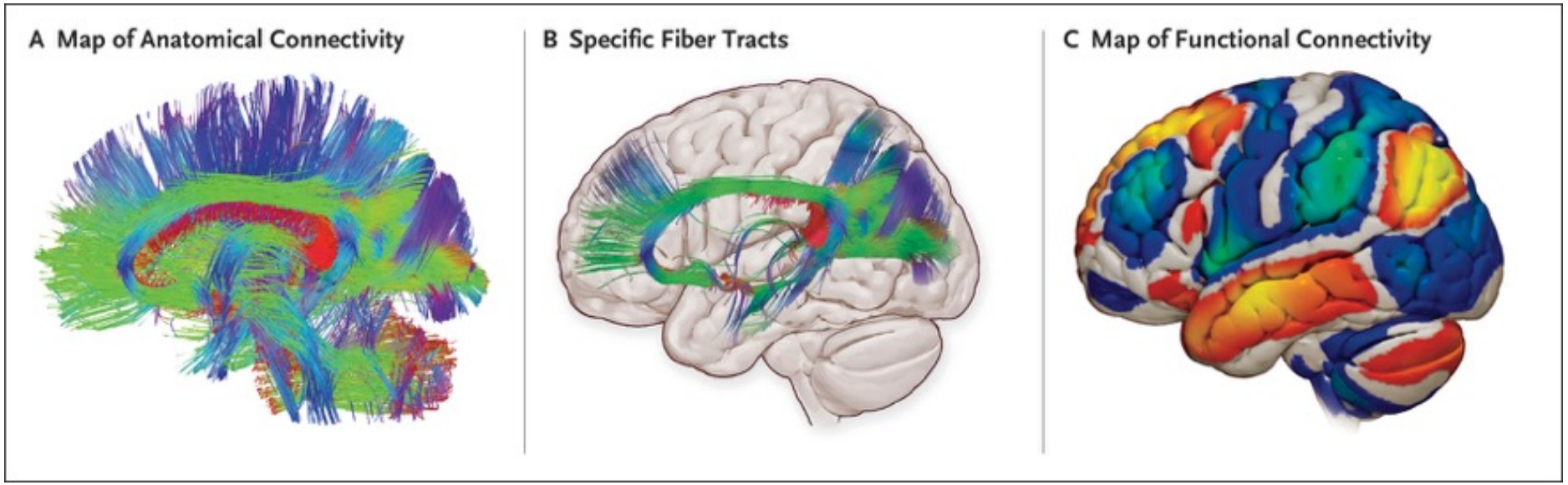

The Human Brain Connectome. Current human brain maps of anatomical connectivity (Panel A) can be used to isolate specific fiber tracts, such as those passing through the posterior cingulate (Panel B). Maps of functional connectivity can be used to identify brain regions with spontaneous activity that is positively correlated (yellow or red) or negatively correlated (blue or green) with any other region, such as the posterior cingulate (Panel C).

Functional neuroimaging

Functional neuroimaging can detect regional changes in brain metabolism, blood flow, blood oxygenation, water diffusion, and electrical activity. Because these physiological changes can be identified in regions that appear anatomically intact, neuroimaging can localize symptoms in patients who have no structural brain lesions. Functional neuroimaging has been particularly useful in the analysis of psychiatric symptoms, such as auditory hallucinations, anxiety, and depression, in which changes in the activity of certain regions may direct attention to potential treatment targets for these symptoms. Two types of connectivity have been explored. Anatomical connectivity is derived from MRI sequences that are sensitive to water diffusion. These reconstructed fiber diagrams correspond reasonably well to postmortem human studies and anatomical tracing studies in nonhuman primates. Functional connectivity is derived from MRI sequences that are sensitive to spontaneous fluctuations in blood oxygenation, an indirect marker of neuronal activity.

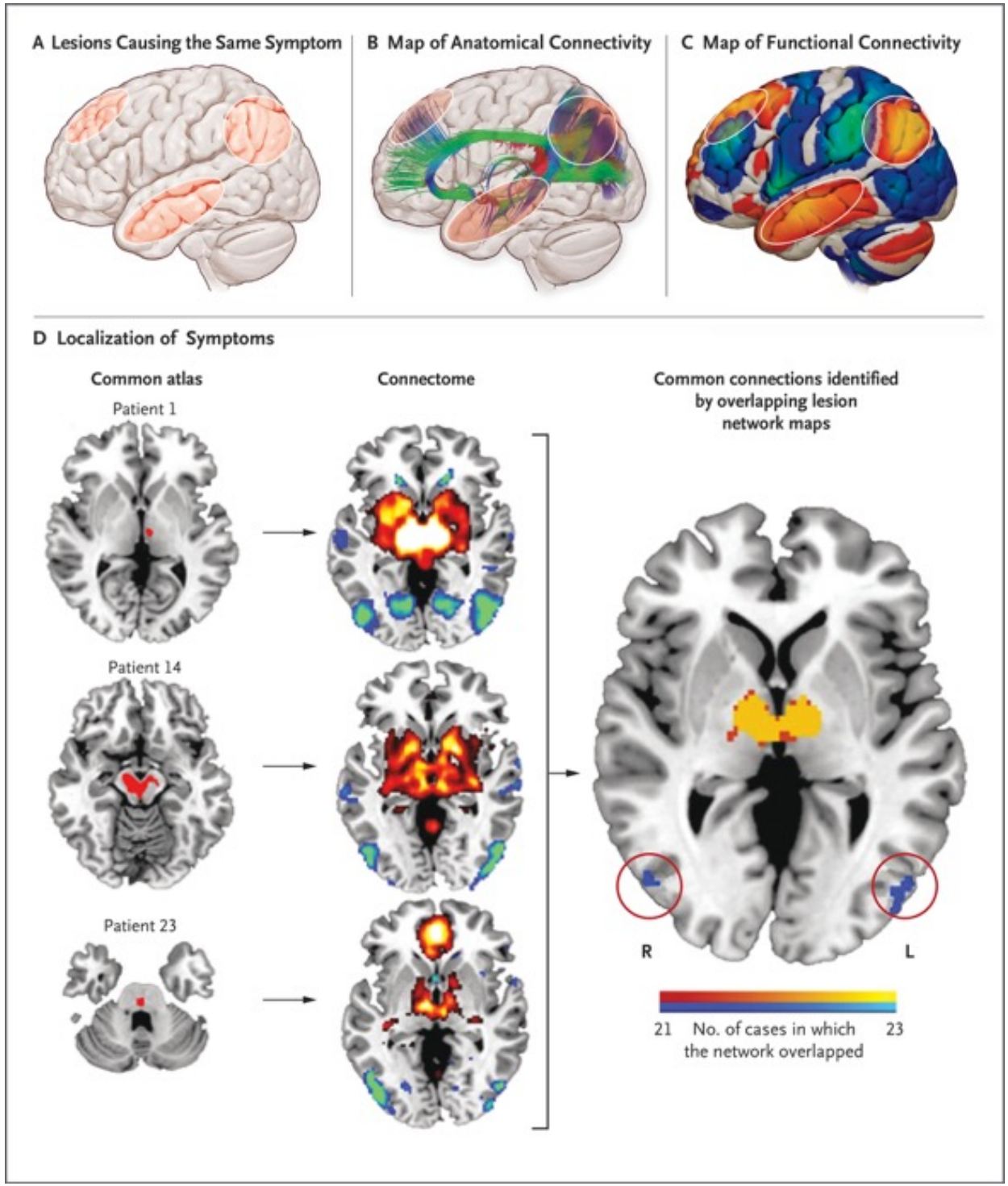

Using the Human Brain Connectome to Localize Symptoms from Focal Brain Lesions.

Lesions that cause the same symptom but occur in different brain locations (Panel A) can be overlaid on a map of anatomical connectivity (Panel B) or functional connectivity (Panel C) to determine whether they are part of the same connected brain network. With lesion network mapping, lesion locations from different patients that cause the same symptom are traced on a common atlas (Panel D, left column). Functional connectivity between each lesion location and the rest of the brain is computed with the use of the connectome (Panel D, middle column). Lesion network maps can then be overlapped to identify common connections (Panel D, right column). In this example, lesion locations that cause visual hallucinations are functionally connected to a part of the brain involved in visual imagery (red circles).

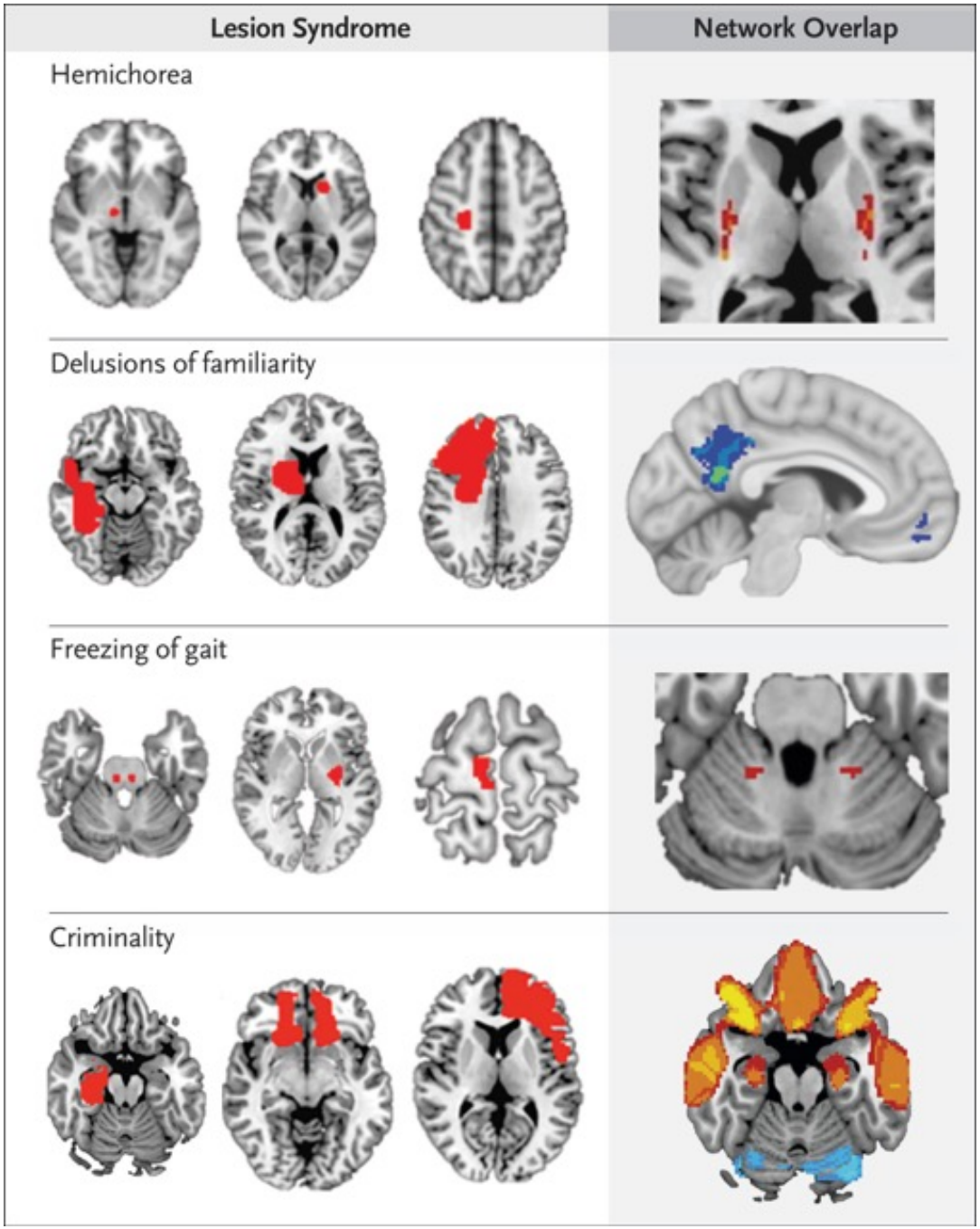

Lesion Network Mapping of Neuropsychiatric Symptoms with Unknown Localization.

Many symptoms are caused by lesions in different locations (three examples for each symptom are shown in red). However, more than 90% of lesion locations that cause the same symptom are functionally connected to the same brain regions (right column). Lesion locations that cause hemichorea are connected to the posterolateral putamen, a region implicated in motor control. Lesion locations that cause delusions of familiarity are connected to the retrosplenial cortex, a region activated by familiar stimuli. Lesion locations that cause freezing of gait are connected to the dorsal medial cerebellum, a region activated by locomotion tasks. Lesion locations that are associated with criminality are connected to the orbitofrontal cortex, a region activated by moral decision making.

Clinical Applications of Lesion Network Mapping

Lesion network mapping is anticipated to identify new symptom-based treatment targets. As a measure of face validity of network mapping to identify treatment targets, some of these targets align with those previously derived through other methods that have led to effective treatment. For example, the extrastriate visual cortex has been targeted with transcranial magnetic stimulation (TMS), a tool to noninvasively alter brain activity, to reduce visual hallucinations; the supplementary motor area, part of the lesion network associated with hemichorea, has been targeted with TMS for relief of chorea in Huntington's disease; and the leg area of motor cortex, part of the gait network, has been targeted with TMS for relief of freezing of gait in Parkinson's disease. Whether new therapeutic targets for symptoms such as delusions or criminality will prove useful are testable hypotheses. It also remains unknown whether these targets will be more useful for patients with brain lesions or, as in the above-mentioned TMS trials, for patients with similar symptoms but without overt structural brain damage.

Therapeutic targets may also be identified through network mapping of lesion locations that alleviate or prevent symptoms. For example, network mapping of spontaneous lesions that relieved tremor identified a therapeutic target in the thalamus that has been effective for tremor relief. Brain stimulation sites can also be incorporated into this type of analysis in order to identify connections that are common to stimulation sites that provide therapeutic benefit. This approach has identified previously unappreciated connections that predict response to deep-brain stimulation in Parkinson's disease, predict response to TMS in depression, and link stimulation sites in different locations that are effective for the same symptom.

Bacterial Vaginosis and Desquamative Inflammatory Vaginitis

Vaginal symptoms are remarkably common. In the United States, vaginal infections are among the 25 most common medical reasons for which women consult a physician, resulting in 5 million to 10 million office visits per year. Vaginal infections affect a woman's quality of life by causing frustration, anxiety, sexual dysfunction, and vulvovaginal discomfort. In addition to direct health care costs associated with the management of vaginal infections, there are indirect costs related to adverse reproductive health consequences. An abnormal vaginal microbiome, or vaginal dysbiosis, which characterizes bacterial vaginosis and desquamative inflammatory vaginitis, has been linked to adverse pregnancy outcomes, pelvic inflammatory disease, an increased risk of sexually transmitted infections, and other reproductive health problems, such as a poor outcome of in vitro fertilization (IVF).

Table 1. Diagnostic Findings in Vaginal Secretions from Women with Healthy Vaginal Flora, Women with Bacterial Vaginosis, and Women with Desquamative Inflammatory Vaginitis.

Variable	Healthy Vaginal Flora	Bacterial Vaginosis	Desquamative Inflammatory Vaginitis
pH	<4.7	≥4.7	≥4.7
Amine odor	Negative	Positive	Negative
Clue cells	Absent	Present	Absent
Epithelial cells	Mature squamous cells	Mature squamous cells	Immature parabasal cells
Neutrophils	Absent	Absent	Present
Flora	Sparse monomorphic bacilli	Abundant polymorphic coccobacilli	Abundant polymorphic cocci and bacilli
Microbiome	Lactobacilli	*Gardnerella vaginalis*, *Atopobium vaginae*, others	*Escherichia coli*, group B streptococci, others
CST*	I, II, V	III, IV	IV

* Community state type (CST) I is dominated by *Lactobacillus crispatus*, CST II by *L. gasseri*, CST III by *L. iners*, and CST V by *L. jensenii*; CST IV is composed of a polymicrobial mixture of strict and facultative anaerobes.[8]

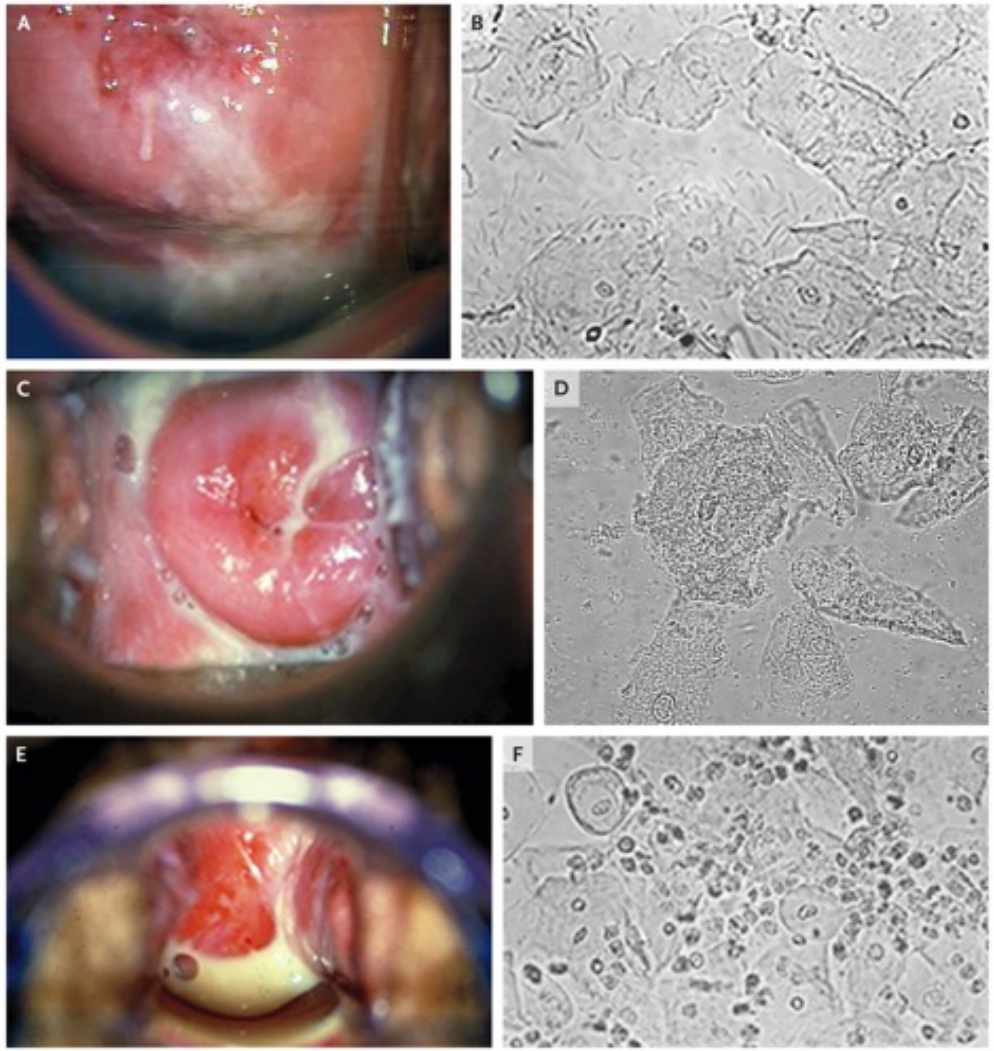

Features of Healthy Vaginal Flora, Bacterial Vaginosis, and Desquamative Inflammatory Vaginitis. Panel A shows healthy cervicovaginal mucosa and a small amount of vaginal discharge, findings that are consistent with a predominance of lactobacilli. Physiological cervical ectopy and clear cervical mucus are evident. In Panel B, microscopic examination of a wet-mount preparation shows rodlike bacteria, which are consistent with lactobacilli. No leukocytes are present. Panels C and D show the features of bacterial vaginosis: heavy, milky, homogeneous vaginal discharge with bubbles (Panel C), which are consistent with gaseous by-products of anaerobic bacteria, and vaginal epithelial cells covered by coccobacilli on microscopic examination (Panel D), a feature of clue cells. No leukocytes are present. Panels E and F show the features of desquamative inflammatory vaginitis: heavy, yellowish vaginal discharge and inflamed cervicovaginal mucosa (Panel E), with microscopic examination showing a high number of leukocytes (with a predominance of mononuclear leukocytes) and round parabasal cells (Panel F), findings that are consistent with inflammation.

Diagnosis

The validation of two standardized, reproducible diagnostic tests for bacterial vaginosis that are based on the use of vaginal swabs has been an important development. One test is laboratory-based Gram's staining for vaginal flora; the other is a bedside, wet-mount microscopic test for vaginal clue cells. Clue cells are epithelial squamous cells covered by coccobacilli in the absence of rods; an absence of rods indicates an absence of lactobacilli. These tests have been introduced into clinical practice and are widely used to determine whether bacterial vaginosis is present. A vaginal pH of less than 4.7 provides an easy-to-read cutoff value for distinguishing between normal flora and bacterial vaginosis and is used to rule out bacterial vaginosis.

Pathogenesis

Bacterial vaginosis can be considered a biofilm infection, with a dense polymicrobial biofilm consisting primarily of *G. vaginalis* adhering to the vaginal epithelium. An *A. vaginae* biofilm is always present with a *G. vaginalis* biofilm, and higher bacterial loads of *G. vaginalis* and *A. vaginae* increase the probability of biofilm formation. The vaginal biofilm appears to create a favorable anaerobic environment for other obligate anaerobic bacteria. An important finding related to upper genital tract complications is that half of women with bacterial vaginosis also have a bacterial vaginosis–associated biofilm covering the endometrium.

Bacterial Vaginosis and Other Sexually Transmitted Infections

Bacterial vaginosis is associated with not only the acquisition but also the transmission of other sexually transmitted infections, especially human immunodeficiency virus (HIV) infection. In women with bacterial vaginosis, CD4 T cells are recruited to the lower genital tract mucosa. Among HIV-infected women, the quantity of HIV in vaginal secretions from women with bacterial vaginosis is increased substantially, as compared with HIV in vaginal secretions from women without bacterial vaginosis.

Overall Disease Burden

Bacterial vaginosis has a large variety of sequelae in the upper genital tract, including increased risks of preterm birth, first-trimester miscarriage in women undergoing IVF, amniotic-fluid infection, chorioamnionitis, endometritis after childbirth or abortion, and infections after hysterectomy, as well as pelvic inflammatory disease, both in general and after abortion.

Table 2. Treatment Guidelines for Bacterial Vaginosis.*

Treatment	Regimen
Recommended treatments	
Metronidazole	500 mg orally twice a day for 7 days
Metronidazole 0.75% gel	One applicator (5 g) intravaginally once a day for 5 days
Clindamycin 2% cream	One applicator (5 g) intravaginally at bedtime for 7 days
Alternative treatments	
Tinidazole	2 g orally once a day for 2 days
Tinidazole	1 g orally once a day for 5 days
Clindamycin	300 mg orally twice a day for 7 days
Clindamycin ovules	100 mg intravaginally at bedtime for 3 days

* The guidelines are from the Centers for Disease Control and Prevention.[58]

Desquamative Inflammatory Vaginitis

Desquamative inflammatory vaginitis is a newly recognized clinical syndrome characterized by persistent purulent vaginal discharge and vaginal erythema, often with submucosal cervicovaginal petechiae. Inflammation is the cardinal feature of this disorder, which has also been called idiopathic inflammatory vaginitis. Donders and colleagues have recently reviewed the literature on this inflammatory vaginitis, which they call “aerobic vaginitis.“ However, the term “desquamative inflammatory vaginitis” holds priority and was first introduced in 1965 by Gray and Barnes. The term “aerobic vaginitis” was introduced in 2002 in reference to a disease entity caused by an abnormal vaginal microbiome genomically defined as CST IV. The published literature on desquamative inflammatory vaginitis is still surprisingly limited, consisting mainly of retrospective case series or short reviews.

Cause

The exact cause of desquamative inflammatory vaginitis is unknown but appears to be a dysbiosis of the normal vaginal microbiome associated with inflammation. In desquamative inflammatory vaginitis, the vagina is colonized with facultative bacteria, not the obligate anaerobic bacteria that colonize the vagina in bacterial vaginosis. The microflora in desquamative inflammatory vaginitis typically consist of *Escherichia coli*, *Staphylococcus aureus*, group B streptococcus, or *Enterococcus faecalis*. The microbiome associated with desquamative inflammatory vaginitis is less well understood than the bacterial vaginosis microbiome. Desquamative inflammatory vaginitis may also represent a systemic inflammatory syndrome that produces vaginal inflammation, resulting in abnormal vaginal flora.

Symptoms and Signs

Clinical manifestations of desquamative inflammatory vaginitis include purulent vaginal discharge and a strong inflammatory reaction. The vaginal discharge is homogeneous and yellowish, with no fishy smell. Vulvar irritation and vaginal mucosal erythema with ecchymotic lesions or erosions are present in severe cases. Symptoms may last for a long time and fluctuate, suggesting a chronic or recurrent natural history.

Diagnosis

Microscopic examination of wet-mount preparations of vaginal secretions reveals an increase in inflammatory cells and parabasal epithelial cells and, and vaginal flora are usually abnormal, with an elevated pH. The point-of-care diagnosis is based on the presence of an increased number of leukocytes and parabasal epithelial cells. Microscopic examination of wet-mount preparations is the preferred diagnostic method for desquamative inflammatory vaginitis, since Gram’s staining of vaginal flora does not discriminate between bacterial vaginosis and desquamative inflammatory vaginitis. The use of routine vaginal cultures is not recommended.

Table 3. Treatment Recommendations for Desquamative Inflammatory Vaginitis.*

Treatment	Regimen
Recommended treatments	
Clindamycin 2% cream	Intravaginally daily at bedtime for 1 to 3 wk; consider maintenance therapy once or twice a week for 2–6 mo
Topical glucocorticoid	
Hydrocortisone, 300–500 mg	Intravaginally daily at bedtime for 3 wk; consider maintenance therapy once or twice a week for 2–6 mo
Clobetasol propionate	Intravaginally daily at bedtime for 1 wk (duration not evidence-based)
Additional recommended treatments†	
Fluconazole	150 mg orally once a week as maintenance therapy
Topical vaginal estrogen	Twice a week

* The recommendations are from Reichman and Sobel.[65] Official treatment guidelines for desquamative inflammatory vaginitis have not been developed.
† Additional recommended treatments are for use in combination with clindamycin or one of the glucocorticoids.

Conclusions and Future Research Directions

The human vaginal ecosystem is highly dynamic. The vaginal microbiome can affect host physiology, and host physiology can affect the vaginal microbiome. Research is needed for a better understanding of the interactions among the vaginal microbiome, host physiology, reproduction, and host defense. Recent genomic research has increased our knowledge of the vaginal microbiome. Future research based on genomic, proteomic, and metabolomic techniques may ultimately have a major effect on women's reproductive health. The mechanisms that initiate and maintain colonization with vaginal lactobacilli, especially *L. crispatus*, in women of reproductive age need to be elucidated. New biomarkers for an abnormal vaginal microbiome are needed for clinical practice.

A lesion in the liver

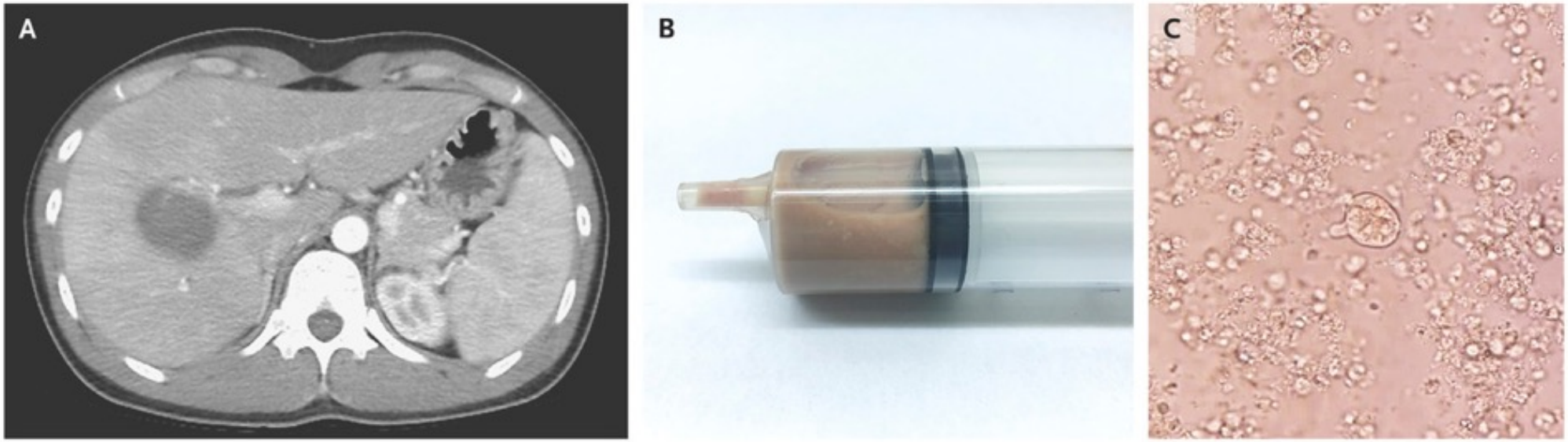

A 29-year-old man infected with the human immunodeficiency virus presented to the emergency department with a 2-day history of fever and pain in the right upper quadrant of the abdomen. His most recent CD4 cell count was 520 per microliter. Laboratory results showed an aspartate aminotransferase level of 208 IU per liter (reference range, 10 to 42), an alanine aminotransferase level of 467 IU per liter (reference range, 10 to 40), and a total bilirubin level of 2.4 mg per deciliter (reference range, 0.2 to 1.0). Computed tomography of the abdomen performed after the administration of contrast material revealed a ring-enhancing lesion in the liver that was suggestive of an abscess (Panel A). A reddish-brown material was obtained on percutaneous drainage of the abscess (Panel B). Microscopic examination revealed unicellular organisms with pseudopods (Panel C). An indirect hemagglutination test for antiamebic antibodies was positive, at a titer of 1:256. A polymerase-chain-reaction assay of stool confirmed infection with *Entamoeba histolytica. E. histolytica* infections result from the ingestion of amebic cysts. Contaminated food or water is typically the source. Metronidazole was administered for 2 weeks and was followed by 10 days of treatment with paromomycin to eliminate intracolonic cysts. The patient's fever and abdominal pain subsided 2 days after the initiation of treatment, and the liver abscess had decreased in size on follow-up abdominal ultrasonography. At a 90-day follow-up visit, the patient had no further symptoms.

Overcoming the Barrier

A 74-year-old man presented to the emergency department with jaundice. Three days earlier, his wife had noted yellow discoloration of his eyes and skin, which was followed by progressive lethargy, confusion, and subjective fevers. He had mild pain in the right upper quadrant that was constant and unrelated to meals. He reported no neck stiffness, chest pain, cough, dyspnea, abdominal distention, changes in bowel habits, dysuria, or rash.

The patient's medical history included hypertension, diabetes, hyperlipidemia, and gout. Three years earlier, he had undergone a laparoscopic cholecystectomy for acute cholecystitis. The procedure was complicated by a common bile duct injury for which he subsequently underwent a hepaticojejunostomy. After this procedure, there was a sustained elevation in the alkaline phosphatase level, which ranged from 262 to 462 U per liter (normal range, 31 to 95). His medications included metformin, glyburide, simvastatin, metoprolol, and allopurinol. He had no history of tobacco, alcohol, or illicit-substance use. He had never traveled outside the northeastern United States.

The patient's temperature was 38.0° C, heart rate 88 beats per minute, blood pressure 157/81 mm Hg, respiratory rate 12 breaths per minute, and oxygen saturation 99% while he was breathing ambient air. He appeared ill. His skin was jaundiced. A cardiopulmonary examination was normal. He had a midline laparotomy scar and mild tenderness in the right upper quadrant. There was no abdominal distention or hepatosplenomegaly. There was no palmar erythema, gynecomastia, spider angiomas, or edema in the legs or feet. He was unable to spell "world" backward, which indicated impaired attention; he had no asterixis, and the remainder of his neurologic examination was normal.

The white-cell count was 11,800 per cubic millimeter, hemoglobin level 11.2 g per deciliter, mean corpuscular volume 99.6 fl, and platelet count 450,000 per cubic millimeter. The basic metabolic panel was normal. The alanine aminotransferase level was 68 U per liter (normal range, 12 to 60), aspartate aminotransferase 84 U per liter (normal range, 17 to 42), and alkaline phosphatase 313 U per liter (normal range, 31 to 95). The total bilirubin level was 8.2 mg per deciliter (140 μmol per liter) (normal range, 0.2 to 1.3 mg per deciliter [3.4 to 22.2 μmol per liter]), direct bilirubin level 4.6 mg per deciliter (79 μmol per liter) (normal level, <0.8 μmol per deciliter [14 μmol per liter]), international normalized ratio (INR) 1.1, and albumin level 3.6 g per deciliter.

Ultrasonography of the right upper quadrant revealed a 3-cm complex cystic lesion in the right hepatic lobe. There was no biliary dilatation, ascites, portal-vein or hepatic-vein thrombosis, or radiographic evidence of cirrhosis. During the next 5 hours, the patient became more disoriented and lethargic. A repeat white-cell count was 32,000 per cubic millimeter, with 85% neutrophils, 8% bands, 4% lymphocytes, 2% monocytes, and 1% basophils. The platelet count was 122,000 per cubic millimeter. His blood sample was reported by the laboratory as hemolyzed; therefore, the serum hemoglobin level and biochemical test results were not available. A peripheral-blood smear showed vacuolated neutrophils with toxic granulations and Döhle bodies, polychromasia, anemia, and mild thrombocytopenia. There were no schistocytes, spherocytes, bite cells, or intracellular organisms. Computed tomography (CT) of the head without contrast enhancement was normal.

CT of the abdomen and pelvis without contrast enhancement revealed a 3.6-cm, air-containing cavity in the posterior right hepatic lobe consistent with a hepatic abscess. The white-cell count increased to 34,700 per cubic millimeter, the platelet count was 136,000 per cubic millimeter, and the INR was 1.5; no other serum test results were available because the blood sample was again reported as hemolyzed. A urinalysis showed 1+ protein, 4+ blood, and 2 red cells and 7 white cells per high-power field. Vancomycin and a combination of piperacillin and tazobactam were administered. General surgery and interventional radiology services were consulted for drainage of the hepatic abscess.

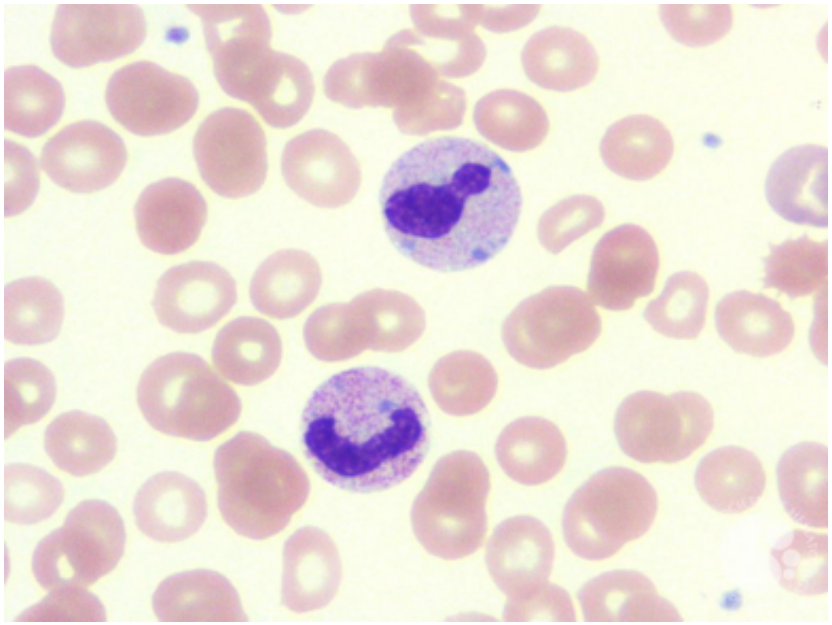

Döhle-Körperchen sind helle blau-graue, oval geformte, basophile Einschlusskörperchen im Pr otoplasma neutrophiler Granulozyten. Die Döhle-Körperchen können unter anderem bei der May-Hegglin-Anomalie, bei Verbrennungen und bestimmten Infektionen (Scharlach, Fleckfieber, Pneumonie), sowie dem Chediak-Higashi-Syndrom diagnostiziert werden.

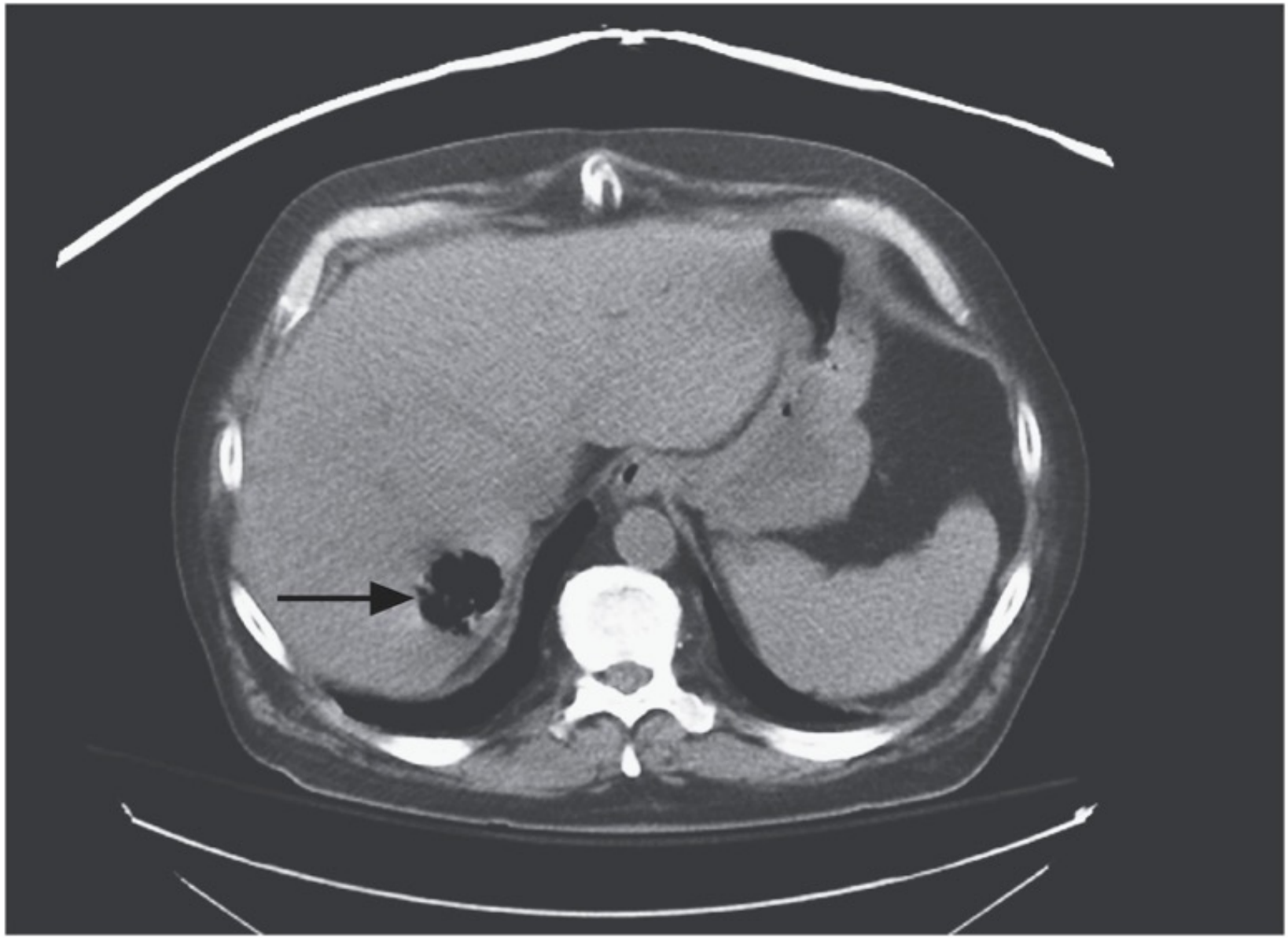

CT Scan of Abdomen and Pelvis without Contrast Enhancement. A computed tomographic (CT) scan of the abdomen and pelvis without contrast enhancement shows a 3.6-cm air-containing cavity (arrow) in the posterior right hepatic lobe, a finding consistent with a hepatic abscess.

The patient had severe respiratory distress that led to intubation and mechanical ventilation. Shortly thereafter, hypotension developed, for which he received four vasopressors. His condition was deemed to be too unstable for surgical intervention. Another blood sample was hemolyzed. Gram's staining of his blood cultures revealed gram-positive rods. Refractory pulseless electrical activity ensued, and the patient died 10 hours after presentation. His blood cultures subsequently grew C. perfringens.

Centrifuged Blood Samples at Time of Presentation and after Presentation. The patient's centrifuged blood sample at the time of presentation (Panel A) shows a normal appearance. The yellow layer (*) represents plasma. The middle white layer (+) represents gel from the collection tube. The bottom red layer (^) reflects the clotting of red cells. The patient's third centrifuged blood sample (Panel B) lacks the yellow plasma layer shown in Panel A. The red discoloration of the top layer (#) represents free hemoglobin (from hemolysis) that has mixed with plasma.

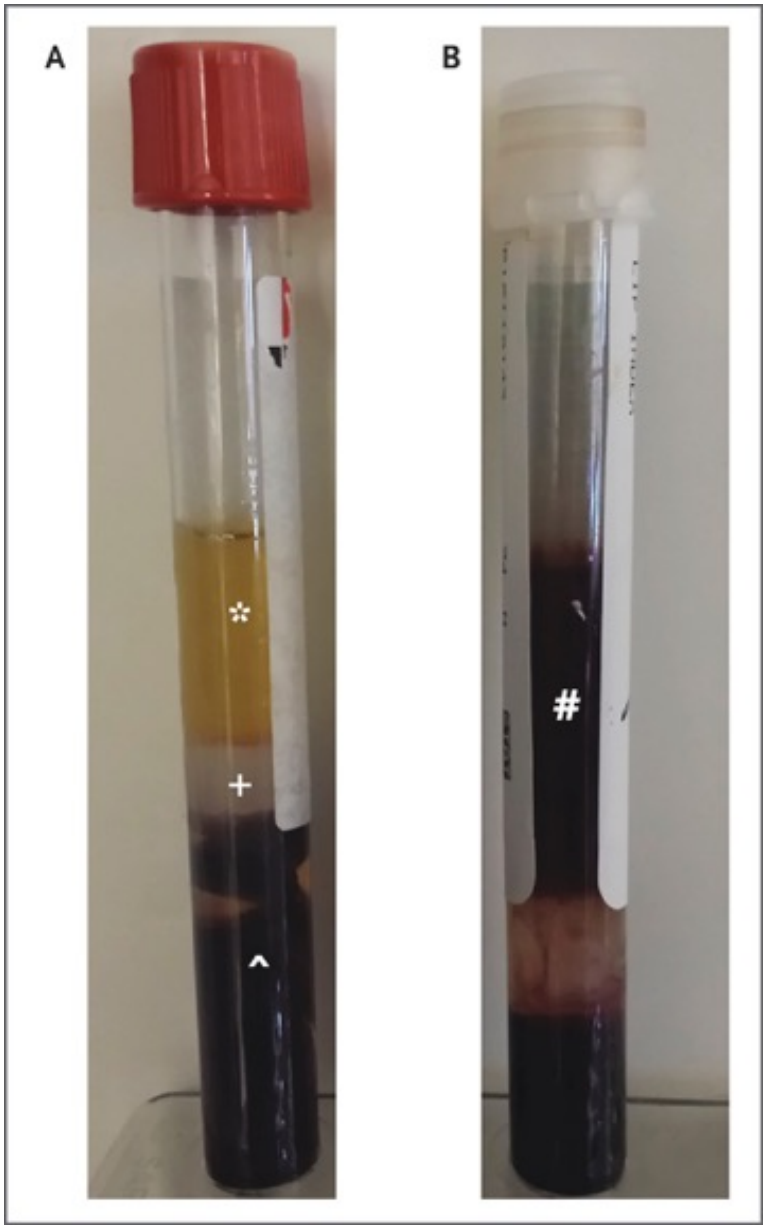

Pyogenic liver abscesses are generally caused by the *Streptococcus anginosus* group, anaerobic gram-negative bacilli (e.g., bacteroides), *Pseudomonas aeruginosa*, *Escherichia coli*, or *Klebsiella pneumoniae*; up to 30% of such abscesses are polymicrobial. Streptococcus species are the most common pathogens in the United States, whereas klebsiella is the predominant organism in Asia. Features in this patient that favored a pyogenic liver abscess over an amebic liver abscess were his advanced age, jaundice, and diabetes mellitus and the fact that he had not traveled to regions where *Entamoeba histolytica* is endemic. A liver abscess caused by *C. perfringens* is rare. Risk factors include diabetes mellitus, gastrointestinal cancer, and cirrhosis. Most patients present with fever and abdominal pain, although some patients have no localizing symptoms. In one case series involving 20 patients with *C. perfringens* liver abscesses, all the patients had evidence of intravascular hemolysis at presentation and had rapid growth of *C. perfringens* in the blood.

C. perfringens is a spore-forming, anaerobic gram-positive bacillus that is a commensal organism of the gastrointestinal and gynecologic tracts and is also found ubiquitously in soil. Ten different exotoxins have been described and account for the spectrum of clinical manifestations associated with this organism. Ingestion of a preformed enterotoxin results in self-limited *C. perfringens* gastroenteritis. The remainder of *C. perfringens* diseases involve endogenous spore germination and toxin production, which are facilitated by anaerobic conditions (e.g., penetrating trauma or ischemic bowel). The most common example is clostridial myonecrosis, a necrotizing infection of the muscle and soft tissues that usually involves a limb.

A pink tinge develops in mild hemolysis, whereas a reddish-brown color is seen with severe hemolysis, reflecting the higher concentration of free hemoglobin. Increasingly, automated instruments on chemical and coagulation analyzers measure the plasma concentration of free hemoglobin to make this assessment. In vitro hemolysis usually results from factors associated with collection of the blood, such as the prolonged application of a tourniquet, the use of small-bore needles, and sampling from intravenous catheters instead of performing direct venipuncture. Issues with the transport, processing, and storage of blood samples account for a smaller fraction of in vitro hemolysis.

Distinguishing in vitro from in vivo hemolysis can be challenging. In both cases, blood test results will show increased potassium and lactate dehydrogenase levels, characteristics that reflect the release of these intracellular components into the serum. In vivo hemolysis is suggested by lactic acidosis, reticulocytosis, indirect hyperbilirubinemia, schistocytes on the peripheral smear, or free hemoglobin in the urine, which can be inferred from a high degree of heme positivity on a urine dipstick without red cells on microscopy.

Mentor (griechisch Μέντωρ) ist eine Gestalt aus der griechischen Mythologie.
Er ist in Homers Odyssee der Sohn des Alkimos aus Ithaka. Als Odysseus in den trojanischen Krieg aufbricht, übergibt er seinen Sohn Telemachos und seinen Hausstand Mentor, seinem Freund und Altersgenossen. Mentor bringt während der Abwesenheit des Odysseus das Treiben der Freier in der Volksversammlung zur Sprache. In die Gestalt Mentors schlüpft immer wieder die Göttin Athena, wenn sie ihrem Schützling Odysseus oder dessen Sohn mit Rat und Tat zur Seite stehen will. So begleitet sie Telemachos in Gestalt des Mentor zu Nestor nach Pylos, als er nach dem Verbleiben seines Vaters forscht, Odysseus selbst macht sie Mut und rüttelt an seiner Ehre, weil er vor dem Kampf mit den Freiern der Penelope zaudert. Im sich ergebenden Konflikt mit den Einwohnern Ithakas vermittelt sie als Mentor den Frieden.
Von der Rolle des Mentor für Telemachos im homerischen Epos leitet sich der Begriff Mentor für einen älteren, klugen und wohlwollenden Berater eines jungen Menschen her.
Mentoring, auch Mentorat, bezeichnet als ein Personalentwicklungsinstrument – insbesondere in Unternehmen, aber auch beim Wissenstransfer in persönlichen Beziehungen – die Tätigkeit einer erfahrenen Person (Mentor). Sie gibt ihr fachliches Wissen oder ihr Erfahrungswissen an eine noch unerfahrenere Person (Mentee oder Protegé) weiter. Ein Ziel ist es dabei, den oder die Mentee bei persönlichen oder beruflichen Entwicklungen zu unterstützen. Bereiche, die in Mentoring-Beziehungen thematisiert werden, reichen von Ausbildung, Karriere und Freizeit bis hin zur Persönlichkeitsentwicklung, Glauben und Spiritualität.

Men's Fear of Mentoring in the #MeToo Era — What's at Stake for Academic Medicine' (Autorinnen = 6 Frauen)

"Me Too" as a slogan to increase awareness about sexual assault dates back about a dozen years, but it has really taken off in the past 2 years as the issue has garnered widespread media attention after dozens of women in the film industry publicly alleged that Hollywood director Harvey Weinstein had engaged in myriad acts of sexual misconduct. #MeToo went viral on social media, and celebrities rallied to launch the Time's Up movement to fight sexual violence and harassment in the workplace. As accusations against other high-profile men surfaced, conversations about sexual harassment and assault shifted to the broader issue of institutionalized sexism and discrimination against women in other industries.

THE OLD BOYS' NETWORK

The problem: Jim has headed up his clinical division for 5 years. He recently hired two excellent young female clinician-researchers — the first women he's ever personally hired. In the past, he made a point of taking new hires out for a beer after work to discuss their new jobs, and he made sure they were invited to join the departmental squash ladder. He worries that if he doesn't do the same for these women they won't fit in as well and might not feel welcomed. He's particularly worried about the beer — what if they got the wrong idea? What if somebody saw them together and it led to gossip?

One recommended approach: Reach out to trusted women leaders to discuss your fears. They can share their experiences, put matters into perspective, and provide potential solutions.

Jim brings up the beer and squash question with a female colleague, and she reminds him that when they started working here, their boss ignored her but took him out to play golf. They reflect on the effect that the old boys' club had on women's inclusion in the division. They discuss how things that are not said or not done can affect the culture of the work environment. She suggests that Jim give the women the option of the traditional one-on-one beer with the boss, both having a joint mentoring session over beer with him, or having a beer with the boss and another mentor of their choice.

At his colleague's suggestion, he also brings up the issue of potential inequitable mentorship for women and other underrepresented groups at their next divisional meeting; the group brainstorms about situations they've encountered, and two senior women give examples of approaches that seem to have worked (or not worked) for their mentees.

Fear as a Social Construct

Conversations about men, women, and mentorship in the #MeToo era illustrate the way we use fear to make sense of our experiences. There is an extensive sociological literature on the nature of fear and its consequences. For thousands of years, humans have responded to fear by creating scapegoats. Groups that are chosen for scapegoating usually lack power and the ability to fight back. Although the reasons for scapegoating vary, fear plays a prominent role. It is part of our everyday lives in an invisible or ambient way.

Moving beyond Fear

Focusing on men's fear deflects attention from the issues that triggered this response in the first place. Being afraid to mentor women is not simply about fearing false accusations of sexual misconduct: it is about discrediting women who speak out against sexual assault and harassment.

BIASED MENTORING

The problem: Spencer is the new physician-in-chief at his hospital. Eating lunch in the food court, he overhears a woman telling colleagues that she was passed over for a leadership position because of gender bias. She can't help but think that taking her mentor's advice to wait until after her maternity leave before assuming a leadership role caused a lag in her promotion, given that her male colleagues are farther along in their careers. Spencer worries: "Am I perceived as sexist or having gender bias when I mentor women?"

One recommended approach: If you're worried about being perceived as sexist, address the fear head-on by initiating an authentic conversation about it with mentees.

Spencer could tell a female mentee that being in a privileged position means that he might not be as sensitive to gender issues as he could be and that he wants to learn from her experiences. He can demonstrate positive intent by being honest and asking her to give him constructive feedback if he says something that might be gendered or seemingly unhelpful to her career. He can tell her that he worries that he might say the wrong thing or be misinterpreted, so in this mentoring relationship, they have to both assume that the other is acting with the best intentions.

Spencer could also shift the power dynamic by characterizing mentorship as a bidirectional relationship. He can express interest in learning about his mentee's current experiences and where she sees herself in the near and more distant future. He can take her lead by asking her to identify ways he can help with her career, while describing what worked for him. He can also ask her how he should give advice in situations where their views of her achievements or capabilities conflict, particularly when the feedback might be perceived as negative. And he can stress the need for patience and open-mindedness.

It also sidelines conversations about the serious consequences for women of limiting their mentorship opportunities, and it threatens to halt progress toward gender equity in leadership roles.

Recommendations for improving gender equity include being transparent in compensation arrangements; supporting universal access to family and medical leave policies; offering leadership-development programs and implicit-bias training; encouraging mentorship and sponsorship programs; and providing flexibility in structuring career paths in academic medicine, with flexible promotions and advancement criteria that reflect the range of responsibilities and unique contributions of female physicians. Among these recommendations, professional guidance and support that encourage self-reflection and address implicit biases toward women are particularly important, because it can be difficult to admit to bias and accept feedback that does not align with our perceptions of our private and professional selves.

PRODUCTIVITY PROBLEMS

The problem: David is the cardiology department chair at an academic medical center. Sarah, an assistant professor in his department, was hired 4 years ago but still has no independent grant support and no published work. A male assistant professor hired at the same time has met these milestones. Sarah had a baby 2 years ago, took 2 months of maternity leave, and has steady day care coverage. David knows he needs to talk to Sarah about her lack of academic productivity, but he's wary of coming off as sexist — and fears that Sarah sees her male colleague's comparative success as the result of discrimination.

One recommended approach: Consider whether expectations are explicit or whether men and women have unequal access to unwritten rules and to mentorship and supervision, then work to correct inequities.

David could examine previous performance reviews to recall what guidance, advice, and mentorship he gave each junior colleague in the past. Was Sarah's lack of productivity pointed out to her previously? Did she have the same mentorship and supervision as her male colleague to increase her chances of obtaining grants? Was she given formal feedback about academic expectations? Are there departmental guidelines outlining expected performance?

If such assistance is in place and all things are equal, David can focus on productivity in his discussion with Sarah and convey that he wants to understand what might be preventing her from meeting expectations. He could assure her that he's there to help her reach her potential, ask what support she needs, and set reasonable timelines moving forward.

If no guidelines exist, then perhaps men are getting more targeted mentorship than women, gaining access to unwritten expectations or rules. People tend to mentor others who remind them of their younger selves, and most of the department leadership is male. David could bring these concerns to his executive committee, which could strategize about improving mentoring for women and create written guidelines on academic expectations. It could also implement a process for negotiating a clock reset for promotion evaluation to accommodate leaves of absence for any reason, such as maternity or elder care.

Die Spondylitis ankylosans, „verbiegende/versteifende Wirbelentzündung“ oder Morbus Bechterew ist eine chronisch entzündliche rheumatische Erkrankung mit Schmerzen und Versteifung von Gelenken. Sie gehört zur Gruppe der Erkrankungen der Wirbelsäulengelenke (Spondylarthropathien) und betrifft vorwiegend die Lenden- und Brustwirbelsäule und die Kreuz-Darmbeingelenke. Außerdem kann es zu Entzündungen der Regenbogenhaut des Auges und selten anderer Organe kommen.
Synonyme sind Bechterewsche Krankheit (nach Wladimir Michailowitsch Bechterew, 1857–1927) oder Bechterew-Strümpell-Marie-Krankheit, ankylosierende Spondylitis, rheumatoide Spondylitis und Spondylarthritis ankylopoetica; das Wort Morbus ist die lateinische (medizinische) Bezeichnung für Krankheit. Seit 2009 ist Morbus Bechterew ein Mitglied der Krankheitsfamilie Axiale Spondyloarthritis (axSpA), welche auch die frühen und weniger ausgeprägten Formen von Morbus Bechterew mit einbezieht. Die „Deutsche Vereinigung Morbus Bechterew e. V.“ spricht von 100.000–150.000 diagnostizierten Fällen in Deutschland. Früher dachte man, Männer seien dreimal so häufig betroffen wie Frauen. Eine Besonderheit ist die enge Assoziation der Erkrankung mit der Präsenz von HLA-B27, einem Histokompatibilitäts-Antigen-Subtyp von dem auf fast allen Körperzellen vorhandenen membrangebundenen Protein HLA-B (Human Leukocyte Antigen).

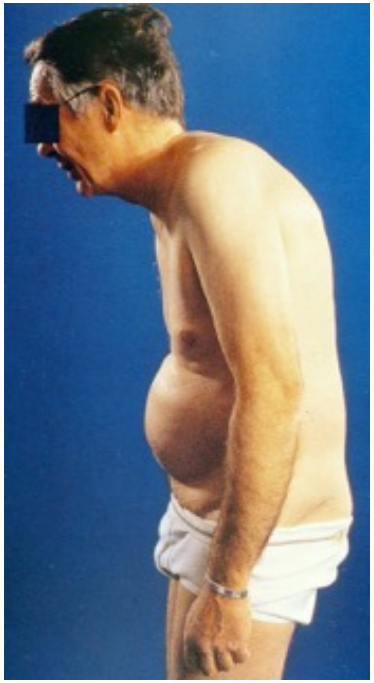

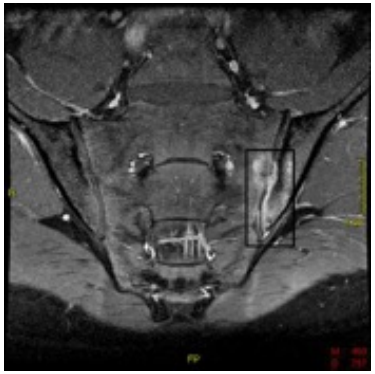

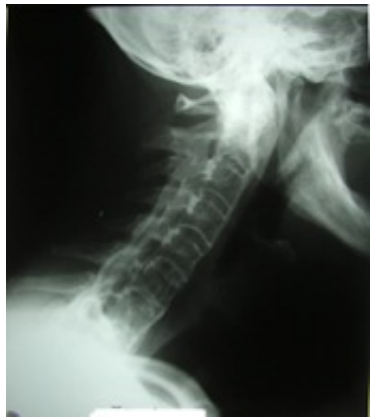

Als Interleukine (von lat/griech. inter = zwischen; leukos = weiß; kinein = sich bewegen) wird eine Gruppe von körpereigenen, kurzkettigen Regulatorproteine (Zytokine) des Immunsystems bezeichnet (IL1-IL38). Interleukine sind Mediatoren für Induktion, Verlauf und Kontrolle der T-Zell-vermittelten zytotoxischen Immunreaktionen sowie der B-Zell-Aktivierung (Antikörperproduktion). Sie werden vorwiegend von stimulierten Leukozyten, Monozyten und Makrophagen gebildet und sezerniert. Bisher sind etwa 38 unterschiedliche Interleukine eindeutig identifiziert. Jedem Zytokin der Interleukingruppe ist nomenklatorisch eine Zahl zu ihrer Klassifikation zugewiesen (IL-1 bis IL-38).
Interleukin-17 ist ein pro-inflammatorisches Zytokin. Es stellt das Signalzytokin des Th17-Zelltyps dar (Interelukin-17-Familie), der mit versch. autoimmunologischrn und nicht-autoimmunologischen Erkrankungen in Verbindung gebracht wird. Die Untereinheit des Interleukin-17, das Interleukin-17A, nimmt bei der Initiierung und Unterhaltung der Immunreaktion bei Psoriasis eine Schlüsselrolle ein. Interleukin-17 wird v.a. durch Lymphozyten vom Typ TH-17 gebildet. Andere Zytokine der Interleukin-17-Familie sind Interleukin-21 und Interleukin-22.
Interleukin-17 ist in seiner biologisch aktiven Form ein Homodimer, dessen Untereinheiten Glykoproteine mit jeweils 155 Aminosäuren sind. IL-17 bindet an seinen Rezeptor IL-17R von dem derzeit 3 Typen bekannt sind: IL17RA, IL17RB, and IL17RC.

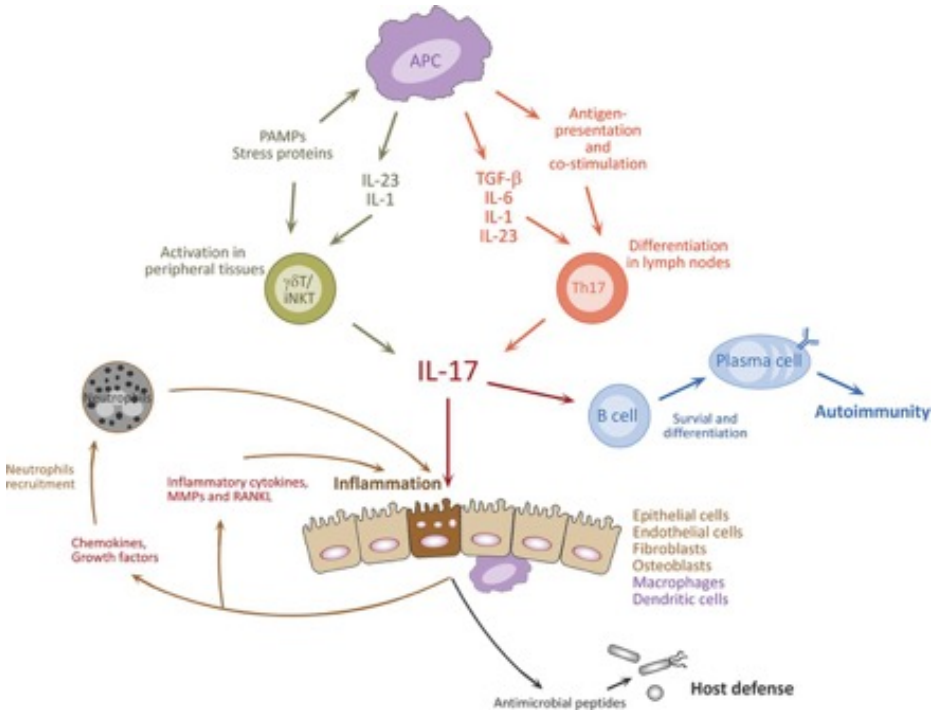

Ixekizumab, an interleukin-17A antagonist in the treatment of ankylosing spondylitis or radiographic axial spondyloarthritis in patients previously untreated with biological disease-modifying anti-rheumatic drugs (COAST-V)

Biological disease-modifying anti-rheumatic drugs (bDMARDs) are recommended for radiographic axial spondyloarthritis, otherwise known as ankylosing spondylitis, when conventional therapies are not effective. We report efficacy and safety data on ixekizumab, a high-affinity monoclonal antibody that selectively targets interleukin-17A (IL-17A), in patients with radiographic axial spondyloarthritis who have not previously been treated with bDMARDs.

In this phase 3, randomised, double-blind, placebo-controlled superiority study of ixekizumab, adult patients with inadequate response or intolerance to non-steroidal anti-inflammatory drugs, an established diagnosis of radiographic axial spondyloarthritis, radiographic sacroiliitis centrally defined by modified New York criteria, and at least one spondyloarthritis feature according to the Assessment of SpondyloArthritis international Society (ASAS) criteria, were recruited from 84 sites (12 countries) in Europe, Asia, and North America. By use of a computer-generated random sequence, patients were randomly assigned (1:1:1:1) to 80 mg subcutaneous ixekizumab every two (Q2W) or four (Q4W) weeks, 40 mg adalimumab Q2W (active reference group), or placebo. The primary objective was to compare the proportion of patients achieving an ASAS40 response, a composite measure of clinical improvement in axial spondyloarthritis, at week 16 for both ixekizumab treatment groups versus the placebo group.

Number of patients positive for HLA-B27	76 (89%)	82 (91%)	75 (90%)	75 (93%)
Number of patients using NSAIDs at baseline	78 (91%)	83 (92%)	79 (95%)	72 (89%)
Use of conventional synthetic DMARDs at baseline	31 (36%)	32 (36%)	29 (35%)	33 (41%)
Sulfasalazine	23 (27%)	25 (28%)	25 (30%)	24 (30%)
Methotrexate	8 (9%)	8 (9%)	4 (5%)	9 (11%)
Mean patient global assessment of disease activity numeric rating score	7·1 (1·7)	7·1 (1·7)	7·1 (1·6)	6·9 (1·5)
Mean CRP concentration, mg/L	16·0 (21·0)	12·5 (17·6)	13·4 (15·3)	12·2 (13·3)
Number of patients with CRP concentration >5 mg/L	60 (70%)	52 (58%)	55 (66%)	52 (64%)

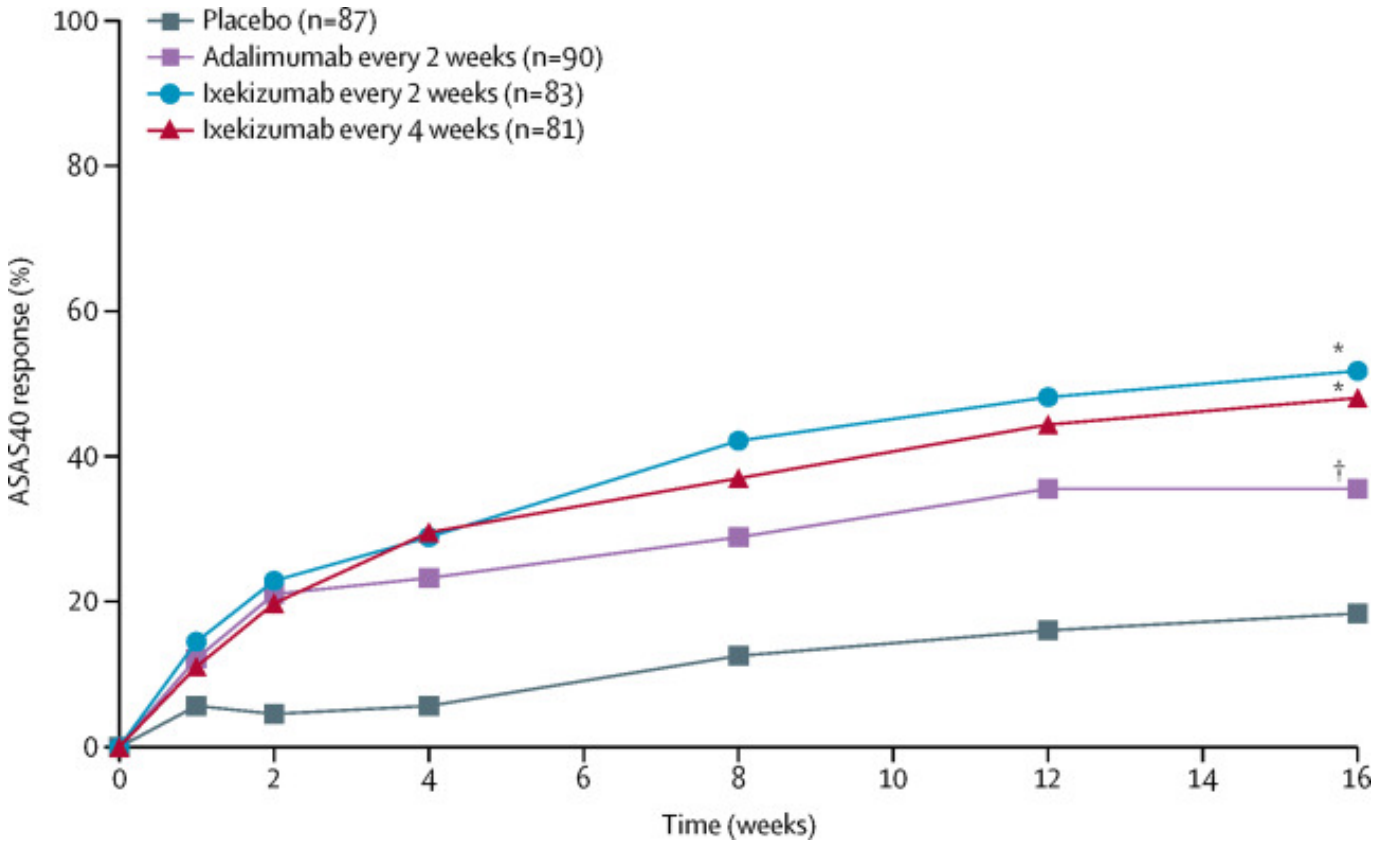

Proportion of patients achieving ASAS40 response through Week 16

Adalimumab represents an active reference group; the study was not powered to test equivalence or non-inferiority of the active treatment groups to each other, including ixekizumab versus adalimumab. ASAS40 response is defined as at least a 40% improvement and an absolute improvement from baseline of at least 2 units (range 0−10) in three or more of four domains (patient global, spinal pain, function, and inflammation) without any worsening in the remaining domain. ASAS=Assessment of SpondyloArthritis international Society. *p<0·0001, †p=0·0053.

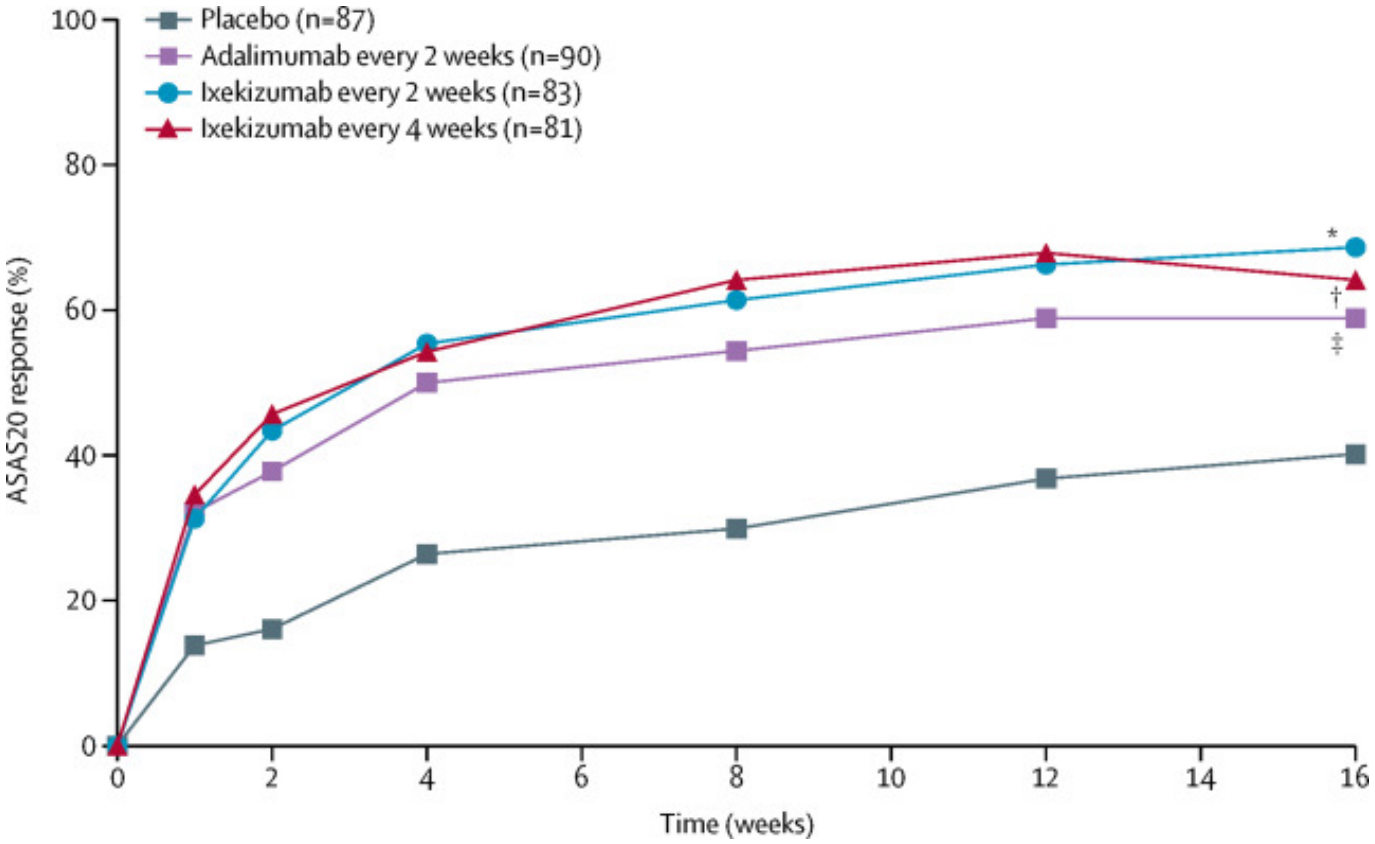

Proportion of patients achieving ASAS20 response through Week 16

Adalimumab represents an active reference group; the study was not powered to test equivalence or non-inferiority of the active treatment groups to each other, including ixekizumab versus adalimumab. ASAS20 response is defined as at least a 20% improvement and an absolute improvement from baseline of at least 1 unit (range 0–10) in three or more of four domains (patient global, spinal pain, function, and inflammation), and no worsening of at least 20% and at least 1 unit (range 0–10) in the remaining domain. ASAS=Assessment of SpondyloArthritis International Society. *p=0·0002, †p=0·0015, ‡p=0·0075.

Added value of this study

The primary and all major secondary endpoints of the COAST-V phase 3 clinical study in radiographic axial spondyloarthritis were achieved at week 16, with a safety profile consistent with studies of ixekizumab in patients with moderate-to-severe psoriasis and active psoriatic arthritis. These findings indicate that ixekizumab, administered every 2 weeks or every 4 weeks, was superior to placebo for the treatment of active radiographic axial spondyloarthritis in patients who had not previously received treatment with bDMARDs. This study is the first to assess the efficacy and safety of ixekizumab for radiographic axial spondyloarthritis in patients previously untreated with bDMARDs and is the first to include both a placebo control group and an active reference group (adalimumab), thereby providing additional context to observed efficacy for ixekizumab. COAST-V is also the first successful phase 3 clinical study in radiographic axial spondyloarthritis to include ASAS40, a stringent composite measure of clinical improvement in axial spondyloarthritis, as the primary endpoint, whereas most other trials of radiographic axial spondyloarthritis have used ASAS20, representing a lower level of response. This higher level of improvement might be more clinically relevant to patients and clinicians.

Implications of all the available evidence

The results of the COAST-V study provide additional evidence supporting the role of IL-17A in the pathogenesis of radiographic axial spondyloarthritis. Ixekizumab was efficacious in the treatment of radiographic axial spondyloarthritis with significant improvements in disease activity, health-related quality of life, day-to-day physical activity, and bone marrow oedema of the spine and sacroiliac joint in patients previously untreated with bDMARDs. Numerically, the responses seen with ixekizumab were similar to those observed in the adalimumab group. Overall, the findings of COAST-V indicate that ixekizumab could be a new treatment option for patients with radiographic axial spondyloarthritis.

Effects of the Learning Together intervention on bullying and aggression in English secondary schools (INCLUSIVE): a cluster randomised controlled trial

Bullying, aggression, and violence among children and young people are among the most consequential public mental health problems.

Bullying, aggression, and violence among children and young people are some of the most consequential public mental health problems. We tested the Learning Together intervention, which involved students in efforts to modify their school environment using restorative practice and by developing social and emotional skills. We did a cluster randomised trial, with economic and process evaluations, of the Learning Together intervention compared with standard practice (controls) over 3 years in secondary schools in south-east England. Learning Together consisted of staff training in restorative practice; convening and facilitating a school action group; and a student social and emotional skills curriculum. Primary outcomes were self-reported experience of bullying victimisation (Gatehouse Bullying Scale; GBS) and perpetration of aggression (Edinburgh Study of Youth Transitions and Crime (ESYTC) school misbehaviour subscale) measured at 36 months. We analysed data using intention-to-treat longitudinal mixed-effects models.

Number of schools		20	20
School sex mix			
	Mixed	15 (75%)	15 (75%)
	Girls only	3 (15%)	4 (20%)
	Boys only	2 (10%)	1 (5%)
School type			
	Voluntary	1 (5%)	3 (15%)
	Community school	3 (15%)	2 (10%)
	Academy (converter mainstream)	9 (45%)	10 (50%)
	Academy (sponsor led)	3 (15%)	3 (15%)
	Foundation school	4 (20%)	2 (10%)

Learning Together had small but significant effects on bullying, which could be important for public health, but no effect on aggression. Interventions to promote student health by modifying the whole-school environment are likely to be one of the most feasible and efficient ways of addressing closely related risk and health outcomes in children and young people.

„Mobbing, Drangsalieren, Schickanieren, Einschüchtern, Tyranniesieren, Nötigen“:

Klingt eigentlich nach:

Er ist wieder da

(Dorothy) Thompson described Hitler in the following terms: "He is formless, almost faceless, a man whose countenance is a caricature, a man whose framework seems cartilaginous, without bones. He is inconsequent and voluble, ill poised and insecure. He is the very prototype of the little man."

Table. Demographic characteristics of participants at baseline, 24 months and 36 months

	Baseline		24 months		36 months	
Outcome	**Control** **n=3,347**	**Intervention** **n=3,320**	**Control** **n=3,195**	**Intervention** **n=3,095**	**Control** **n=3,087**	**Intervention** **n=2,873**
Age mean (SD)	11·75 (0·44)	11·76 (0·43)	13·72 (0·59)	13·76 (0·45)	14·75 (1·20)	14·70 (0·82)
Sex n (%)						
Male	1,639 (49·85)	1,464 (44·88)	1,580 (49·45)	1,357 (43·84)	1,462 (47·36)	1,232 (42·88)
Female	1,649 (50·15)	1,804 (55·20)	1,543 (48·29)	1,675 (54·12)	1,521 (49·27)	1,563 (54·40)
Ethnicity n (%)						
White British	1,391 (41·47)	1,221 (37·32)	1,265 (39·59)	1,028 (33·21)	1,127 (36·51)	966 (33·62)
White other	291 (8·78)	273 (8·34)	308 (9·64)	285 (9·21)	322 (10·43)	273 (9·50)
Asian/Asian British	859 (25·92)	786 (24·02)	837 (26·20)	762 (24·62)	816 (26·43)	687 (23·91)
Black/Black British	384 (11·59)	535 (16·35)	365 (11·42)	489 (15·80)	377 (12·21)	473 (16·46)
Chinese/Chinese British	11 (0·33)	35 (1·07)	14 (0·44)	29 (0·94)	15 (0·49)	26 (0·90)
Mixed ethnicity	238 (7·18)	224 (6·85)	231 (7·23)	229 (7·40)	217 (7·03)	191 (6·65)
Other	140 (4·22)	198 (6·05)	145 (4·54)	232 (7·50)	170 (5·51)	219 (7·62)
Religion n (%)						
None	983 (29·59)	787 (23·99)	1,037 (32·46)	808 (26·11)	1,043 (33·79)	802 (27·92)
Christian	1,073 (32·30)	1,173 (35·76)	923 (28·89)	1,019 (32·92)	871 (28·22)	900 (31·33)
Jewish	9 (0·27)	13 (0·40)	11 (0·34)	17 (0·55)	15 (0·49)	18 (0·63)
Muslim/Islam	878 (26·46)	817 (24·91)	843 (26·38)	774 (25·01)	810 (26·24)	726 (25·27)
Hindu	90 (2·71)	176 (5·37)	79 (2·47)	149 (4·81)	83 (2·69)	144 (5·01)
Sikh	71 (2·14)	88 (2·68)	69 (2·16)	87 (2·81)	70 (2·27)	81 (2·82)
Don't know	145 (4·36)	126 (3·84)	148 (4·63)	114 (3·68)	91 (2·95)	91 (3·17)
Other	73 (2·20)	100 (3·05)	57 (1·78)	85 (2·75)	69 (2·24)	67 (2·33)
Family structure n (%)						
Two parents	2,393 (71·91)	2,369 (72·05)	2,200 (68·86)	2,137 (69·05)	2,073 (67·15)	1,958 (68·15)
Single mothers	604 (18·15)	626 (19·04)	627 (19·62)	649 (20·97)	624 (20·21)	584 (20·33)

Figure: Intervention logic model

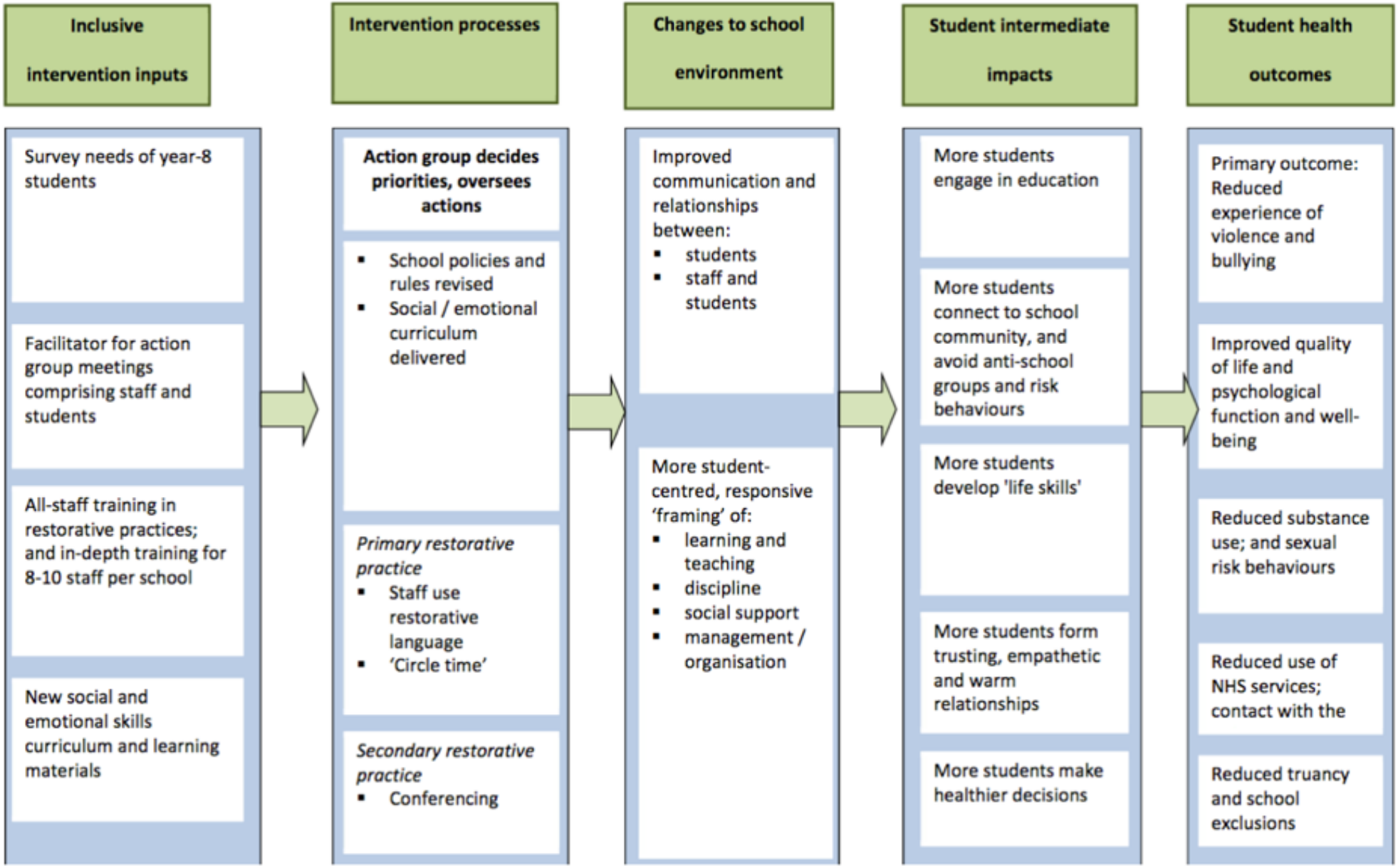

We found an effect of the intervention on bullying at 36 months (as hypothesised for our primary outcome) but not at 24 months, and we found a similar strengthening of effects over time for most secondary outcomes. This probably reflects the time needed for components of the intervention to be translated into organisational change within schools, consistent with evidence from the Gatehouse Project, a previous trial of an intervention to modify the whole-school environment to reduce health risk behaviours among Australian adolescents.
Although many schools did not deliver formal intervention components so well in the third year as earlier, our process evaluation suggested that by the third year schools had integrated components of the intervention into mainstream school structures and processes.

We report results of the first randomised controlled trial of restorative approaches to reduce bullying and aggression and promote student health, using a whole-school approach, engaging students in school decision making, and providing social and emotional skills education. Learning Together reduced student reports of bullying victimisation compared with schools continuing their standard practice. We did not identify a reduction in overall student reports of aggression. Learning Together seemed to have larger benefits for many secondary outcomes, from improved psychological function, wellbeing, and quality of life, to reductions in police contact, smoking, and alcohol and drug use. The effects on bullying and other continuous outcomes by the third year approximated 0·1 SD, which could be important at the population level. We found intervention effects both in the whole sample and in schools with higher levels of bullying or aggression at baseline, implying that the intervention worked to curtail existing bullying and aggression (secondary prevention) as well as prevent new bullying (primary prevention). We also found that the Learning Together intervention had greater effects for boys than in girls for secondary psychological and behavioural outcomes, although not for primary outcomes. The intervention was cheap, falling into the very low cost category for UK school interventions.
The costs of trainers, facilitators, and school staff were an additional £47–58 per pupil in the intervention group compared with control schools over the 3 years.

Research in context

Evidence before this study

Reviews have shown the pervasive effect of bullying in adolescence on contemporary and later health, wellbeing, and social functioning. Systematic reviews indicate that whole-school interventions are among the most promising approaches to the promotion of young people's health, and that these are effective in reducing bullying victimisation. Restorative practice is increasingly used in schools to address bullying and antisocial behaviour. We undertook a systematic review in January, 2018, of PubMed using the search terms (((((“Schools”[Mesh]) AND “Randomized Controlled Trial” [Publication Type]) AND (“Bullying”[Majr]) OR “Aggression”[Majr]))) AND restorative justice. We identified no published randomised trials or systematic reviews of restorative practice interventions in schools.

Added value of this study

We present the first evidence from a randomised trial that a whole-school intervention including restorative practice and social and emotional learning elements, has positive effects on bullying; mental health and wellbeing; quality of life; smoking, alcohol and drug use; and police contact. The Learning Together intervention is very low cost compared with other educational interventions and offers a coherent means of addressing clustered risks and health outcomes in schools.

Implications of all the available evidence

Interventions aiming to promote student health by modifying the whole-school environment can have effects of public health importance across a broad range of important outcomes in young people. The inclusion of restorative practice within such interventions can reduce bullying among all young people and reduce aggressive behaviour in those with high baseline aggression.

Promoting school climate and health outcomes with the SEHER multi-component secondary school intervention in Bihar, India: a cluster-randomised controlled trial

School environments affect health and academic outcomes. With increasing secondary school retention in low-income and middle-income countries, promoting quality school social environments could offer a scalable opportunity to improve adolescent health and wellbeing. We did a cluster-randomised trial to assess the effectiveness of a multi-component whole-school health promotion intervention (SEHER) with integrated economic and process evaluations in grade 9 students (aged 13–14 years) at government-run secondary schools in the Nalanda district of Bihar state, India. Schools were randomly assigned (1:1:1) to three groups: the SEHER intervention delivered by a lay counsellor (the SEHER Mitra [SM] group), the SEHER intervention delivered by a teacher (teacher as SEHER Mitra [TSM] group), and a control group in which only the standard government-run classroom-based life-skills Adolescence Education Program was implemented. The primary outcome was school climate measured with the Beyond Blue School Climate Questionnaire (BBSCQ).

The multi-component whole-school SEHER health promotion intervention had substantial beneficial effects on school climate and health-related outcomes when delivered by lay counsellors, but no effects when delivered by teachers.

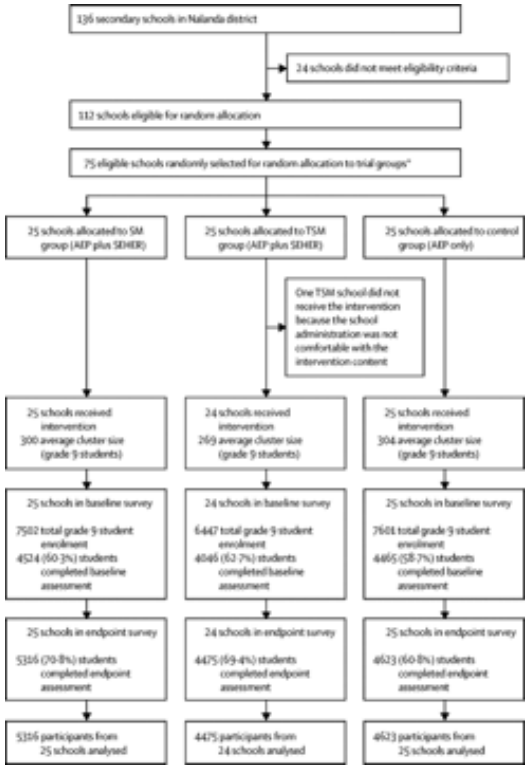

Whole-school activities

The following themes were addressed through whole-school activities outlined below: hygiene, bullying, mental health, substance use, reproductive and sexual health, gender and violence, rights and responsibilities, and study skills. Each month had a dedicated theme, and all the whole-school activities were geared towards the theme of the month.

- School Health Promotion Committee: each school was encouraged to form a School Health Promotion Committee, consisting of representatives from the management, parents, teachers, and student body. The principal was the chairperson and the SM or TSM was the secretary. The committee was responsible for monitoring the programme in the school and met twice during an academic year—ie, at the beginning and in the latter half of the academic year. The agenda for the meetings of the committee included reporting and discussion on issues submitted by the students, feedback from committee members on the activities conducted in the previous academic year, and activities planned for the upcoming year (frequency: twice per year).
- Awareness generation: the SEHER Mitra (SM) or teacher as SEHER Mitra (TSM) facilitated activities such as skit presentation, role play, and group discussion during the general assembly of the school (frequency: four assemblies per month).
- Speak-out box: the speak-out box was a letterbox providing a platform for students to raise concerns, complaints, and suggestions anonymously. The box was opened once per week by the SM or TSM and issues were addressed through one-to-one counselling if the student had self-identified. For anonymous contributions, the SM or TSM addressed the concerns through discussion during various activities of the intervention. In case of issues that were deemed severe or required urgent action, the SM or TSM contacted the supervisor or the principal for consultation. The issues that could not be addressed quickly were discussed in the School Health Promotion Committee meeting and a plan of action was developed to address them.
- Wall magazine: a monthly wall magazine issue was developed to build knowledge on the theme chosen for the month. All students, teachers, and the principal could contribute to the wall magazine issue through write-ups, poems, pictures, artwork, etc. The SM or TSM assessed the materials submitted for appropriateness before posting on the wall magazine (frequency: one issue per month).
- Competitions: the SM or TSM organised monthly competitions for the students, such as elocution, debate, poster making, sports, quizzes, and essay writing, linked to the monthly topic of the wall magazine. A prize of appreciation was given to the students during the assembly (frequency: one competition per month).

Whole-school activities

The following themes were addressed through whole-school activities outlined below: hygiene, bullying, mental health, substance use, reproductive and sexual health, gender and violence, rights and responsibilities, and study skills. Each month had a dedicated theme, and all the whole-school activities were geared towards the theme of the month.

- School Health Promotion Committee: each school was encouraged to form a School Health Promotion Committee, consisting of representatives from the management, parents, teachers, and student body. The principal was the chairperson and the SM or TSM was the secretary. The committee was responsible for monitoring the programme in the school and met twice during an academic year—ie, at the beginning and in the latter half of the academic year. The agenda for the meetings of the committee included reporting and discussion on issues submitted by the students, feedback from committee members on the activities conducted in the previous academic year, and activities planned for the upcoming year (frequency: twice per year).
- Awareness generation: the SEHER Mitra (SM) or teacher as SEHER Mitra (TSM) facilitated activities such as skit presentation, role play, and group discussion during the general assembly of the school (frequency: four assemblies per month).
- Speak-out box: the speak-out box was a letterbox providing a platform for students to raise concerns, complaints, and suggestions anonymously. The box was opened once per week by the SM or TSM and issues were addressed through one-to-one counselling if the student had self-identified. For anonymous contributions, the SM or TSM addressed the concerns through discussion during various activities of the intervention. In case of issues that were deemed severe or required urgent action, the SM or TSM contacted the supervisor or the principal for consultation. The issues that could not be addressed quickly were discussed in the School Health Promotion Committee meeting and a plan of action was developed to address them.
- Wall magazine: a monthly wall magazine issue was developed to build knowledge on the theme chosen for the month. All students, teachers, and the principal could contribute to the wall magazine issue through write-ups, poems, pictures, artwork, etc. The SM or TSM assessed the materials submitted for appropriateness before posting on the wall magazine (frequency: one issue per month).
- Competitions: the SM or TSM organised monthly competitions for the students, such as elocution, debate, poster making, sports, quizzes, and essay writing, linked to the monthly topic of the wall magazine. A prize of appreciation was given to the students during the assembly (frequency: one competition per month).

Research in context

Evidence before this study

We did not do a formal literature search before starting this trial. Our review of the published literature included a synthesis of international reviews on WHO's Health Promoting Schools and whole school interventions. Existing evidence indicates that whole-school interventions are more effective in achieving health and educational outcomes than classroom-only or single-intervention approaches. However, most of the studies contributing to this evidence are from high-income countries, mainly the USA and European nations. This situation raises the questions of feasibility and sustainability of the whole-school interventions in low-income and middle-income countries. We supplemented this evidence with a review of evaluation studies on school-based health promotion in India. School-based health promotion interventions have generally been delivered by existing human resources such as teachers and health-care providers. However, these interventions can compete with teaching duties and other commitments. The evaluation of our whole-school intervention in Goa (India) suggested that a lay school counsellor could be an effective delivery agent for such interventions.

Added value of this study

To the best of our knowledge, this study is the first report of findings from a low-income or middle-income country assessing the effectiveness and cost-effectiveness of a whole-school, multi-component intervention in secondary schools targeting school environments, delivered either by a lay counsellor or teacher, compared against a government-run life skills classroom programme alone. The intervention, when delivered by lay counsellors, showed large effects on improving school climate and a range of health-related outcomes including depressive symptoms, bullying, violence, attitude towards gender equity, and knowledge of reproductive and sexual health, compared with both the standard life skills intervention and the teacher-delivered intervention. However, the results showed no effect of the teacher-delivered intervention when compared with the standard government-run life skills intervention.

Implications of all the available evidence

A whole-school, multi-component intervention targeting school environments delivered by lay counsellors in government-run secondary schools is acceptable, feasible, and effective for enhancing school climate and improving health-related outcomes in adolescents. These findings need to be replicated in other contexts, so that the intervention can potentially be scaled up as a relatively low-cost strategy to improve adolescent health outcomes.

The 2018 report of the *Lancet* Countdown on health and climate change

The Lancet Countdown was established to provide an independent, global monitoring system dedicated to tracking the health dimensions of the impacts of, and the response to, climate change. The *Lancet* Countdown tracks 41 indicators across five domains: climate change impacts, exposures, and vulnerability; adaptation, planning, and resilience for health; mitigation actions and health co-benefits; finance and economics; and public and political engagement.

This report is the product of a collaboration of 27 leading academic institutions, the UN, and intergovernmental agencies from every continent. The report draws on world-class expertise from climate scientists, ecologists, mathematicians, geographers, engineers, energy, food, livestock, and transport experts, economists, social and political scientists, public health professionals, and doctors.

Recommendation 1: invest in climate change and public health research

Since 2007, the number of published articles on health and climate change in scientific journals has increased by 182% (indicator 5.2).

Recommendation 2: scale up financing for climate-resilient health systems

Spending on direct health adaptation as a proportion of total adaptation spending increased in 2017 to 4·8% (£11·68 billion), which is an increase in absolute and relative terms from the previous year (indicator 2.7). Health-related adaptation spending (including disaster response and food and agriculture) was estimated at 15·2% of total adaptation spend. Although this national-level spending is increasing, climate financing for mitigation and adaptation remains well below the US$100 billion per year committed in the Paris Agreement (indicator 2.8).

Recommendation 3: phase out coal-fired power

Coal consumption remains high, but continued to decline in 2017, a trend which is largely driven by China's decreased reliance and continued investment in renewable energy (indicators 3.2 and 3.3). The Powering Past Coal Alliance (an alliance of 23 countries including the UK, Italy, Canada, and France) was launched at the 23rd Conference of the Parties to the UN Framework Convention on Climate Change (UNFCCC) in December, 2017 (COP23), committing to phase out coal use by 2030 or earlier.

Recommendation 4: encourage city-level low-carbon transition to reduce urban pollution

In 2017, a new milestone was reached, with more than 2 million electric vehicles on the road, and with global per-capita electricity consumption for road transport increasing by 13% from 2013 to 2015 (indicator 3.6). China is responsible for more than 40% of electric cars sold globally.

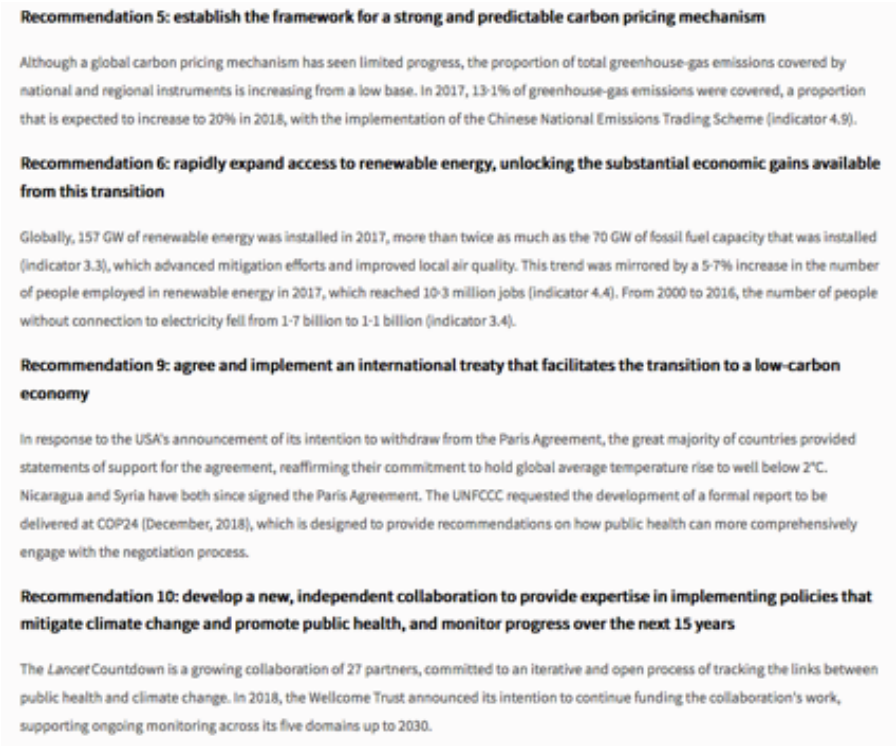

Recommendation 5: establish the framework for a strong and predictable carbon pricing mechanism

Although a global carbon pricing mechanism has seen limited progress, the proportion of total greenhouse-gas emissions covered by national and regional instruments is increasing from a low base. In 2017, 13·1% of greenhouse-gas emissions were covered, a proportion that is expected to increase to 20% in 2018, with the implementation of the Chinese National Emissions Trading Scheme (indicator 4.9).

Recommendation 6: rapidly expand access to renewable energy, unlocking the substantial economic gains available from this transition

Globally, 157 GW of renewable energy was installed in 2017, more than twice as much as the 70 GW of fossil fuel capacity that was installed (indicator 3.3), which advanced mitigation efforts and improved local air quality. This trend was mirrored by a 5·7% increase in the number of people employed in renewable energy in 2017, which reached 10·3 million jobs (indicator 4.4). From 2000 to 2016, the number of people without connection to electricity fell from 1·7 billion to 1·1 billion (indicator 3.4).

Recommendation 9: agree and implement an international treaty that facilitates the transition to a low-carbon economy

In response to the USA's announcement of its intention to withdraw from the Paris Agreement, the great majority of countries provided statements of support for the agreement, reaffirming their commitment to hold global average temperature rise to well below 2°C. Nicaragua and Syria have both since signed the Paris Agreement. The UNFCCC requested the development of a formal report to be delivered at COP24 (December, 2018), which is designed to provide recommendations on how public health can more comprehensively engage with the negotiation process.

Recommendation 10: develop a new, independent collaboration to provide expertise in implementing policies that mitigate climate change and promote public health, and monitor progress over the next 15 years

The *Lancet* Countdown is a growing collaboration of 27 partners, committed to an iterative and open process of tracking the links between public health and climate change. In 2018, the Wellcome Trust announced its intention to continue funding the collaboration's work, supporting ongoing monitoring across its five domains up to 2030.

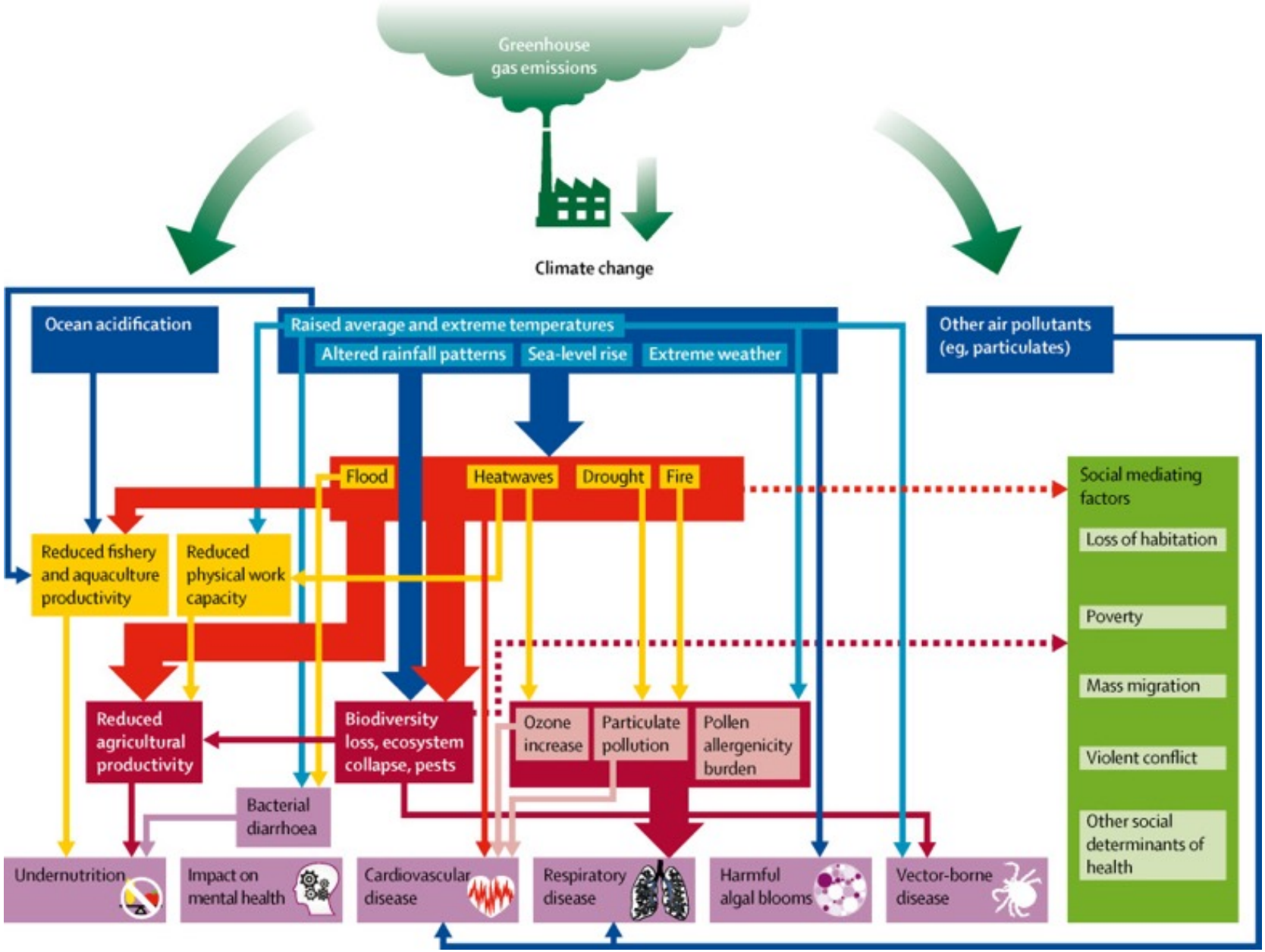
Greenhouse gas emissions
Climate change
Ocean acidification
Raised average and extreme temperatures
Altered rainfall patterns
Sea-level rise
Extreme weather
Other air pollutants (eg, particulates)
Flood
Heatwaves
Drought
Fire
Social mediating factors
Loss of habitation
Poverty
Mass migration
Violent conflict
Other social determinants of health
Reduced fishery and aquaculture productivity
Reduced physical work capacity
Reduced agricultural productivity
Biodiversity loss, ecosystem collapse, pests
Ozone increase
Particulate pollution
Pollen allergenicity burden
Bacterial diarrhoea
Undernutrition
Impact on mental health
Cardiovascular disease
Respiratory disease
Harmful algal blooms
Vector-borne disease

Mean summer warming relative to the 1986–2005 average

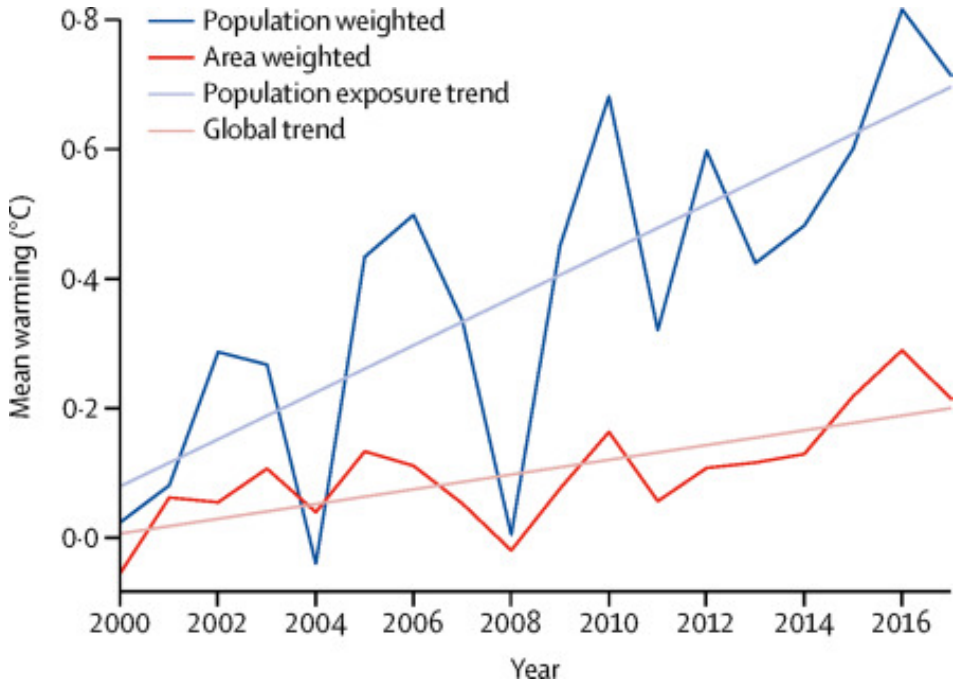

Headline finding: the mean global temperature change to which humans are exposed is more than double the global average change, with temperatures rising 0·8° C versus 0·3° C

The rising vulnerability to heat-related risks of climate change (indicator 1.1) is mirrored by greater human exposures to higher temperatures. In 2017, although the global mean temperature increase relative to the 1986–2005 reference period was 0·3° C, the increase in human exposure temperature (the temperature increase in populated zones) was more than double at 0·8° C. This continues an accelerating trend globally, which was identified in the Lancet Countdown's previous report.

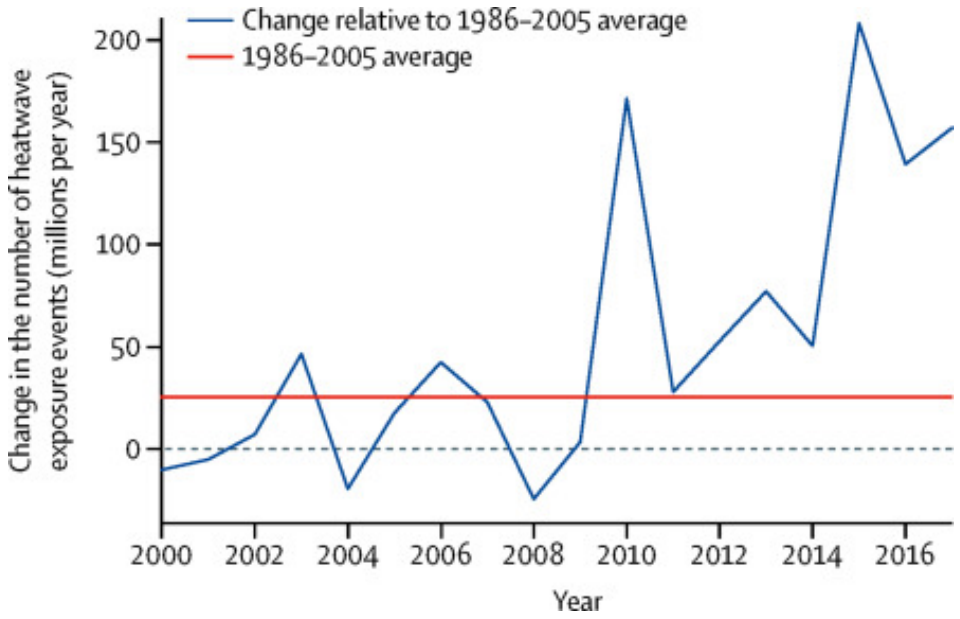

The strong upward trend noted in the 2017 *Lancet* Countdown report, with notable peaks in heatwave exposure observed in 2010, and 2015, continues in this 2018 report. On average, each person was exposed to an additional 1·4 days of heatwave from 2000 to 2017 (compared with the 1986–2005 baseline). Furthermore, in 2017, an additional 157 million exposure events occurred (one exposure event being one heatwave experienced by one person), 18 million more than in 2016.

Change in the number of heatwave exposure events (with one exposure event being one heatwave experienced by one person) compared with the historical average number of events (1986–2005 average)

Mean change in total hours of labour lost at the 400 W activity level over the 2000–17 period relative to the 1986–2005 baseline

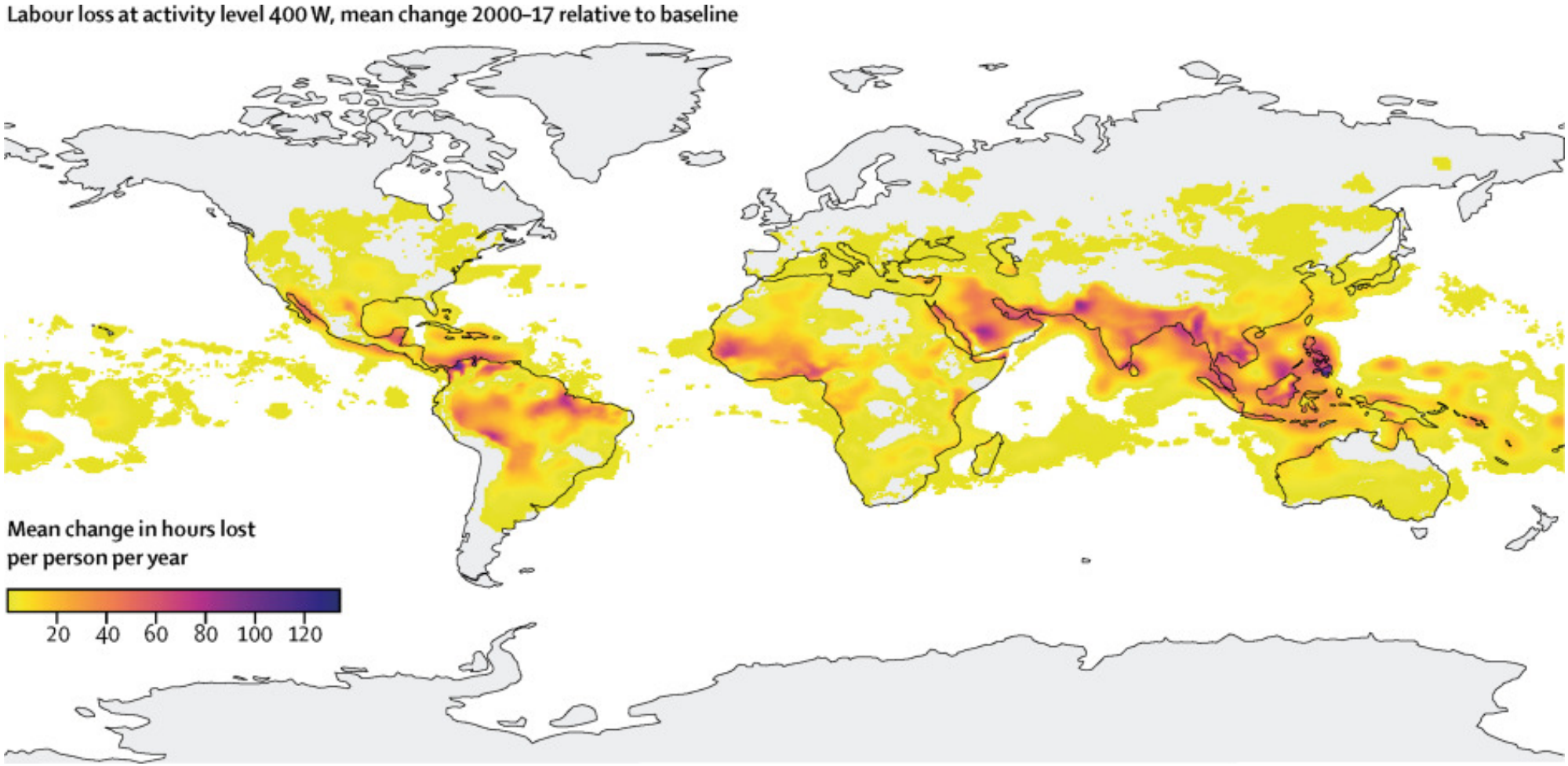

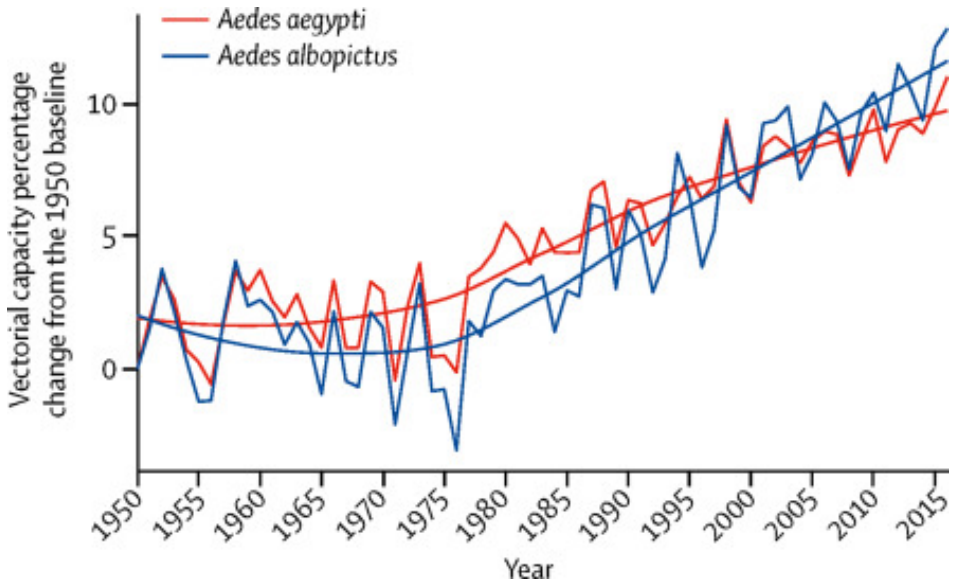

Vectorial capacity is a measure of the capacity for vectors to transmit a pathogen to a host and is influenced by vector, pathogen, and environmental factors. Compared with the 1950s baseline, climatic changes have increased global vectorial capacity for dengue virus in the 2010s (2011–16 average) by 7·8% for *A aegypti* and 9·6% for *A albopictus*. For both vectors, 2016 was the most suitable year on record. In addition, the seasonal dynamics of vectorial capacity for dengue virus for both vectors have lengthened and strengthened. Model projections suggest this rise will continue for both vectors in step with greenhouse gas emissions. The contribution of mobility and globalisation to the expansion of the dengue virus vector and dengue disease burden is important to note, alongside the impact of climate change.

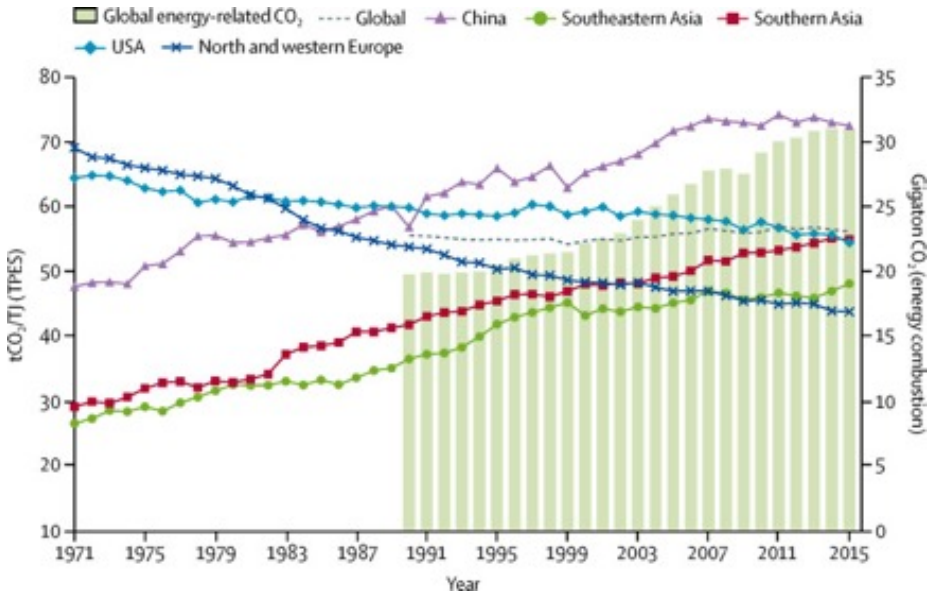

Headline finding: since 1990, the carbon intensity of TPES has remained static with no reduction at 55–57 tCO_2/TJ

This year's report includes 4 years of additional data compared with the 2017 *Lancet* Countdown report, and shows that the global trend in carbon intensity remains broadly unchanged. This means an ever-widening gap from the required path of rapid reduction towards zero emissions by 2050 to fulfil the Paris Agreement, which would require a decline in carbon intensity approximately equivalent to an average reduction of 1·0–1·6 tCO_2/TJ per year.

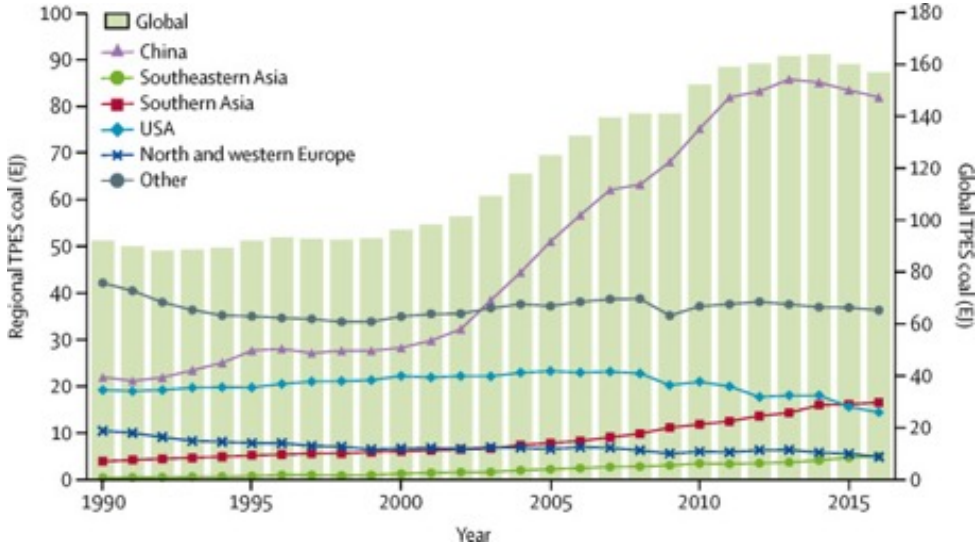

Headline finding: since 2013, coal use has declined, resulting largely from reductions in coal consumption in China, enhanced efficiency in coal-fired power generation, and continued increase in use of shale gas in the USA.

In 2016, this downward trend continued; however, preliminary data suggest coal consumption might increase slightly in 2017 and 2018

Accelerating the downward trend in coal demand will be crucial to meeting the climate goals embodied in the Paris Agreement. For example, to meet the 1·5° C warming-limit target, coal use needs to be at 20% of 2010 usage by 2040, or around 30 EJ

Conclusion: the *Lancet* Countdown in 2018

The *Lancet* Countdown: tracking progress on health and climate change monitors progress on health and climate change across five domains: climate change impacts, exposures, and vulnerabilities; adaptation, planning, and resilience for health; mitigation actions and health co-benefits; finance and economics; and public and political engagement. The collaboration is committed to an iterative and open process, and will continue to develop the methods and data sources its indicators draw on, publishing annually in *The Lancet* through to 2030.

In 2018, many of the global trends previously identified accelerated, both in terms of the health impacts of climate change, and the mitigation and adaptation interventions being implemented around the world. The first section of the report made clear that vulnerable populations are continually exposed to more severe climate hazards, with indicators reporting 157 million heatwave exposure events for such groups in 2017, more than 153 billion hours of labour lost due to rising temperatures, and that climatic conditions are at their most suitable for the transmission of dengue fever virus since 1950. Section 2 explored the various ways in which ministries of health, cities, and health systems are planning to enhance resilience and adaptation, providing more detailed insight into the quality and comprehensiveness of these strategies, and highlighted the fact that only 3·8% of adaptation funds available for development were allocated specifically for public health. Although more than 2·9 million premature deaths were caused by ambient pollution from $PM_{2·5}$ globally in 2015, promising trends reported in sections 3 and 4 showed a continued phase-out of coal-fired power, accelerated deployment of renewable energy, and continued divestment from fossil fuels, which should help to reduce premature mortality from air pollution. Indicators in the final section pointed to the same conclusions—that engagement in health and climate change is increasing, enabling this engagement to be an important driver of policy change globally.

Four key messages emerge from the 41 indicators of the *Lancet* Countdown's 2018 report. First, present day changes in labour capacity, vector-borne disease, and food security provide early warning of compounded and overwhelming impacts expected if temperature continues to rise. Trends in climate change impacts, exposures, and vulnerabilities show an unacceptably high risk for the current and future health of populations across the world. Second, slow progress in reducing emissions and building adaptive capacity threatens both human lives and the viability of the national health systems they depend on, with the potential to disrupt core public-health infrastructure and overwhelm health services. Third, despite these delays, trends in a number of sectors are helping to generate the beginning of a low-carbon transition, and clearly the nature and scale of the response to climate change will be the determining factor in shaping the health of nations for centuries to come. And fourth, ensuring a widespread understanding of climate change as a central public-health issue will be vital in delivering an accelerated response, with the health profession beginning to rise to this challenge.

What the U.S. elections mean for science *p. 731*

Dendrite turnover in Down syndrome neurons *p. 793*

Social networks drive success in art *p. 825*

Science

$15
16 NOVEMBER 2018
sciencemag.org
AAAS

SPECIAL ISSUE

DIET AND HEALTH

Optimizing human metabolism

Optimizing the diet

In every stage race, competitive cyclists perform an experiment of sorts to discover who can most efficiently turn dietary energy sources into maximal power output on the bike. More broadly, we're all interested in diet because abundant evidence shows that diet has major effects on human health and resistance to rampant diseases associated with aging, such as obesity, cardiovascular disease, and diabetes. Advice on what constitutes a healthy diet is more prevalent and more inconsistent than ever. For this special issue, we checked in with the experts. On the question of how much fat we should eat, recommendations have swung from one extreme to the other. We consulted with a group of scientists representing different sides in the debate over the proportion of fat in a healthy diet and, importantly, which particular fats are most healthful. We share our meals with trillions of bacteria in the digestive system, so a promising and emerging area of investigation explores how diet influences our give-and-take interaction with gut symbionts. It's not just what you eat but when you eat it, and periods of fasting have some remarkable benefits. A pervasive theme is that much of the disagreement and confusion reflects a lack of solid scientific studies on humans. Clearly, many more well-designed studies are needed to determine the best diet for people, and how that varies with activity, at different life stages and for different individuals. And individual needs can be extreme—a cyclist at the top of the sport recorded massive carbohydrate loading before an intense stage, eating the equivalent of 85 slices of bread!

Dietary fat: From foe to friend?

For decades, dietary advice was based on the premise that high intakes of fat cause obesity, diabetes, heart disease, and possibly cancer. Recently, evidence for the adverse metabolic effects of processed carbohydrate has led to a resurgence in interest in lower-carbohydrate and ketogenic diets with high fat content. However, some argue that the relative quantity of dietary fat and carbohydrate has little relevance to health and that focus should instead be placed on which particular fat or carbohydrate sources are consumed. This review, by nutrition scientists with widely varying perspectives, summarizes existing evidence to identify areas of broad consensus amid ongoing controversy regarding macronutrients and chronic disease.

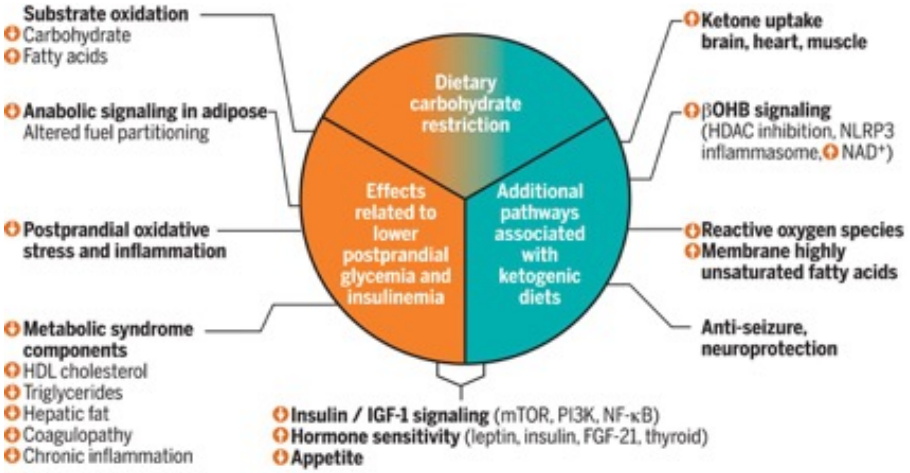

From a pathophysiological perspective, low-carbohydrate, high-fat diets may directly target underlying metabolic dysfunction in insulin resistance and type 2 diabetes, characterized by defects in the body's ability to oxidize ingested carbohydrate. With insulin resistance, dietary carbohydrate is diverted at increased rates into hepatic de novo lipogenesis, resulting in increased hepatic triglyceride synthesis and abnormal concentrations of lipids in the blood (60). From a historical perspective, some aboriginal hunting and fishing cultures (e.g., Inuit of the Arctic and First Nations groups in Canada) survived for millennia with little available dietary carbohydrate. In fact, mild ketosis was the "normal" metabolic state for many cultures before the advent of agriculture (i.e., for all but the last 1% or less of the existence of humans as a species). When these ethnic groups underwent a transition from their low-carbohydrate and high-fat traditional diets, the prevalence of obesity and type 2 diabetes increased markedly, although changes in other lifestyle factors may have also had a role.

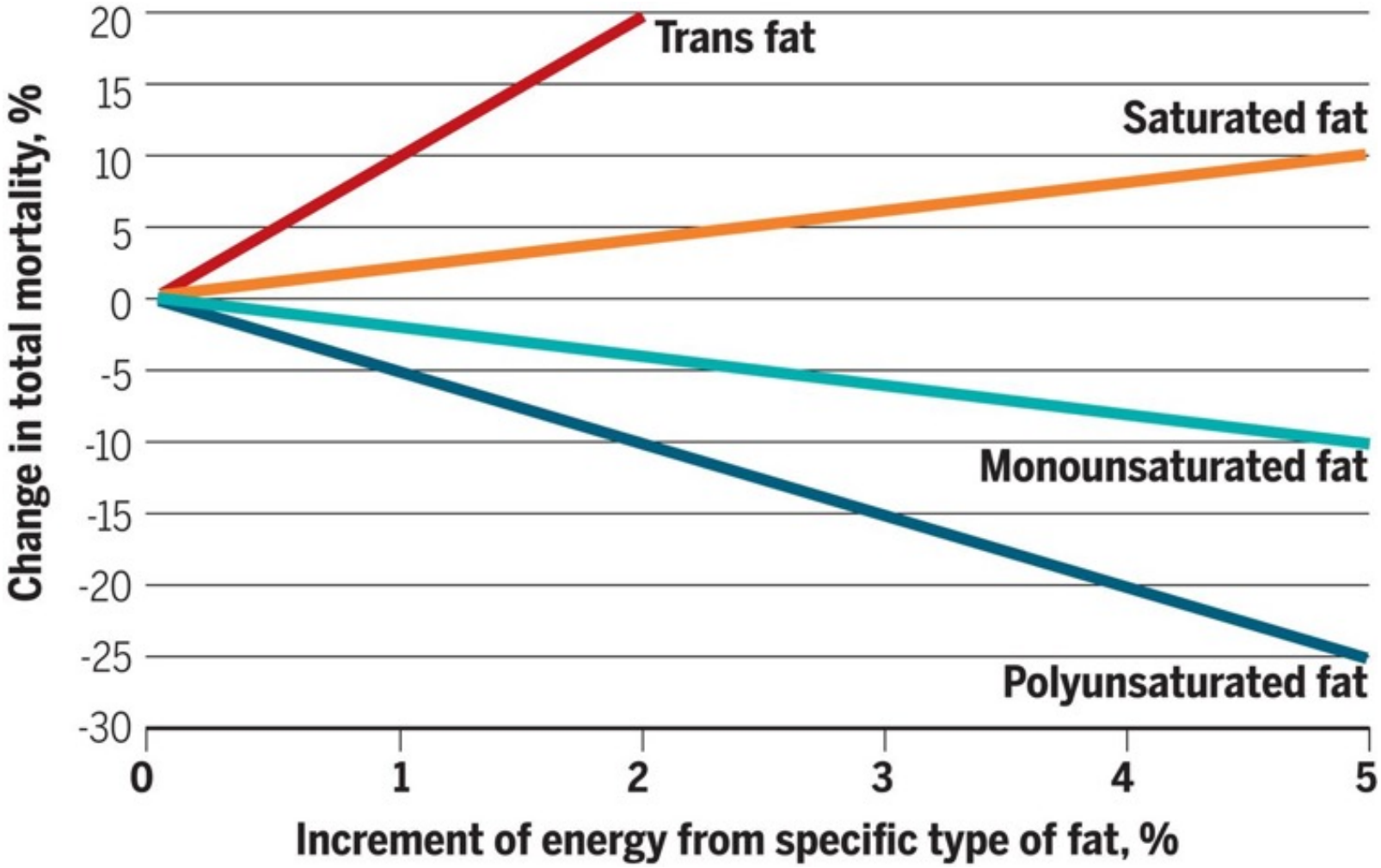

Conclusion

The optimal proportion of carbohydrate to fat in the diet for obesity treatment and chronic disease prevention has been a topic of debate for decades, often generating more heat than light. Of course, any meaningful assessment of a diet's impact on health must extend far beyond macronutrient quantity, to include the myriad qualitative aspects of food and food combinations that influence hormonal response, gene expression, and metabolic pathways. Further complicating this issue is the likelihood that inherent or acquired biological differences among individuals or populations, especially related to glucose homeostasis, affect response to specific diets.

Current controversies.

1. Do diets with various carbohydrate-to-fat proportions affect body composition (ratio of fat to lean tissue) independently of energy intake? Do they affect energy expenditure independently of body weight?

2. Do ketogenic diets provide metabolic benefits beyond those of moderate carbohydrate restriction? Can they help with prevention or treatment of cardiometabolic disease?

3. What are the optimal amounts of specific fatty acids (saturated, monounsaturated, polyunsaturated) in the context of a very-low-carbohydrate diet?

4. What is the relative importance for cardiovascular disease of the amounts of LDL cholesterol, HDL cholesterol, and triglycerides in the blood, or of lipoprotein particle size, for persons on diets with distinct fat-to-carbohydrate ratios? Are other biomarkers of equivalent or greater importance?

5. What are the effects of dietary fat amount and quality across the lifespan on risk of neurodegenerative, pulmonary, and other diseases that have not been well studied?

6. What are the long-term efficacies of diets with different carbohydrate-to-fat proportions in chronic disease prevention and treatment under optimal intervention conditions (designed to maximize dietary compliance)?

7. What behavioral and environmental interventions can maximize long-term dietary compliance?

8. What individual genetic and phenotypic factors predict long-term beneficial outcomes on diets with various fat-to-carbohydrate compositions? Can this knowledge inform personalized nutrition, with translation to prevention and treatment?

9. How does variation in the carbohydrate-to-fat ratio and in sources of dietary fat affect the affordability andenvironmental sustainability of diets?

A time to fast.

Nutrient composition and caloric intake have traditionally been used to devise optimized diets for various phases of life. Adjustment of meal size and frequency have emerged as powerful tools to ameliorate and postpone the onset of disease and delay aging, whereas periods of fasting, with or without reduced energy intake, can have profound health benefits. The underlying physiological processes involve periodic shifts of metabolic fuel sources, promotion of repair mechanisms, and the optimization of energy utilization for cellular and organismal health. Future research endeavors should be directed to the integration of a balanced nutritious diet with controlled meal size and patterns and periods of fasting to develop better strategies to prevent, postpone, and treat the socioeconomical burden of chronic diseases associated with aging.

Feeding regimen	Description	Macronutrient balance (Fat, Protein, Carbohydrate)	Feeding time (Fasting, Feeding)	Median life-span increase	Effects on health
Caloric restriction (CR)	Daily reduction by 15 to 40% of caloric intake without malnutrition			Yes 	Prevention of obesity, diabetes, oxidative stress, hypertension, cancer, cardiovascular disease
Time-restricted feeding (TRF)	Daily food consumption restriced to 4- to 12-hour window	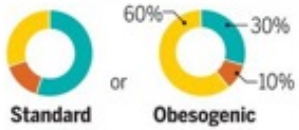		No data	Defense against type II diabetes, hepatic steatosis, hypercholesterolemia
Intermittent or periodic fasting (IF or PF)	**IF:** Alternation of 24-hour fasting or very low calories (25% of energy needs) with a 24-hour ad libitum eating period **PF:** 1 to 2 days fasting or very low calories followed by a 5-day ad libitum eating period (5:2)			Yes 	Protection against obesity, oxidative stress, cardiovascular disease, hypertension, neurodegeneration, diabetes
Fasting-mimicking diet (FMD)	Reduced caloric intake (~30% of energy needs) for five consecutive days before returning to normal eating cycles of FMD once a month or every 3 to 4 months per year			Yes 	Protection from cancer and diabetes, improved risk factors associated with multiple age-related diseases

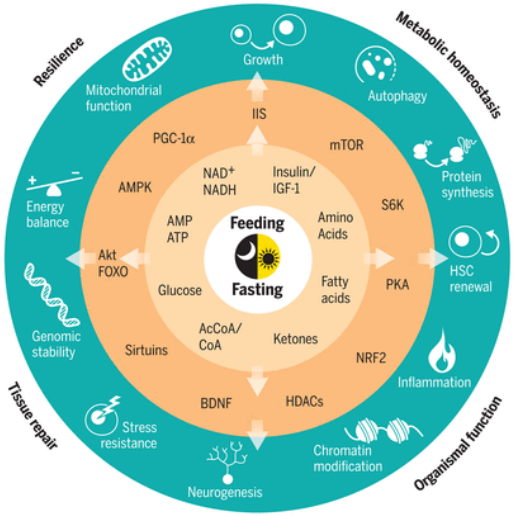

Fasting time and energy restriction share biological responses implicated in metabolite-controlled longevity pathways.Reduction of calories by continuous energy restriction or prolonged fasting periods trigger metabolic adaptations characterized by increased amounts of circulating ketones, whereas circulating fatty acids, amino acids, glucose, and insulin are maintained at low concentrations. Adaptive cellular responses involve alterations in the ratios of adenosine monophosphate (AMP) to adenosine triphosphate (ATP), of oxidized nicotinamide adenine dinucleotide (NAD^+) to the reduced form NADH, and of acetyl-CoA to CoA. After a few hours of fasting, increased AMP to ATP ratios activate AMPK, which triggers repair and inhibits anabolic processes. Acetyl-CoA and NAD^+ serve as cofactors for epigenetic modifiers such as histone acetyltransferases and NAD^+-dependent deacetylases, the sirtuins, thus linking nutrition, energy metabolism, and post-translational modifications of histone proteins. Sirtuins deacetylate FOXOs and peroxisome proliferator-activated receptor γ coactivator 1α (PGC-1α), factors respectively involved in stress resistance and mitochondrial biogenesis. Production of ketone bodies such as β-hydroxybutyrate from fatty-acid catabolism may operate as endogenous histone deacetylase (HDAC) inhibitors and may contribute to epigenetic control of gene expression, DNA repair, and genome stability. Ketogenesis also promotes synaptic plasticity and neurogenesis by increasing the expression of brain-derived neurotrophic factor (BDNF). Periodic cycles of fasting have systemic anti-inflammatory effects and increase progenitor stem cells. Down-regulation of the insulin–IGF-1 signaling (IIS) pathway and reduction of circulating amino acids repress the activity of mTOR and its downstream effector, the ribosomal protein S6 kinase beta-1 (S6K). This mechanism inhibits global protein synthesis and promotes recycling of macromolecules by stimulation of autophagy. CR promotes the expression and activity of NRF2, which induces a number of antioxidative and carcinogen-detoxifying enzymes. Collectively, the organism responds to a low-energy challenge by minimizing anabolic processes (synthesis, growth, and reproduction), favoring maintenance systems, and enhancing stress resistance, tissue repair, and recycling of damaged molecules. Improvement in resilience, metabolic homeostasis, tissue repair, and organismal function can act as direct modifiers of the four domains of the aging phenotype: body composition; balance between energy availability and energy demand; signaling networks that maintain homeostasis; and neurodegeneratio. Each of these domains can be assessed readily by routine clinical tests.

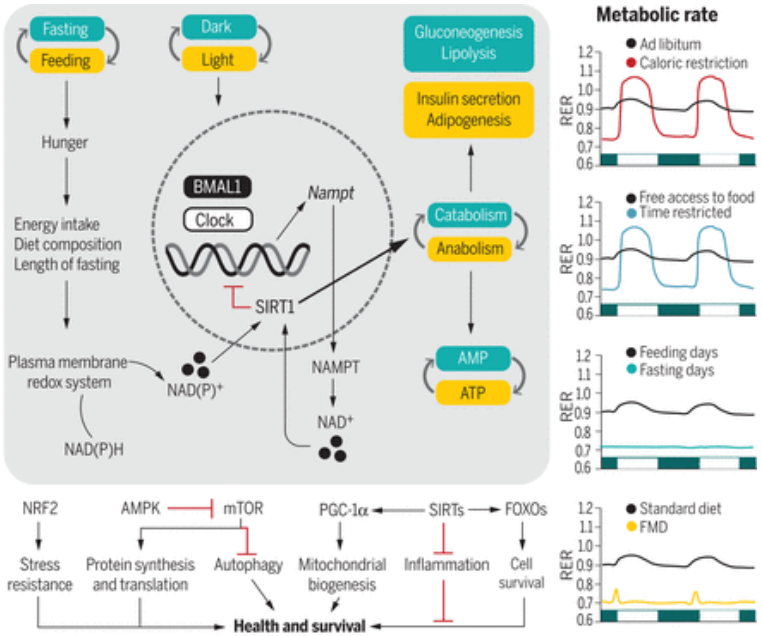

Integration of the circadian rhythms and feeding-fasting cycles with metabolism.(**Left**) The transcriptional activators BMAL1 and CLOCK are at the core of a cell-autonomous molecular circuit that governs circadian rhythms. Fasting increases hunger, the extent of which depends on the overall energy intake, diet composition, and length of fasting. The internal circadian clock also increases hunger independent of food intake and other behaviors. Intermittent energy restriction increases concentrations of the plasma membrane redox system enzymes, NADH-cytochrome b5 reductase and NAD(P)H-quinone oxidoreductase, contributing to oscillations in the NAD(P)H [reduced form of $NAD(P)^+$] to $NAD(P)^+$ (nicotinamide adenine dinucleotide phosphate) ratio. The circadian rhythmicity of CLOCK and BMAL1 expression regulates the transcription of NAMPT, a key regulatory enzyme involved in the generation of NAD^+, a metabolite required for the deacetylase activity of SIRT1. Active SIRT1 influences metabolism through its effects on catabolic and anabolic reactions and mediates BMAL1 deacetylation, which inhibits the circadian clock machinery. During the active phase (yellow boxes), increased production of ATP sustains anabolic pathways. During the resting phase (green boxes), a shift toward AMP gears metabolism toward catabolic processes. These intermediate energy carriers activate downstream transcription factors, kinases, and deacetylases like NRF2, AMPK, PGC-1α, sirtuins, and FOXOs, whose activation influences health and survival. (**Right**) At the organismal level, fasting or feeding states are paralleled by changes in the metabolic rate. AL–fed animals set their RERs at around 0.9, showing an intermediate preference between fat and carbohydrate metabolism. Both CR and TRF regimens increase the amplitude of RER oscillations, characterized by higher RER (utilization of carbohydrates) during feeding and lower RER (utilization of lipids) during fasting. Under prolonged fasting, lipids are the only source of energy, as opposed to feeding time. The FMD diet results in lower RER with a slight peak after the meal. The RER traces are idealized and may be close to what is seen in nocturnal rodents.

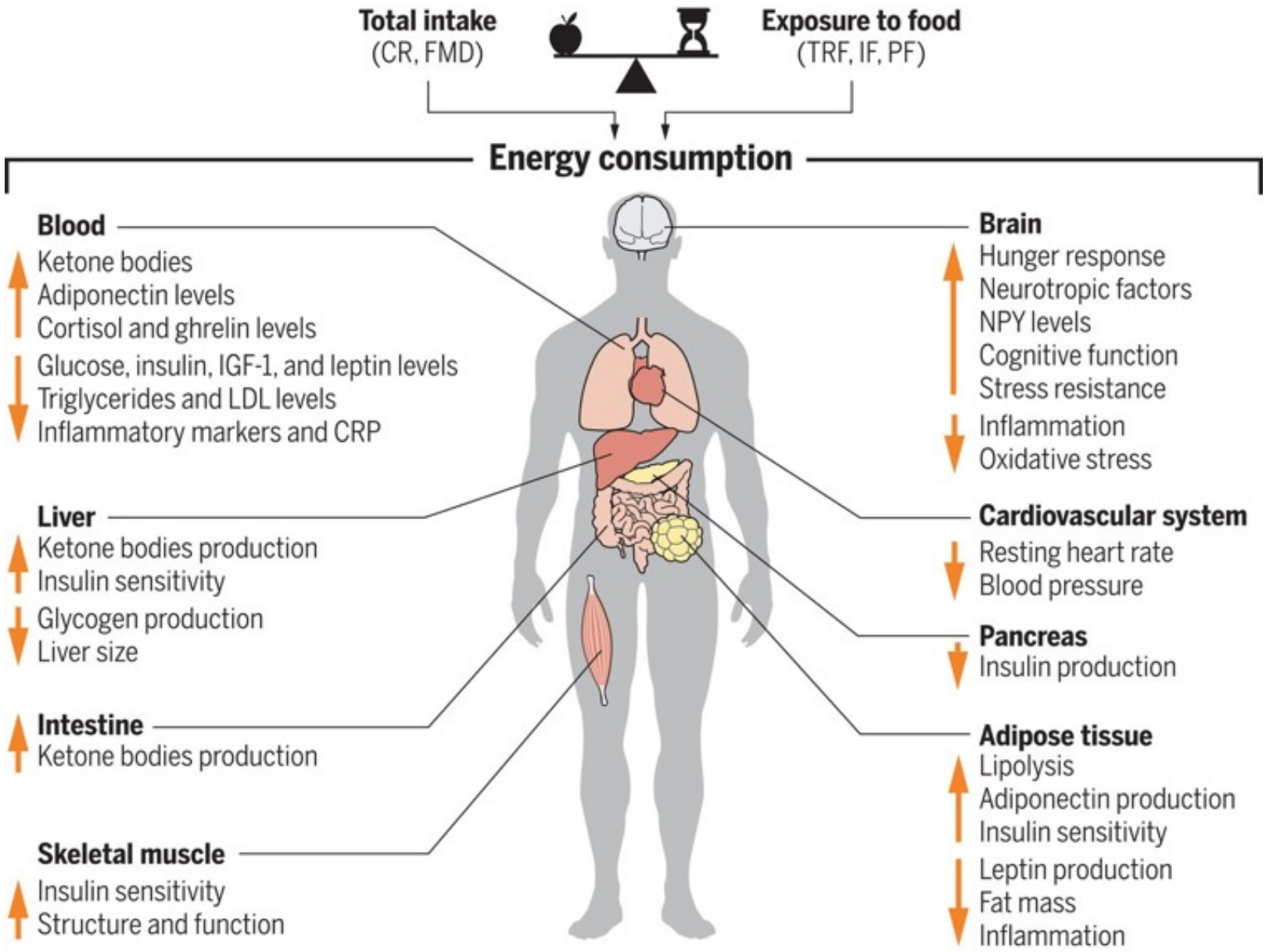

Conclusions

Pharmacological interventions with proven effectiveness are often accompanied by a range of unwanted side effects. Many elderly people take multiple medications, which can cause adverse geriatric outcomes linked to increases in morbidity and mortality.

The gut microbiota at the intersection of diet and human health

Abstract

Diet affects multiple facets of human health and is inextricably linked to chronic metabolic conditions such as obesity, type 2 diabetes, and cardiovascular disease. Dietary nutrients are essential not only for human health but also for the health and survival of the trillions of microbes that reside within the human intestines. Diet is a key component of the relationship between humans and their microbial residents; gut microbes use ingested nutrients for fundamental biological processes, and the metabolic outputs of those processes may have important impacts on human physiology. Studies in humans and animal models are beginning to unravel the underpinnings of this relationship, and increasing evidence suggests that it may underlie some of the broader effects of diet on human health and disease.

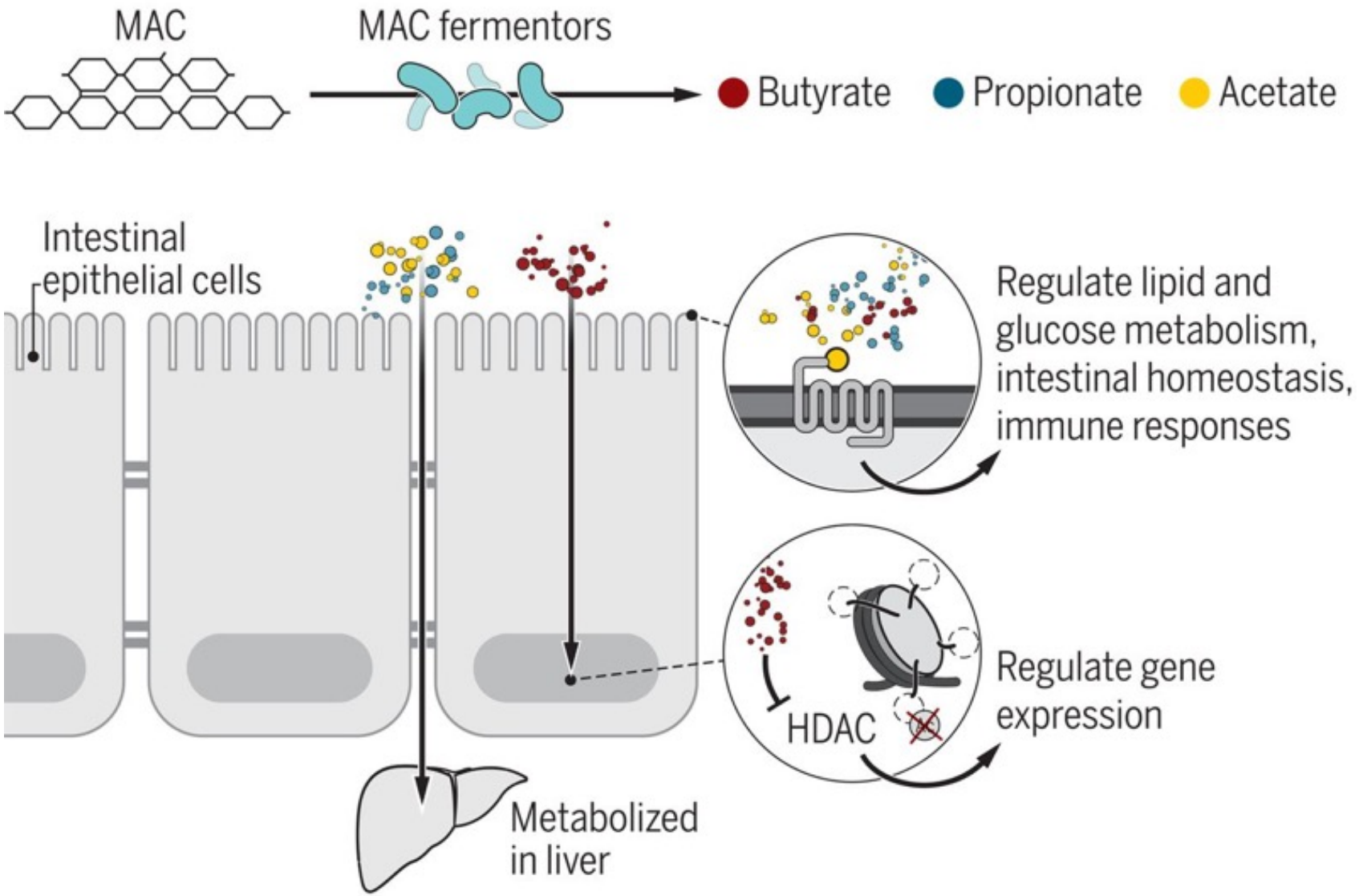

Microbiota-accessible carbohydrates

MAC fermentors produce SCFAs that can have multiple interactions with host tissues.Butyrate is taken up by epithelial cells and used as a primary source of energy for these cells. Butyrate (and to a lesser degree, propionate) can block histone deacetylases (HDAC) to regulate gene expression. All of the SCFAs can bind with varying affinities to G protein receptors in the intestines and other cells to regulate energy metabolism, intestinal homeostasis, and immune responses. Acetate and propionate are primarily metabolized in the liver, where propionate is used as a substrate for gluconeogenesis and acetate is used as an energy source and for fatty acid synthesis.

Interactions between amino acids and the gut microbiota.Microbial metabolism of the amino acid carnitine produces trimethylamine (TMA), which is subsequently oxidized in the liver to TMAO in a reaction catalyzed by flavin-containing monooxygenase (FMO). Increased levels of circulating TMAO have been linked to metabolic disease. Gut microbes metabolize the amino acid tryptophan into various substances, including indolepropionic acid (IPA) and indole-3-acetic acid (I3A), both of which can enter the general circulation. The metabolic effects of IPA, I3A, and other microbially derived amino acid metabolites are only now beginning to emerge.

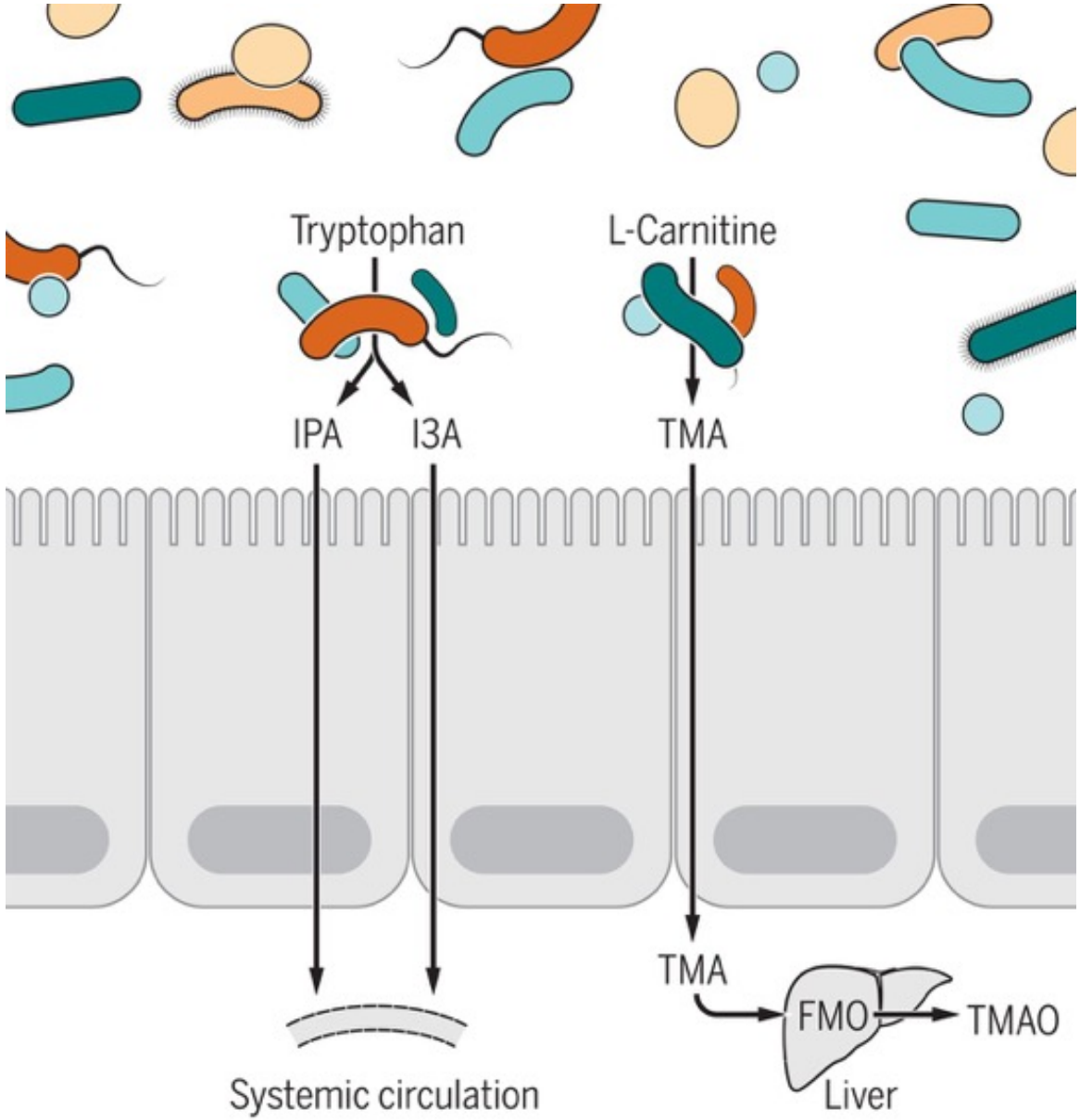

Dietary patterns

One obvious limitation to studying the health effects of individual nutrients is that those nutrients are rarely consumed in isolation; thus, experimental manipulation of an individual macronutrient invariably alters intake of other macronutrients that may have metabolic effects unto themselves.

Ketogenic diet

The ketogenic diet is characterized by very low CHO consumption (5 to 10% of total caloric intake), sufficient to enhance ketone production. It was originally developed as a treatment for refractory childhood epilepsy, and response of the gut microbiota to a ketogenic diet appears to play a role in the efficacy of this intervention in epileptic children.

Paleolithic diet

The Paleolithic diet, which seeks to mimic the dietary patterns of pre-agricultural societies, is often implemented as a high-protein/low-CHO diet for weight loss by individuals in Western societies. Clinically, the Paleolithic diet is being explored for management of inflammatory bowel disease (IBD), and although initial findings were promising, the study was conducted in a small cohort, and additional nutrient supplementation was required to curtail iron and vitamin D deficiencies.

Vegan/vegetarian diets

Plant-rich diets have long been a key feature of dietary recommendations, and vegan/vegetarian diets are associated with positive health outcomes and reduced disease risk. These beneficial effects may extend to the gut microbiota. Plant-based foods constitute the primary source of dietary MACs, and the microbiota of individuals who consume vegetarian or predominantly plant-based diets exhibit greater capacity for MAC fermentation.

Mediterranean diet

The Mediterranean diet emphasizes consumption of a variety of foods (fruits, vegetables, legumes, unsaturated fats, and limited red meat intake) rather than the exclusion of particular food groups or confinement to specific macronutrient ratios. Numerous epidemiologic studies and clinical trials have demonstrated that following a Mediterranean diet reduces the risk of all-cause mortality and multiple chronic diseases.

Microbiota-targeted diets

A number of microbiota-targeted diets have recently emerged with the growing public awareness of the gut microbiota and its potential to influence human health. Although the scientific premise of many of these diets is logically rooted in prevailing paradigms, they fail to acknowledge the many gaps in our knowledge regarding diet-microbiome-host interactions.

Perspectives and future directions

Data collected over the past decade have identified the gut microbiota as an important factor defining interindividual variation in disease risk and dietary response. The ascension of the gut microbiota as a key regulator of human physiology has generated tremendous excitement within and beyond the scientific community, as exemplified by the exponential increase in microbiota-focused publications and by the growth of the probiotic market into a multibillion-dollar industry. The rapidity of this ascension, however, poses a substantial challenge in that commercialization and popularity of microbiota-targeted therapies have accelerated despite the fact that fundamental questions regarding the microbiota and its relation to diet and human health remain unresolved. For example, much of the current data linking the microbiota to disease processes have been generated in animal models, and human feeding studies are needed to confirm their relevance before they can be translated to practical nutrition advice.

The plasticity of the microbiota makes microbiome-targeted interventions an attractive approach for disease prevention and treatment. However, despite reported alterations of the gut microbiota in response to short-term dietary interventions, long-term dietary patterns are associated with stable microbiota conformations that are difficult to alter. Despite current unresolved questions that limit practical and clinical translation of microbiota research, several new developments promise continued advancement of the field. Integration of proteomic and metabolomic data with existing DNA-based methods of microbiota assessment could circumvent the need to define healthy versus unhealthy microbial populations as more accurate functional profiling emerges. These examples demonstrate how realization of the potential for microbiota-diet interactions could change future approaches to nutrition.

Swifter, higher, stronger: What’s on the menu?

Abstract

The exploits of elite athletes delight, frustrate, and confound us as they strive to reach their physiological, psychological, and biomechanical limits. We dissect nutritional approaches to optimal performance, showcasing the contribution of modern sports science to gold medals and world titles. Despite an enduring belief in a single, superior ”athletic diet,” diversity in sports nutrition practices among successful athletes arises from the specificity of the metabolic demands of different sports and the periodization of training and competition goals. Pragmatic implementation of nutrition strategies in real-world scenarios and the prioritization of important strategies when nutrition themes are in conflict add to this variation. Lastly, differences in athlete practices both promote and reflect areas of controversy and disagreement among sports nutrition experts.

Ancient Olympians manipulated their diets according to prevailing beliefs, with Pythagoras being credited (probably incorrectly) for introducing athletes to meat and protein-rich foods in place of traditional figs, cereals, and cheese. Meanwhile, modern-day athletes are bombarded with social media “warriors” who evangelize vegan, Paleo, and low-carb “keto” diets for peak performance. In contrast to the battle over the perfect menu, contemporary sports nutrition embraces diversity in dietary practices, underpinning the demands of training and competition with the philosophies of specificity, periodization, and personalization

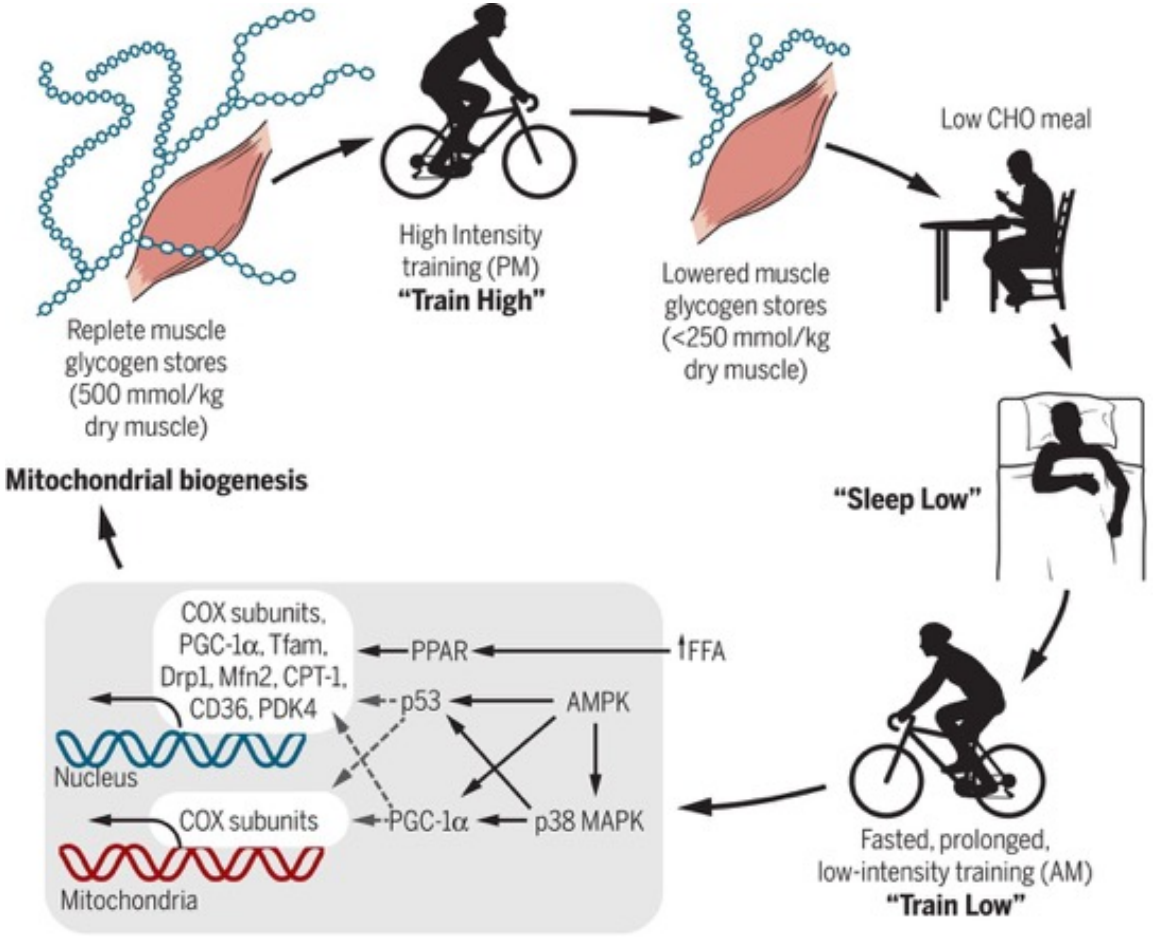

Periodized nutrition: Evolution of a nutritional practice.Commencing endurance training with lowered muscle glycogen stores (training low) results in greater transcriptional activation of enzymes involved in CHO and fat oxidation, as well as greater mitochondrial biogenesis, than undertaking exercise with a normal or elevated glycogen content. Restricting CHO availability during the early (1 to 5 hours) postexercise recovery period also acutely up-regulates various markers of substrate metabolism and endurance training adaptation in skeletal muscle. Against this background, we formulated a novel approach in which we can undertake high-quality, high-intensity training and then prolong the duration of low CHO availability during recovery and subsequent aerobic exercise, thereby potentially extending the time course of transcriptional activation of metabolic genes and their target proteins. We have termed this practice “train high, sleep low”. PPAR, peroxisome proliferator–activated receptor; AMPK, 5′-AMP–activated protein kinase; MAPK, mitogen-activated protein kinase; COX, cyclooxygenase.

Nutrition can beat competition fatigue.Many factors that commonly cause fatigue (a periodic or sustained decline in the athlete’s ability to optimally perform) in sporting events can be addressed by nutritional strategies that reduce the effects of these factors or delay their onset.

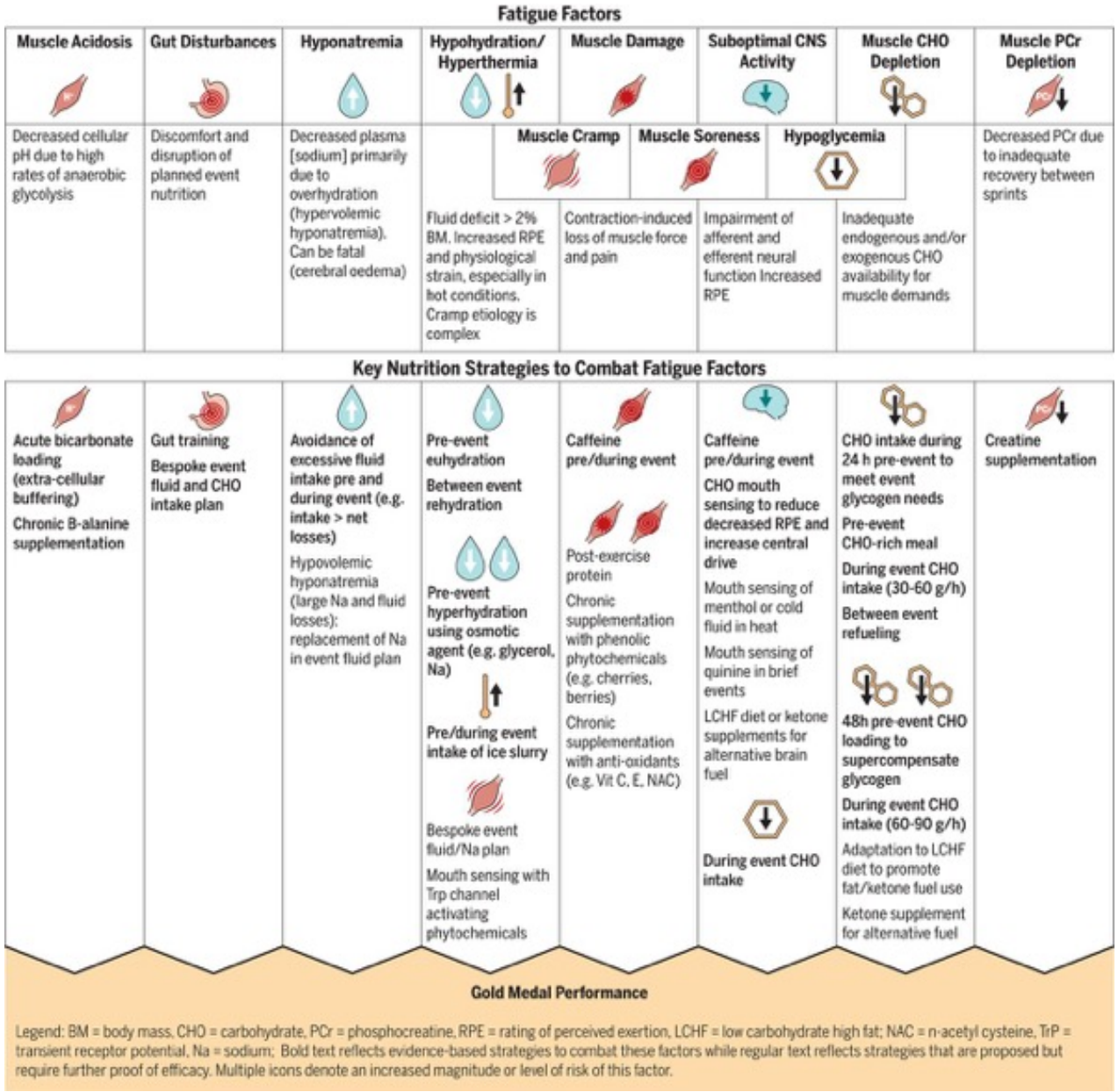

Performance in a bottle.

Sports products represent a lucrative portion of the worldwide explosion in the manufacture and marketing of supplements; according to one report, sports supplements generated global revenue of $9 billion in 2017, with a doubling of this value forecasted by 2025. Surveys confirm the high prevalence of sports food and supplement use among athletes, including greater use at higher levels of competition. Despite earlier reluctance, many expert groups, including the International Olympic Committee, now pragmatically accept the use of supplements passing a risk-benefit analysis as being safe, effective, legal, and appropriate to an athlete's age and maturation in their sport. Supplements used by athletes fall into different categories: nutrient supplements for the treatment or prevention of deficiencies (e.g., iron and vitamin D); sports foods providing energy or nutrients when it is impractical to consume everyday foods (e.g., sports drinks and protein supplements); performance supplements that directly enhance exercise capacity; and supplements that provide indirect benefits through recovery, body composition management, and other goals. Despite enthusiastic marketing, from the latter two groups, only a few products enjoy robust evidence of efficacy [e.g., caffeine, creatine monohydrate, bicarbonate, β-alanine, and nitrate.

Elite athletes are different

Scrutiny of the evidence base for current sports nutrition guidelines reveals that the individuals who contribute blood, sweat, and tears to scientific investigations are at best well trained, often male, and almost always subelite. Interventions with world-class athletes are rare: By definition, such athletes are few in number, and they are generally disinclined to interrupt successful training or nutrition programs or submit to invasive experimental techniques for the sake of science. It is reasonable to ask, therefore, whether the results of studies on nonelite populations apply to their elite counterparts. Issues include application of the intervention to the specific scenarios in which elite athletes train or compete, the inability of underpowered studies to detect small but worthwhile differences or changes in performance that could alter the outcomes of elite sport, and the translation of putative mechanisms to athletes who undertake substantially larger volumes of specialized training and potentially possess favorable genetic traits.

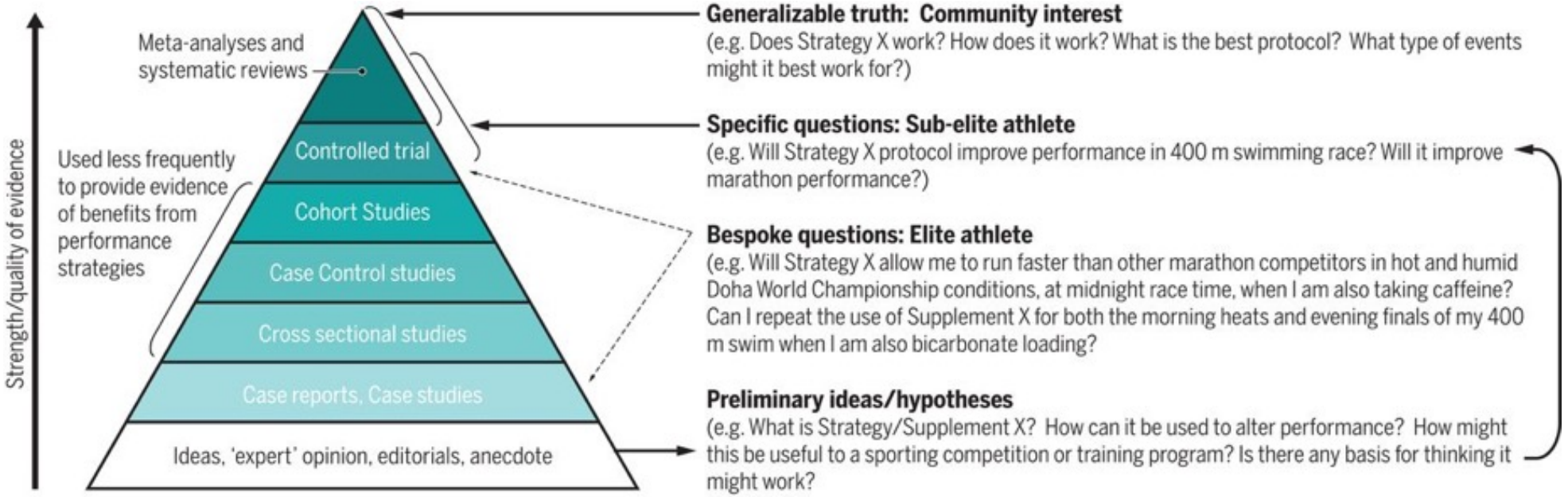

Perspectives on the evidence base for elite athlete practices.Developing an evidence base for the nutritional practices of elite athletes requires acknowledgment that specific answers to research questions and interpretations of guidelines are needed.

In the final analyses, modern sports nutrition offers a feast of opportunities to assist elite athletes to train hard, optimize adaptation, stay healthy and injury free, achieve their desired physique, and fight against fatigue factors that limit success. Although there will be challenges and changes to sports nutrition guidelines as they evolve beyond the frontiers of current knowledge and practice, we can be excited to know that sports science in many guises contributes to the outcomes that delight and amaze us from our sofas and the grandstand.

Die Dermoidzyste ist ein Hohlraum, der von Oberhautgewebe ausgekleidet ist. Die Dermoidzyste gehört zu den Teratomen.
Sie ist ein Keimzelltumor, ein reifes Teratom, das aus vollkommen verschiedenen Gewebearten besteht. Daher kann es innerhalb der Dermoidzyste zur Ausbildung von Gewebestrukturen wie Muskulatur, Knorpel, kleinen Knochen, Haaren und auch völlig ausgebildeten Zähnen kommen.

Spinale Dermoidzyste

Im Rahmen des Neuralrohrverschlusses können sich auch an der Wirbelsäule, meist lumbal, Dermoidzysten ausbilden. Sie gelten als sehr selten.

Epidermoidzysten zählen zu den monodermalen Geschwulsten und treten an verschiedenen Stellen des menschlichen Körpers auf. In der Dermis lokalisierte gutartige Zysten, die aus epidermalen Zellen bestehen, jedoch keine Hautanhangsgebilde aufweisen. Diese Zysten entstehen durch die Zellproliferation von Epidermalzellen in der sie umgebenden Haut. Histologisch bestehen sie aus einer dünnen Plattenepithelschicht mit Hornlamellen, die zum Teil abgeschilfert sein können. Bei Hautverletzungen können kleinere Teile der Epidermis in die Tiefe der Wunde verlagert werden. Die verpflanzten Epidermisteile wachsen im Inneren der Wunde weiter und bilden Hornmassen, die dann zur Entstehung einer Epidermoidzyste führen.
Die Epidermoidzysten finden sich oft im Gesicht, Hals und Rumpfbereich.

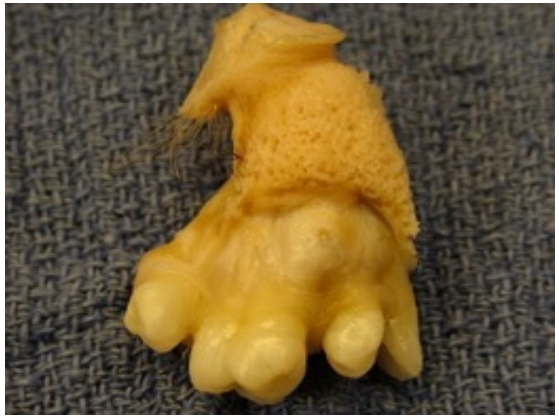

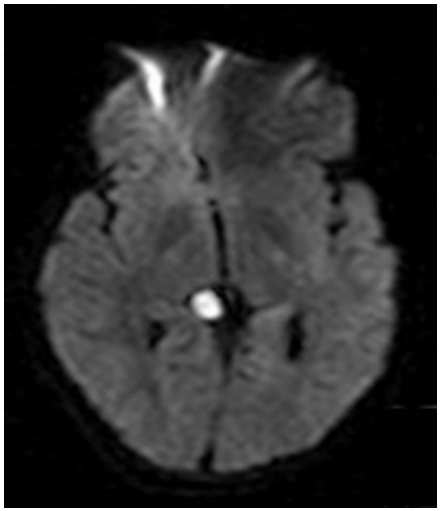

Lobulierte, irreguläre, blumenkohlartige Raumforderung mit liquorähnlicher (Flüssigkeit) Dichte, welche keine Kontrastmittelanreicherung aufweist. In der Magnetresonanztomographie ist sie vor allem dadurch zu unterscheiden, dass sie in der Flair-Sequenz nicht vollständig signalsupprimiert ist, d. h., es besteht eine Hyperintensität im Vergleich zu Liquor. In 10–25 % der Fälle sind Verkalkungen vorhanden. Am häufigsten finden sich Epidermoidzysten im Kleinhirnbrückenwinkel (75 %) und im 4. Hirnventrikel (20 %). Sie entstehen individuell aus Einschlüssen an der Hautoberfläche der Haut während des Neuralrohrverschlusses. Hier eine in der Penialisregion.

Figure: A tight squeeze with an intracranial epidermoid brain tumour. (A) CT scan shows large lesion has not changed since original CT scan (B) and MRIs (C and D) undertaken at the time of the initial diagnosis: the T1-weighted MRIs shows strands of high signal in the lesion-possibly representing fat. The diffusion-weighted MRI shows and confirms the diagnosis ofanepidermoid cyst (E).

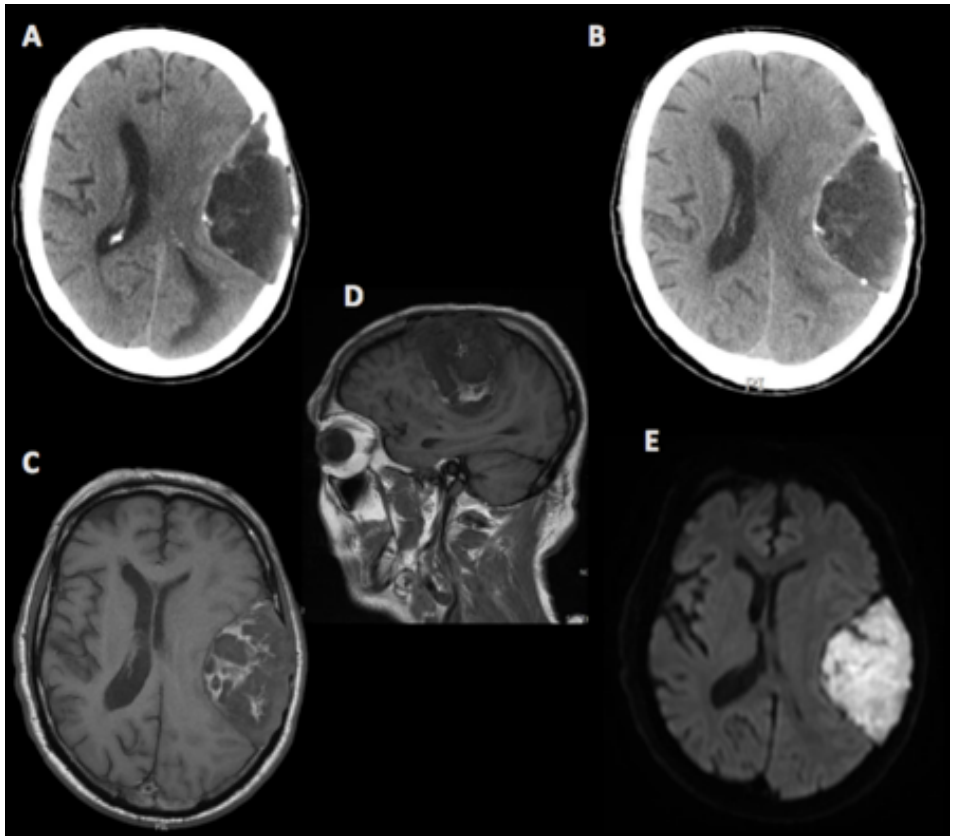

An 80-year-old man presented to our hospital with a 4-day history of a throbbing pain in the front part of his head that was not relieved by analgesics. The pain had developed gradually and was not associated with any weakness in his arms or legs, numbness or visual symptoms. His medical history included a diagnosis of an intracranial epidermoid cyst, hypertension, and depression. A full clinical neurological examination showed no abnormalities. A CT scan of his head showed no additional changes to those seen in a CT scan and an MRI and done 4 months earlier; at the time when the epidermoid cyst was first found, it was a 9 cm × 7·5 cm mass in the left parietal region, thinning and scalloping of the skull vault, and a slight midline shift to the right. No acute bleeds or infarcts were found. The patient was told his symptoms were due to the epidermoid cyst. At the time the cyst was first diagnosed, it was jointly decided by the patient and us to avoid any surgical interventions because epidermoid cysts are usually slow growing, benign, and asymptomatic.

In such cases it is important to differentiate an epidermoid cyst from a dermoid cyst: the CT scans in this case showed a lesion of low density, which might have been fat—typically associated with dermoid cysts. An MRI with the appropriate enhancement was needed to differentiate the two. T1-weighted MRI showed strands of high signal in the lesion, which could also have represented fat. However, the diffusion-weighted

MRI, which showed restricted diffusion, confirmed the diagnosis. Furthermore, these striking images—in a patient with no neurological signs—show how a large lesion can be accommodated by a relatively atrophic brain with increased cerebrospinal fluid (CSF) filled spaces and the clinical relevance of the Monro–Kellie doctrine. Normal intracranial pressure is maintained in the presence of an expanding intracranial mass—firstly, as CSF is forced out of the ventricles and secondly, as intracranial venous volume reduces, both effects resulting in the creation of up to 150 mL of space. Essentially, the changes in the CSF and venous blood volume buffer the effect of an expanding intracranial mass within the rigid skull. Neurological symptoms—such as headaches, visual disturbances, and sensorimotor deficits—only develop when these mechanisms are exhausted, and at this point surgery may be indicated.

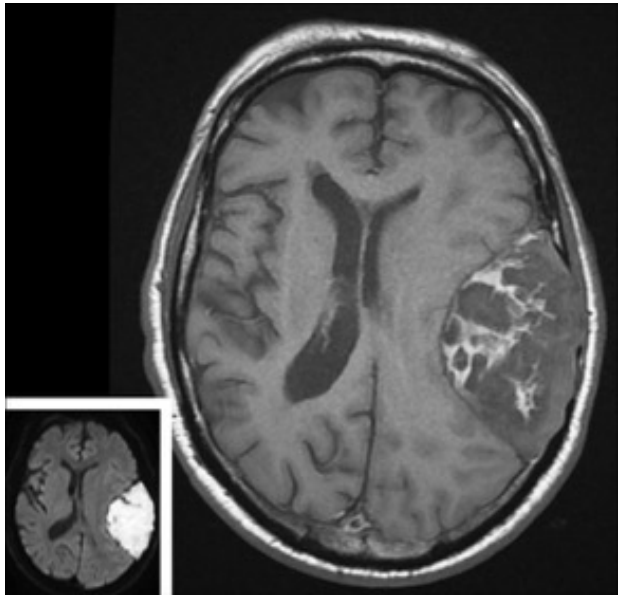

T1-weighted MRI shows strands of high signal in the lesion—possibly representing fat. The diffusion-weighted MRI shows and confirms the diagnosis of an epidermoid cyst (inset)